Inside Track with Kevin Kelly, LGS Innovations | 26

Wireless Challenges in the IoT | 46

Smarter Antenna Tuning Can Change the Game | 63

microwaves&rf

FEBRUARY 2017 TRUSTED ENGINEERING RESOURCE FOR OVER 50 YEARS www.mwrf.com

SPECTRUM ANALYZERS:

Small Size, BIG Performance

p | 68

$10.00 Powered by Penton

TAKE IT TO THE EXTREME

INTRODUCING THE WORLD'S FIRST ULTRAPORTABLE FAMILY OF mmWAVE SPECTRUM ANALYZERS TO 110GHZ.

Now taking it to the extreme just got easier. The footprint for up to 110 GHz measurements is now a whole lot smaller, and so is the price tag. Anritsu introduces a new family of 9 kHz to 110 GHz direct-connect solutions which offer superior dynamic range in the mmWave bands and in a form factor that fits in your pocket! Nothing on the market comes close.

ANRITSU MS2760A SPECTRUM MASTER

mmWAVE
Test and measurement for Automotive Radar, Satellite, 5G, WiGig and more

ULTRAPORTABLE
Benchtop power from a smartphone-sized instrument that fits in your pocket

PERFORMANCE
Best-in-class dynamic range, sweep speed, and amplitude accuracy

Anritsu

WWW.ANRITSU.COM/TEST-MEASUREMENT

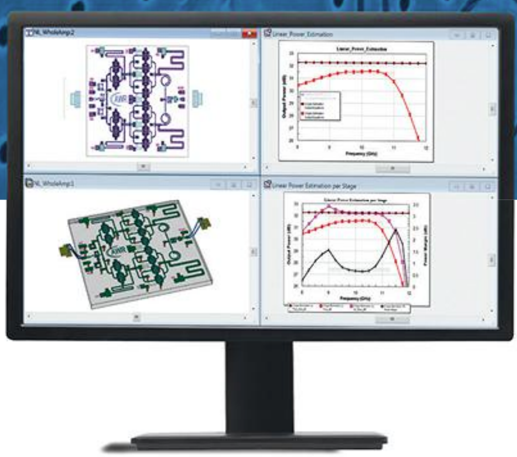

VOLUME 56, ISSUE 2

In This Issue

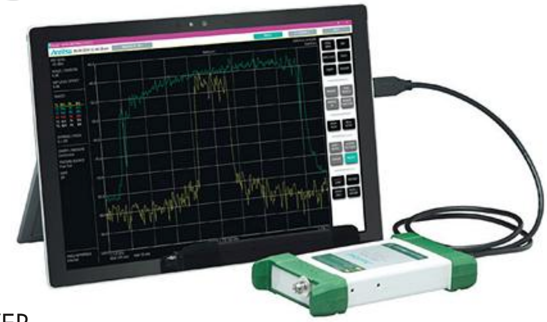

68

FEATURES

68 **COVER STORY:**
POCKET-SIZED ANALYZERS SCAN MILLIMETER-WAVE FREQUENCIES
Barely larger than many smartphones, this line of ultraportable spectrum analyzers doesn't skimp on performance, with models available for measurements to 110 GHz.

33 A ROBUST, LARGE-SIGNAL MODEL FOR LDMOS RF POWER TRANSISTORS
Accurate empirical LDMOS transistor models are critical to achieving first-pass design success.

42 BASICS OF MODULATION AND DEMODULATION, PART 1
Radio waves can carry audio, video, and digital information over great distances by using changes in a carrier wave's amplitude, frequency, or phase to represent the information being transmitted.

46 IoT GROWTH BANKS ON RELIABLE COMMUNICATION
To meet the needs of the Industrial Internet of Things (IIoT), communication systems must demonstrate a high level of reliability while maintaining low costs.

50 ANALYZE RF JFETs FOR LARGE-SIGNAL BEHAVIOR
A new field-effect-transistor architecture can be biased for improved efficiency and output power at RF and microwave frequencies.

56 FIND SOLUTIONS FOR TRANSIENT DELAYS IN GaAs MMIC SWITCHES
The fast speeds of GaAs MMIC switches can be hindered by step voltage functions employed for bias sequencing of power amplifiers.

63 REVERSING 25 YEARS OF ANTENNA DEGRADATION
As mobile communication ramps up in complexity, smarter antenna tuning could prove to be a game-changer in meeting demands.

42

46

PRODUCT TECHNOLOGY

72 Higher-Density ICs
75 Manufacturing Semiconductors
77 High-Level Frequency Synthesizers
81 Portable Spectrum Monitoring
82 Creating Accurate Antenna Models

NEWS & COLUMNS

10 ON MWRF.COM
13 EDITORIAL
18 FEEDBACK
20 NEWS
26 INSIDE TRACK with Kevin Kelly, LGS Innovations

28 R&D ROUNDUP
66 APPLICATION NOTES
85 NEW PRODUCTS
88 ADVERTISERS INDEX

JOIN US ONLINE

follow us @MicrowavesRF

become a fan at facebook.com/microwavesRF

63

Featured MACOM MMIC Devices

Application	Function	Part Number
Aerospace & Defense	Low Noise Amplifier Octave Band VCO Power Amplifier	MAAM-011229, 0.05 - 4 GHz MAOC-415000, 10 - 20 GHz MAAP-011232, 0.1 - 3 GHz
SATCOM	Ka-Band Power Amplifier Doubler Power Amplifier L-Band Power Amplifier Module	MAAP-011289, 28 - 30.5 GHz MAFC-011009, 28 - 30 GHz MAAP-011060, 1616 - 1627 MHz
Test & Measurement	Wideband Power Amplifier Wideband Low Noise Amplifier Wideband DBL BAL Mixer	MAAP-011247, DC - 22 GHz MAAL-011141, DC - 26.5 GHz MAMX-011036, 8 - 43 GHz
Industrial, Scientific & Medical	Low Noise Amplifier Gain Block	MAAL-011129, 18 - 32 GHz MAAM-011206, DC - 15 GHz
Wired Broadband	Variable Gain Amplifier Gain Block Very Low Noise Amplifier	MAAM-011194, 45 - 1218 MHz MAAM-011220, 45 - 1218 MHz MAAL-011136, 45 - 1218 MHz

on microwaves&rf.com

THE FUTURE OF VEHICULAR TECH

http://mwrf.com/systems/driving-future-vehicular-technology

The interest of automotive manufacturers in producing fully autonomous vehicles has been well publicized, and the overall growth of electronic content within new-model automobiles represents a heartily growing market for electronic devices such as microprocessors and wireless transceivers, as well as software that can help build the road to the "driverless" vehicle of the future.

IMPROVING HEALTH WITH MICROWAVE ENERGY

http://mwrf.com/systems/microwave-energy-aims-improve-health

Medical devices are now being implanted, worn, and mounted for monitoring in homes and hospitals to provide cutting-edge health benefits via modern wireless technology.

USING SOUND WAVES TO ANALYZE MIMO

http://mwrf.com/systems/using-sound-waves-analyze-mimo

At the University of Madrid, low-cost audio speakers and sound waves were used to model the effects of multipath propagation on MIMO wireless communications systems.

THE MYSTERIES OF TRANSMISSION LINES

http://mwrf.com/systems/untangle-mysteries-transmission-lines

Transmission lines vary structurally and performance-wise, and create challenges during the fabrication process when using different active- and passive-circuit components.

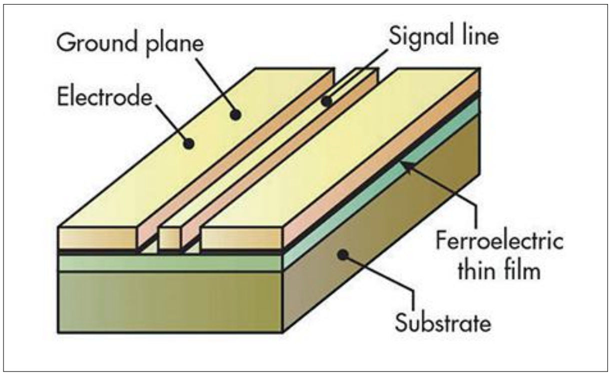

join us online

twitter.com/MicrowavesRF facebook.com/microwavesrf

NEW! RF Switches

SWITCH-N-SAVE by CEL

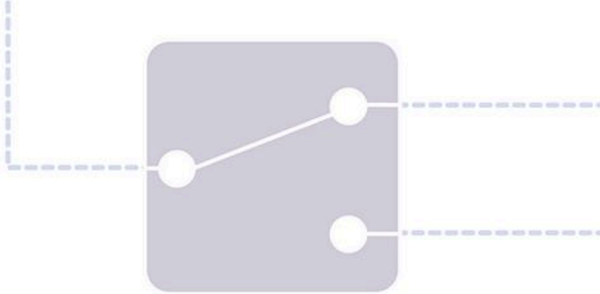

SWAP THEM WITH OTHER SUPPLIER SWITCHES FOR BIG SAVINGS

LOWER COST SOLUTIONS

Cost Savings for New and Existing Customers

HIGHER RF PERFORMANCE

Better RF Performance than other RF Switches

HIGH JAPANESE QUALITY

Manufactured in Japan with High Quality, Packaging and Testing

CEL Part Numbers	Switch Type	MAX Freq. (GHz)	Insertion Loss (dB)		Isolation (dB)		Compression point @ 3V (dBm)		Package Type (mm)
			2.5 GHz	6.0 GHz	2.5 GHz	6.0 GHz	2.5 GHz	6.0 GHz	
CG2163X3	SPDT	6.0	0.40	0.50	40	31	+33 @ P1.0dB	+32 @ P1.0dB	(1.5 x 1.5 x 0.37)
JUST ADDED CG2164X3	DPDT	6.0	0.50	0.65	25	17	+32 @ P0.5dB	+30 @ P0.5dB	(1.5 x 1.5 x 0.37)
CG2176X3	Absorptive SPDT	6.0	0.45	0.55	30	22	+37.5 @ P0.5dB	+37.5 @ P0.5dB	(1.5 x 1.5 x 0.37)
CG2179M2	SPDT	3.0	0.45	N/A	26	N/A	+30 @ P0.1dB	NA	(2.0 x 1.25 x 0.9)
CG2185X2	SPDT	6.0	0.35	0.40	28	26	+29 @ P0.1dB	+29 @ P0.1dB	(1.0 x 1.0 x 0.37)
CG2214M6	SPDT	3.0	0.35	N/A	25	N/A	+30 @ P0.1dB	NA	(1.5 x 1.1 x 0.55)
JUST ADDED CG2409M2	SPDT	3.8	0.45	N/A	27	N/A	+37.5 @ P0.1dB	NA	(2.0 x 1.25 x 0.9)
JUST ADDED CG2409X3	SPDT	6.0	0.40	N/A	26	N/A	+37.5 @ P0.1dB		(1.5 x 1.5 x 0.37)
CG2415M6	SPDT	6.0	0.35	0.45	32	26	+31 @ P0.1dB	+31 @ P0.1dB	(1.5 x 1.1 x 0.55)
CG2430X1	SP3T	6.0	0.50	0.60	28	25	+28 @ P0.1dB	+28 @ P0.1dB	(1.5 x 1.5 x 0.37)

ULTRA-REL™
CERAMIC MMIC AMPLIFIERS

10 MHz to 7 GHz

Low NF from 0.5 dB *High IP3 up to +42 dBm* *Low DC current 65 mA* from $7.45 ea. (qty 20)

When failure is not an option! Our CMA family of ceramic MMIC amplifiers is expanding to meet your needs for more critical applications. Designed into a nitrogen-filled, hermetic LTCC package just 0.045" high, these rugged models have been qualified and are capable of meeting MIL standards for a whole battery of harsh environmental conditions:

Qualified for: *(see website for complete list and details)*

Gross and Fine Leak	*HTOL (1700 hours @ +105°C)*
Mechanical Shock	*Steam Aging*
Vibration	*Solder Heat Resistance*
Acceleration	*Autoclave*
PIND	*And More!*

**Gross leak only*

Robust performance across wide bandwidths makes them ideal for military and defense applications, hi-rel instrumentation, and anywhere long-term reliability adds bottom-line value. Go to minicircuits.com for all the details today, and have them in your hands as soon as tomorrow!

Electrical Specifications *(-55 to +105°C)*

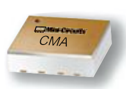

3 x 3 x 1.14 mm

Model	Freq. (GHz)	Gain (dB)	P_{OUT} (dBm)	IP3 (dBm)	NF (dB)	DC (V)	Price $ ea. (qty 20)
CMA-81+	DC-6	10	19.5	38	7.5	5	8.95
CMA-82+	DC-7	15	20	42	6.8	5	8.95
CMA-84+	DC-7	24	21	38	5.5	5	8.95
CMA-62+	0.01-6	15	19	33	5	5	7.45
CMA-63+	0.01-6	20	18	32	4	5	7.45
CMA-545+	0.05-6	15	20	37	1	3	7.45
CMA-5043+	0.05-4	18	20	33	0.8	5	7.45
CMA-545G1+	0.4-2.2	32	23	36	0.9	5	7.95
CMA-162LN+	0.7-1.6	23	19	30	0.5	4	7.45
CMA-252LN+	1.5-2.5	17	18	30	1	4	7.45

RoHS compliant

Mini-Circuits®

www.minicircuits.com P.O. Box 350166, Brooklyn, NY 11235-0003 (718) 934-4500 sales@minicircuits.com

Editorial

CHRIS DeMARTINO
Technical Editor
chris.demartino@penton.com

Norway Turns Off the Lights on FM Radio

Recently, news came forth that Norway is planning to be the first nation to eliminate FM radio. It goes without saying that this move is significant given how long FM radio has been in existence. Norway's intention is to replace FM with digital audio broadcasting (DAB); the transition is expected to be completed by the end of the year. Proponents of DAB point out its advantages, including better reception and lower operating costs.

However, many Norwegians do not support this move—some 66%, according to a recent poll. Although the government says this move will save a significant amount of money, critics have not been shy in voicing their opinion. Some have said that the country is simply not prepared to eliminate FM radio. For example, many cars on the road do not even have DAB receivers. Many radios in homes will no longer work when FM radio is shut down.

No question, it will be interesting to follow Norway's transition away from FM. It will also be interesting to see which other nations ultimately decide to follow in its footsteps. Several other European countries, such as Switzerland, Denmark, and the U.K., are strong candidates to similarly eliminate FM radio in the future, so they will surely be interested to see how this all unfolds.

While a similar move is not likely to happen in the U.S. anytime soon, it does beg the question of what life would be like without FM radio. Although there are some who do not listen to FM radio much—if at all—countless others still rely on this "old" technology. Without a doubt, many people would surely be unhappy if FM radio ever did go away.

This "old vs. new" debate also led me to think about the "print vs. digital media" argument. While many outlets have transitioned away from print media, a large number of people still prefer the "old school" approach of reading a physical magazine. If you are holding this magazine in your hands right now, then you are already bearing witness to that. For many, print media is still something that is appreciated.

With all of this being said, both old-fashioned FM radio and print magazines (at least this one) can still be enjoyed here in the U.S. That's (hopefully) good news for many. mw

JOIN US ONLINE twitter.com/MicrowavesRF
become a fan at facebook.com/MicrowavesRF

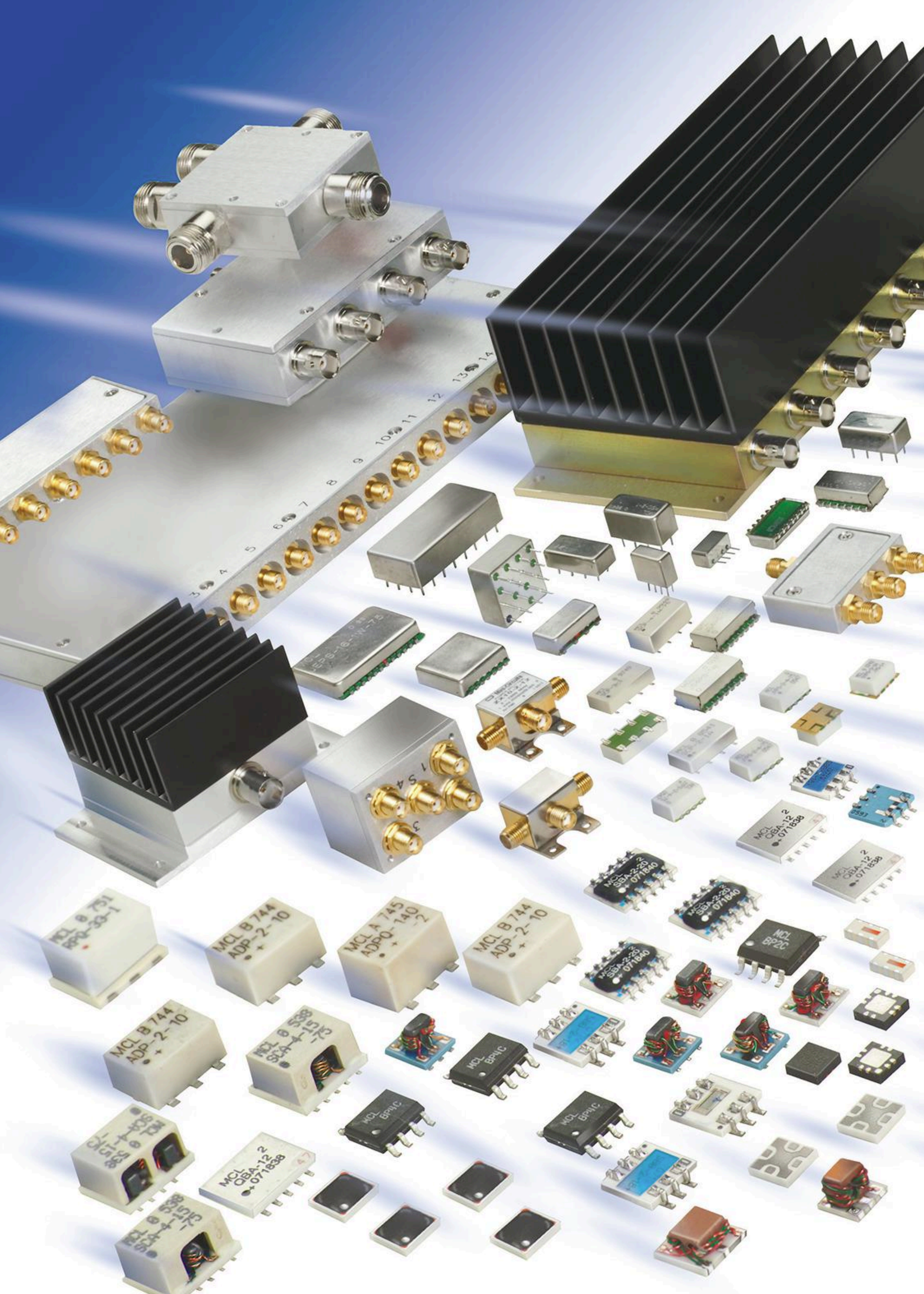

MCL B 744
ADP-2-10
MCL A 745
MCL
BP4C
MCL
BP2C
MCL
QBA-12
071838
MCL
SBA-2-20
071840

RF Amplifiers and Sub-Assemblies for Every Application

Delivery from Stock to 2 Weeks ARO from the catalog or built to your specifications!

- Competitive Pricing & Fast Delivery
- Military Reliability & Qualification
- Various Options: Temperature Compensation, Input Limiter Protection, Detectors/TTL & More
- Unconditionally Stable (100% tested)

ISO 9001:2000 and AS9100B CERTIFIED

OCTAVE BAND LOW NOISE AMPLIFIERS

Model No.	Freq (GHz)	Gain (dB) MIN	Noise Figure (dB)	Power-out @ P1-dB	3rd Order ICP	VSWR
CA01-2110	0.5-1.0	28	1.0 MAX, 0.7 TYP	+10 MIN	+20 dBm	2.0:1
CA12-2110	1.0-2.0	30	1.0 MAX, 0.7 TYP	+10 MIN	+20 dBm	2.0:1
CA24-2111	2.0-4.0	29	1.1 MAX, 0.95 TYP	+10 MIN	+20 dBm	2.0:1
CA48-2111	4.0-8.0	29	1.3 MAX, 1.0 TYP	+10 MIN	+20 dBm	2.0:1
CA812-3111	8.0-12.0	27	1.6 MAX, 1.4 TYP	+10 MIN	+20 dBm	2.0:1
CA1218-4111	12.0-18.0	25	1.9 MAX, 1.7 TYP	+10 MIN	+20 dBm	2.0:1
CA1826-2110	18.0-26.5	32	3.0 MAX, 2.5 TYP	+10 MIN	+20 dBm	2.0:1

NARROW BAND LOW NOISE AND MEDIUM POWER AMPLIFIERS

Model No.	Freq (GHz)	Gain (dB) MIN	Noise Figure (dB)	Power-out @ P1-dB	3rd Order ICP	VSWR
CA01-2111	0.4 - 0.5	28	0.6 MAX, 0.4 TYP	+10 MIN	+20 dBm	2.0:1
CA01-2113	0.8 - 1.0	28	0.6 MAX, 0.4 TYP	+10 MIN	+20 dBm	2.0:1
CA12-3117	1.2 - 1.6	25	0.6 MAX, 0.4 TYP	+10 MIN	+20 dBm	2.0:1
CA23-3111	2.2 - 2.4	30	0.6 MAX, 0.45 TYP	+10 MIN	+20 dBm	2.0:1
CA23-3116	2.7 - 2.9	29	0.7 MAX, 0.5 TYP	+10 MIN	+20 dBm	2.0:1
CA34-2110	3.7 - 4.2	28	1.0 MAX, 0.5 TYP	+10 MIN	+20 dBm	2.0:1
CA56-3110	5.4 - 5.9	40	1.0 MAX, 0.5 TYP	+10 MIN	+20 dBm	2.0:1
CA78-4110	7.25 - 7.75	32	1.2 MAX, 1.0 TYP	+10 MIN	+20 dBm	2.0:1
CA910-3110	9.0 - 10.6	25	1.4 MAX, 1.2 TYP	+10 MIN	+20 dBm	2.0:1
CA1315-3110	13.75 - 15.4	25	1.6 MAX, 1.4 TYP	+10 MIN	+20 dBm	2.0:1
CA12-3114	1.35 - 1.85	30	4.0 MAX, 3.0 TYP	+33 MIN	+41 dBm	2.0:1
CA34-6116	3.1 - 3.5	40	4.5 MAX, 3.5 TYP	+35 MIN	+43 dBm	2.0:1
CA56-5114	5.9 - 6.4	30	5.0 MAX, 4.0 TYP	+30 MIN	+40 dBm	2.0:1
CA812-6115	8.0 - 12.0	30	4.5 MAX, 3.5 TYP	+30 MIN	+40 dBm	2.0:1
CA812-6116	8.0 - 12.0	30	5.0 MAX, 4.0 TYP	+33 MIN	+41 dBm	2.0:1
CA1213-7110	12.2 - 13.25	28	6.0 MAX, 5.5 TYP	+33 MIN	+42 dBm	2.0:1
CA1415-7110	14.0 - 15.0	30	5.0 MAX, 4.0 TYP	+30 MIN	+40 dBm	2.0:1
CA1722-4110	17.0 - 22.0	25	3.5 MAX, 2.8 TYP	+21 MIN	+31 dBm	2.0:1

ULTRA-BROADBAND & MULTI-OCTAVE BAND AMPLIFIERS

Model No.	Freq (GHz)	Gain (dB) MIN	Noise Figure (dB)	Power-out @ P1-dB	3rd Order ICP	VSWR
CA0102-3111	0.1-2.0	28	1.6 Max, 1.2 TYP	+10 MIN	+20 dBm	2.0:1
CA0106-3111	0.1-6.0	28	1.9 Max, 1.5 TYP	+10 MIN	+20 dBm	2.0:1
CA0108-3110	0.1-8.0	26	2.2 Max, 1.8 TYP	+10 MIN	+20 dBm	2.0:1
CA0108-4112	0.1-8.0	32	3.0 MAX, 1.8 TYP	+22 MIN	+32 dBm	2.0:1
CA02-3112	0.5-2.0	36	4.5 MAX, 2.5 TYP	+30 MIN	+40 dBm	2.0:1
CA26-3110	2.0-6.0	26	2.0 MAX, 1.5 TYP	+10 MIN	+20 dBm	2.0:1
CA26-4114	2.0-6.0	22	5.0 MAX, 3.5 TYP	+30 MIN	+40 dBm	2.0:1
CA618-4112	6.0-18.0	25	5.0 MAX, 3.5 TYP	+23 MIN	+33 dBm	2.0:1
CA618-6114	6.0-18.0	35	5.0 MAX, 3.5 TYP	+30 MIN	+40 dBm	2.0:1
CA218-4116	2.0-18.0	30	3.5 MAX, 2.8 TYP	+10 MIN	+20 dBm	2.0:1
CA218-4110	2.0-18.0	30	5.0 MAX, 3.5 TYP	+20 MIN	+30 dBm	2.0:1
CA218-4112	2.0-18.0	29	5.0 MAX, 3.5 TYP	+24 MIN	+34 dBm	2.0:1

LIMITING AMPLIFIERS

Model No.	Freq (GHz)	Input Dynamic Range	Output Power Range Psat	Power Flatness dB	VSWR
CLA24-4001	2.0 - 4.0	-28 to +10 dBm	+7 to +11 dBm	+/- 1.5 MAX	2.0:1
CLA26-8001	2.0 - 6.0	-50 to +20 dBm	+14 to +18 dBm	+/- 1.5 MAX	2.0:1
CLA712-5001	7.0 - 12.4	-21 to +10 dBm	+14 to +19 dBm	+/- 1.5 MAX	2.0:1
CLA618-1201	6.0 - 18.0	-50 to +20 dBm	+14 to +19 dBm	+/- 1.5 MAX	2.0:1

AMPLIFIERS WITH INTEGRATED GAIN ATTENUATION

Model No.	Freq (GHz)	Gain (dB) MIN	Noise Figure (dB)	Power-out @ P1-dB	Gain Attenuation Range	VSWR
CA001-2511A	0.025-0.150	21	5.0 MAX, 3.5 TYP	+12 MIN	30 dB MIN	2.0:1
CA05-3110A	0.5-5.5	23	2.5 MAX, 1.5 TYP	+18 MIN	20 dB MIN	2.0:1
CA56-3110A	5.85-6.425	28	2.5 MAX, 1.5 TYP	+16 MIN	22 dB MIN	1.8:1
CA612-4110A	6.0-12.0	24	2.5 MAX, 1.5 TYP	+12 MIN	15 dB MIN	1.9:1
CA1315-4110A	13.75-15.4	25	2.2 MAX, 1.6 TYP	+16 MIN	20 dB MIN	1.8:1
CA1518-4110A	15.0-18.0	30	3.0 MAX, 2.0 TYP	+18 MIN	20 dB MIN	1.85:1

LOW FREQUENCY AMPLIFIERS

Model No.	Freq (GHz)	Gain (dB) MIN	Noise Figure dB	Power-out @ P1-dB	3rd Order ICP	VSWR
CA001-2110	0.01-0.10	18	4.0 MAX, 2.2 TYP	+10 MIN	+20 dBm	2.0:1
CA001-2211	0.04-0.15	24	3.5 MAX, 2.2 TYP	+13 MIN	+23 dBm	2.0:1
CA001-2215	0.04-0.15	23	4.0 MAX, 2.2 TYP	+23 MIN	+33 dBm	2.0:1
CA001-3113	0.01-1.0	28	4.0 MAX, 2.8 TYP	+17 MIN	+27 dBm	2.0:1
CA002-3114	0.01-2.0	27	4.0 MAX, 2.8 TYP	+20 MIN	+30 dBm	2.0:1
CA003-3116	0.01-3.0	18	4.0 MAX, 2.8 TYP	+25 MIN	+35 dBm	2.0:1
CA004-3112	0.01-4.0	32	4.0 MAX, 2.8 TYP	+15 MIN	+25 dBm	2.0:1

CIAO Wireless can easily modify any of its standard models to meet your "exact" requirements at the Catalog Pricing.

Visit our web site at **www.ciaowireless.com** for our complete product offering.

Ciao wireless

Ciao Wireless, Inc. 4000 Via Pescador, Camarillo, CA 93012

Tel (805) 389-3224 Fax (805) 389-3629 sales@ciaowireless.com

MAKE FOUNDRIES A FOCUS

After receiving your January issue in the mail, I read with great interest your story on II-VI and their acquisition and reclamation of EpiWorks (p. 24). The article mentions the production of device technologies such as GaAs and InP and the many applications for semiconductor devices they're used to fabricate: applications like optoelectronic devices, lasers, and high-frequency wireless ICs.

Not that I don't enjoy reading your publication, but this story reveals one of the shortcomings in your coverage of the high-frequency industry (especially for designers of semiconductor devices): editorial coverage of the foundry side of the business. Rarely do I see reviews of the different commercial semiconductor foundries, or even of the captive foundries at defense contractors that are used to fabricate devices like GaN-based amplifiers for pulsed radar applications.

In terms of performance, commercial products will always lag behind the performance levels of military electronic systems. It would be educational not just for me, but for all of your readers interested in semiconductors, to know more about the various semiconductor foundries in the industry and the role they play in fabricating devices.

If a report on semiconductor foundries is not on your schedule, I implore you to add it, for the benefit of your readers. It's certainly possible to Google information about these foundries, but poring through each of these companies' websites (while trying to make sense of information which is often poorly written and presented) is tedious and time-consuming. Please do what you can to help by presenting reviews of foundries in clear, understandable fashion.

Joseph Suarez

EDITOR'S NOTE

Thank you for your note. Ironically, *Microwaves & RF's* technical editor, Chris DeMartino, recently visited one of these "captive" semiconductor foundries—BAE Systems—and some of the details can be found in a review of the foundry's capabilities (see p. 75). Although BAE fabricates many devices and circuits for defense-related projects, the foundry's services are also available to outside customers.

And, to your point about the need for more coverage of semiconductor foundries, contractors such as Northrop Grumman offer impressive services to both internal and external customers, but little would be known of them without the editorial coverage. To that end, a review of NG's foundry will appear in the March edition of our *Defense Electronics* supplement.

Jack Browne
Technical Contributor

News

GALLIUM NITRIDE
to Gradually Move Out of the Periphery

If the mark of critical technology is that companies are willing to sue to protect it, and governments are blocking other countries from buying it, then gallium nitride will only grow more widespread as it supplants silicon in power and wireless electronics.

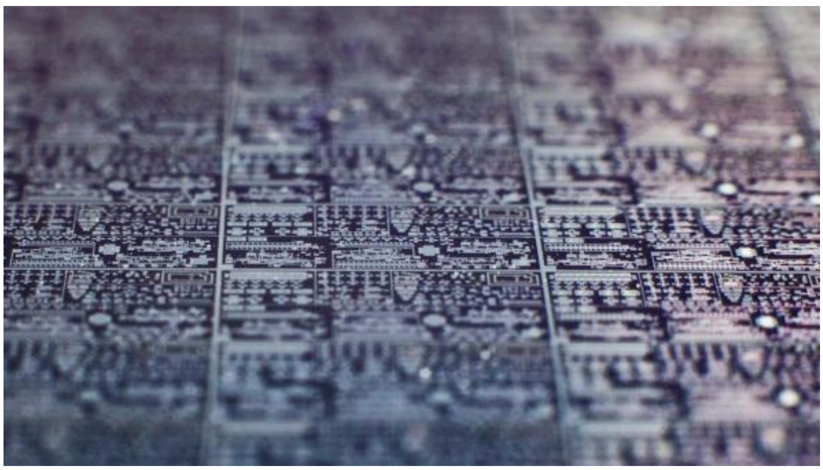

Gallium nitride, also known as GaN, stands out from materials like silicon for having a wide bandgap, which allows it to handle higher voltages and hotter temperatures. *(Image courtesy of Eric Gorski, Creative Commons)*

In December 2016, a federal court ordered that Infineon stop making gallium nitride chips that could infringe on patents owned by Macom Technology Solutions, which sued the German chipmaker in April 2016. John Croteau, Macom's chief executive, said that Infineon's attempt to alter its patent licensing deal confirmed that gallium nitride is "at the tipping point for market adoption, threatening large incumbents like Infineon."

Last year, the U.S. government blocked Aixtron, a German maker of semiconductor tools from selling itself to a Chinese chip supplier. The reason was likely that Aixtron's tools are critical for making light-emitting diodes based on gallium nitride, which has vital military applications. An American regulatory panel also blocked the sale of a Philips subsidiary with similar manufacturing insight.

These quarrels over gallium nitride are not insignificant. The material is replacing silicon in sophisticated radar for antiballistic missiles and an Air Force radar system, called Space Fence, for tracking space debris. The market for the technology is also growing: from around $870 million in 2014 to $3.4 billion in 2024, according to a recent report from Transparency Market Research. The market will grow 17% per year over the next eight years, the report said.

The largest suppliers of gallium nitride, including Efficient Power Conversion and GaN Systems, are focusing on power electronics and light-emitting diodes, according to the report. But their growth mirrors what is happening with gallium nitride in radio frequency applications. Some of the industry leaders—including NXP Semiconductors, Macom, and Qorvo as well as defense contractors like Raytheon and Lockheed Martin—are turning their eyes toward this market.

Gallium nitride stands out from materials like silicon for having a wide bandgap, which allows it to handle higher voltages and hotter temperatures. With limited power consumption, it outperforms other materials in radio frequency applications, including gallium arsenide and silicon structures known as LDMOS.

These benefits have not come easy, though. Troubles with packaging and producing gallium nitride chips have slowed an ascent that industry analysts once thought would quickly remove silicon from the high-power equation. But recent advances in plastic packaging and larger wafers leaving factories have kept the market at a slow burn.

For years, the defense sector was the major force in the market for gallium nitride, which was used in electronic warfare, radar, communications, and jammers for improvised explosive devices. But that is set to change with new radio equipment for 5G communications, according to Transparency Market Research. The equipment will require power amplifiers based on gallium nitride that run more efficiently at high voltages than gallium arsenide, generating more power to transmit signals.

New applications are pending in healthcare and home appliances, according to industry executives. Mark Murphy, senior director of marketing at Macom, recently told *Microwaves & RF* that gallium nitride could be used to generate heat for pain-relief procedures like ablation. Power amplifiers based on the technology could also be used for cooking food more efficiently than microwave ovens.

Many companies are not stopping at power amplifiers, though. Charles Trantanella, a chief scientist at Custom MMIC, used the material to create mixers that modulate and convert radio signals with high linearity. Akoustis, a start-up firm, is using gallium nitride in filters that block out stray signals that leak into smartphone or radio equipment.

The future is bright for the wireless applications of gallium nitride, though the material will still make a larger impact in power electronics. After enduring its growing pains, the market for radio frequency gallium nitride is expected to reach $688.5 million in 2020, up from around $300 million in 2015, according to technology research firm Strategy Analytics.

There are signs that chipmakers are buying the tools to carve out part of the market. Last year, Infineon said that it was buying Cree's power and radio frequency business, which has expertise in gallium nitride, for $850 million. For wireless applications, that Wolfspeed unit had developed a process for layering gallium nitride on substrates of silicon carbide, which is used alone in power electronics.

Reinhard Ploss, Infineon's chief executive, said that the acquisition would help Infineon to remain relevant in a future increasingly powered by electricity and connected through radios. "With Wolfspeed we will become number one in SiC-based power semiconductors. We also want to become number one in RF power," he says.

"This will accelerate the market introduction of these innovative technologies, addressing the needs of modern society—such as energy efficiency, connectivity and mobility." ■

NEW MILLIMETER-WAVE TECHNOLOGY Helps Guide the Blind

RESEARCHERS AT THE VTT Technical Research Centre of Finland are testing wearable scanners that guide the blind or visually impaired by mapping the environment with radio pulses.

Guide Sense, as the technology is called, bounces millimeter waves off objects to measure distance, speed, and where the objects are located in relation to the wearer. The device conveys information to users either with voice feedback or vibrations to indicate how close something is.

The result of a two-year project at VTT, the radar is designed with the same millimeter wave technology used in airport security checkpoints to check underneath people's clothes for weapons and in radios for transmitting large packets of wireless data between cell towers.

With specialized algorithms, the technology can also be used by security systems for tracking people or imaging tumors in the human body without X-rays. Northrop Grumman engineers have devised millimeter-wave chips for radio astronomy and airplane landing systems.

The high frequencies of millimeter waves enable the radar antennas to be shrunk down and worn, according to Tero Kiuru, a senior scientist at VTT. He said that their system can be strapped around a person's chest like a heart rate monitor and worn under clothing.

The system is still in the testing and development stage, but early trials have been positive, according to Kiuru. Working with the Finnish Federation of the Visually Impaired, the researchers tested the device on 25 visually impaired people. Of those, 14 were blind, seven had limited eyesight, and four were both partially deaf and blind.

In tests approved by Finland's National Supervisory Authority for Welfare and Health, the researchers found that 92% of the users reported the GuideSense helped them perceive their surroundings and 32% of users would immediately start using the test device in its current form.

But there are improvements that Kiuru and other researchers are eyeing. For one, the radar has trouble sensing objects like branches and bushes in parks. For another, many of the testers were confused by the vibration-based feedback and imprecision of some distance measurements. ■

Guide Sense is designed with the same millimeter-wave technology used in airport security checkpoints to check underneath people's clothes for weapons and in radios for transmitting large packets of wireless data between cell towers. *(Image courtesy of VTT Technical Research Centre of Finland)*

MULTI-PROTOCOL CHIP Tries to Desegregate the Internet of Things

THE NEW WIRELESS CHIP recently released by Qorvo is the latest specimen to incorporate multiple radios that can improve reliability and connect things like heating systems and light bulbs. The new product, also known as the GP695, enables devices to connect devices that might have been isolated on a single type of network.

The new chip is built with hardware that supports Zigbee, Bluetooth, and Thread as well as personal area networks based on the IEEE 802.15.4 standard, like Linear Technology's Wireless Hart and Microchip's MiWi standards.

Using the type of chip like Qorvo's, "designers can let consumers control their smart homes without worrying about evolving IoT standards," says Cees Links, the general manager of Qorvo's wireless connectivity business, formerly GreenPeak Technologies before Qorvo bought the company in 2016.

For example, a homeowner could use a mobile phone to connect a door lock equipped with the GP695 to a smart-home hub using the phone's Bluetooth transmitter. The door lock could then be opened or closed from the mobile phone over Bluetooth or over Zigbee when security cameras in the house detect no one home.

Qorvo is not alone in etching different types of radio circuits onto a single chip. In May 2016, the Belgian electronics research center Imec unveiled a radio chip that contains hardware for more than five different low-power wide area networks, including the popular LoRa and Sigfox, as well as Zigbee and Thread. Hmicro, a startup making wireless sensors for hospitals, has built a platform that integrates circuits for Wi-Fi, medical frequency bands, and ultra-wideband channels.

The GP695 uses an ARM Cortex-M4 microcontroller and features Qorvo Wi-Fi interference mitigation technology and has an extended range. GP695 complements the multi-protocol GP712, which was released in 2016 for use with smart-home gateways. ■

The GP695 uses an ARM Cortex-M4 microcontroller and features Qorvo Wi-Fi interference mitigation technology and has an extended range.

INTEL ATTEMPTS TO CLEAN SLATE with 5G Modem

OVER THE LAST year, Intel cleaned the slate after failing to sell computer processors at the heart of smartphones. The company ended its mobile processor line, announced around 12,000 layoffs to focus on cloud computing and connected devices, and made wireless modems for smartphones a new priority.

Now the Santa Clara, Calif., company is starting 2017 with an aggressive step to build up its modem business. At the International Consumer Electronics Show in Las Vegas in January, Intel revealed plans to sell a new modem chip for handling 5G wireless communications. Samples will be available starting in the second half of this year, said the company's executives.

Aicha Evans, Intel's vice president of communications and devices, said that the modem chip will deliver downloads around 5 gigabits per second, making it around five times faster than the latest wireless modems and 20 times speedier than the most advanced 4G networks.

The announcement makes Intel the latest chip maker to release 5G hardware even though the wireless standard is far from set in stone. Wireless companies are still hammering out the final version of the technology, which will connect smartphones and other gadgets to 5G networks. Widespread 5G networks are still years out, but the first networks are not expected until 2020.

Verizon has promised to open preliminary 5G networks as soon as this year, and South Korea carriers are trying to deploy networks by 2018. That's because 5G technology will provide major improvements over current wireless technology. For instance, it will allow smartphone users to browse the internet and stream videos much faster and with fewer interruptions.

But device manufacturers need special hardware to tap into them.

Intel is not the only company working to etch 5G features into silicon. In October 2016, Qualcomm revealed its own 5G modem called the X50, which it said would sample in the second half of 2017 and first appear in products in 2018. The modem will

Intel's 5G modem chip will deliver downloads around 5 gigabits per second, making it around five times faster than the latest wireless modems. *(Image courtesy of Intel)*

operate around 5 gigabits per second, Qualcomm executives said at the time.

That performance could be critical to connecting delivery drones, virtual reality headsets, and billions of wireless sensors. These devices need networks that respond quickly and exchange reams of data with the cloud, where it can be pooled and processed by machine learning programs. Intel is the biggest supplier of server chips in data centers.

Intel's new chip, also known as Gold Ridge, contains features that are likely to be included in the final 5G standard. It is designed to coordinate multiple antennas, which shortens the time it takes for devices to send and receive messages, and to steer antenna beams electronically. It also has the ability to access higher frequency bands ignored by current wireless standards.

These features could help factory robots and autonomous cars to talk to each other wirelessly. Intel said that Gold Ridge is part of its new autonomous driving platform, which enables cars to share location information to help make snap decisions about avoiding obstacles. The chip could also send details about a car's surroundings to update online traffic maps.

In a blog post, Evans said that the chip would be used in early trial networks and "to lay a foundation enabling accelerated development of products" that support 5G wireless technology. The modem will grant devices access to a wide array of frequency bands that companies in the United States, Europe, Korea, and Japan are using in trials. ■

Inside TRACK with Kevin Kelly,

CEO, LGS Innovations

The last 20 years have seen the massive adoption of mobile communications and data services by the global user community, a remarkable expansion in worldwide wireless network capacity, and a meteoric rise in the wireless equipment and enabling technology markets. This virtuous cycle has driven both technological innovation and a continuously increasing demand for a decidedly finite resource in this ecosystem: RF spectrum. Microwaves & RF talked with Kevin Kelly, CEO of LGS Innovations, about the evolving trends in this arena.

Interview by CHRIS DeMARTINO, Technology Editor

What are some of the specific challenges associated with today's crowded RF spectrum?

The origins of today's crowded RF spectrum are diverse, and pose real concerns. Spectrum is a finite resource, and not all frequencies are equally desirable. The most desirable frequency bands (VHF, UHF, and the low microwave bands) are already very crowded, and the explosive growth of cellular communications and the Internet of Things (IoT) are driving tremendous pressure for spectrum access.

At the Consumer Electronics Show (CES), an estimated one of three displays pertained to IoT, with devices as diverse as automobiles, washing machines, and wearables featuring embedded wireless transmitters. Considering the possibility of nearly every person having multiple transmitters—many communicating nearly continuously and concurrently—it is easy to see how quickly spectrum is becoming an even more valuable resource.

This resource needs to be utilized in an optimal manner in order to extract every bit of spectrum availability. It requires an approach that allows for the simultaneous dynamic sharing of this resource across the dimensions of frequency, time, physical-layer code, multiple-input, multiple-output (MIMO), multiplexed channel, and/or geography.

More users accessing ever-scarcer spectrum increases overall RF noise and RF interferers. Nulling interferers and reducing noise gets more difficult—both technically and from a policy perspective—in this evolving, heterogeneous spectral environment.

Can you explain some of the concerns of government agencies regarding spectrum usage?

Government agencies that once enjoyed seemingly limitless (and free) spectrum access must now learn to share bandwidth with industry and consumers. The challenges of sharing spectrum are clear, but not trivial. Sharing spectrum means that new RF interference will be present that could negatively impact an agency's mission. Agency managers need to protect their ability to execute upon the mission while allowing other spectrum users to realize the value of their spectrum investment.

As the FCC, NTIA, and other regulatory bodies further outline government/industry spectrum-sharing opportunities and policies, government agencies will find themselves working with industry partners to establish a mutually beneficial partnership. Are their new partners viewing the government agency's mission critically through the same lens and operating in a manner that allows them to execute on their missions? How can they protect themselves if this is not the case? How will new types and levels of RF interference impact their systems? How can they tell who is interfering? Do they need to develop new internal expertise to monitor and manage RF interference?

Safe and effective spectrum sharing requires new systems and technologies. The government should be looking for technologies available to solve this problem, and how they can/should procure this technology.

For our military, compliance with U.S. spectrum allocations is only a small part of the problem. Military radars, communications, sensors, and weapon systems must maneuver within and around spectrum, which is allocated differently around the world.

For example, a Navy ship training off the U.S. coast must comply with U.S. spectrum allocations, but must also adapt to different allocations, laws, and policies (or the absence thereof) when operating in other parts of the world. A ship may operate in dozens of international spectrum-regulated areas on a single deployment, and may be limited or restricted in its use of sensors and systems that are essential for their missions and self-defense.

Moreover, these spectrum-management issues are mission-critical. Adversaries knowing our spectrum allocations or limitations can target their use of specific bands to detect, jam, spoof, or otherwise disable our defense systems.

Can you describe spectrum-management solutions?

Conventional spectrum management is generally a static process. Users are assigned exclusive rights to bands of frequencies to be employed in specific geographical regions. In this model, the main strategy for sharing spectrum is to partition the available spectrum into finer and finer spectral swaths. This forces industry to develop more efficient modulation schemes, where more bits of data can be transported per unit of frequency (hertz). Although many modulation techniques have been developed over the past 20 years, we are rapidly approaching the number of bits per hertz that can be transported efficiently.

Once allocations are set, spectrum management is composed of verification and enforcement of allocations in a rather manual fashion. One example of this could be a government agency employing a manual, human-intensive RF interference hunting approach using only the most basic tools, such as spectrum analyzers and large form-factor directional finding tools. Their goal would be to identify and locate violators of spectrum access agreements, and then apply appropriate regulatory methods to protect their spectrum from interference.

This approach does not scale well with large numbers of competing users interfering with each other, and would render reliable communication of data impractical.

A better, more sustainable solution for spectrum management should feature highly concurrent, dynamic, seamless, and at least semi-autonomous (if not fully self-governing) allocation of the spectrum for multiple competing users with different data-capacity and data-traffic requirements. The cognitive sensing of actual spectrum usage in real time will prove a key enabler of autonomous network awareness and bandwidth management.

Proactive and dynamic spectrum awareness and management approaches such as this will require three components:

- First, new methods are needed to monitor spectrum utilization with enhanced resolution over multiple resource dimensions (e.g., frequency, time, space, and signal analysis) in order to provide dynamic awareness of the RF environment.
- Next, dynamic spectrum access and monitoring techniques will enable multiple competing users to efficiently and safely exchange data.
- Third, techniques and algorithms are needed to facilitate multi-dimensional, autonomous resource allocation.

By applying these new methods for spectrum monitoring, dynamic spectrum access, and resource allocation, a scaled solution for spectrum management can avoid excessive "human-in-the-loop" requirements while allowing for enforcement of spectrum access agreements.

Tell us about the software that enables spectrum management.

Spectrum management covers a diverse set of applications and requires an equally diverse set of software technologies. To succeed in a crowded RF environment, a spectrum-management system will need to assess the behavior of relevant emitters. This involves using signal processing to identify and characterize RF sources; eliciting the frequency usage and temporal patterns of those sources; and perhaps demodulating and decoding the signals to extract information for understanding the environment.

The increasing complexity of RF systems requires spectrum-management systems become increasingly intelligent to detect and track the behavior of the systems emitting in the environment. This "pattern of life" analysis enables prediction of system behavior and determination of how best to achieve mission objectives. Rules-based processing, efficient database-management techniques, and machine-learning methods will be necessary to accomplish this goal.

In addition to monitoring emitters in the environment, many spectrum-management applications (i.e., aboard ship or aircraft) might carry responsibility for managing their own emitters. This can require scheduling algorithms, optimization techniques, and in some cases, collaboration with other systems in the environment. Generally, spectrum-management systems have to be adaptive, flexible, robust enough to react to unexpected changes in the environment, and able to work in real time.

Spectrum-management software solutions must be modular, scalable, and distributable, with the capacity and flexibility to support and integrate with small, embedded sensor systems as well as large, dispersed "systems of systems" involving thousands of complex sensors. Similarly, spectrum-management systems will need to interface with current and future standards-based infrastructure. Consequently, many systems-level features must be built into a spectrum-management solution, including the ability to tailor and adapt the user interface/user experience and ensure compliance with security and secure networking protocols and standards.

(Continued on page 80)

CREATE AN EM MODEL for a Human Head

CONCERN FOR THE growing use of wireless devices, such as mobile phones, that expose a user's head to electromagnetic (EM) field energy has motivated a number of studies on the effects of EM radiation on the brain. An important part of that research is to develop accurate models of the human head for simulating the effects of EM radiation on human tissues.

One research team has created a human-head model for studying the effects of different EM specific absorption rates (SARs) on the human brain. This high-resolution model allows for accurate simulation of 49 different tissues and organs within the human head. It is hoped that work with the model will lead to the design of safer multiple-band antennas for wireless electronic products.

Research on the EM head model was performed by investigators mainly in China, but also in the United States. The engineering team consists of Lei Zhao, director of the Center for Computational Science and Engineering and associate dean of the School of Mathematics and Physics of Jiangsu Normal University of China; Qin Ye, a visiting scholar at the School of Biology of Jiangsu Normal University of China; Ke-Li Wu, a professor at The Chinese University of Hong Kong; Geng Chen, a visiting student at the Center for Computational Electromagnetics at the University of Illinois; and Wenhua Yu, a visiting professor at Jiangsu Normal University of China and director of the Jiangsu Big Data Key Lab for Education Science and Engineering.

The new human-head model is meant to provide further insights into EM exposure levels from such devices as closely held cellular phones, in addition to the calculated SARs used by various regulatory bodies for determining safe EM exposure limits.

This first Chinese EM human-head model (CMODEL) was developed at The Third Military Medical University and the Chinese University of Hong Kong, initially based on photographs of a female human head. Great attention was paid to preserve the integrity of different structures and materials, such as teeth, within the head model.

Cross-sectional imaging and measurements were used to identify the different visible biological tissues. Data on a large number of tissues were provided by the U.S. Federal Communications Commission (FCC), including fat, muscle, grey matter, cartilage, blood, and spinal-cord nerve tissue. Different colors were used in the head model to identify the energy paths for different tissues.

To validate the head model, three versions with different dimensions were developed and subjected to EM energy from a dual-band mobile-phone antenna operating at 900 and 1,800 MHz. The final model achieved a resolution of $0.16 \times 0.16 \times 0.25$ mm^3 for the head and $0.16 \times 0.16 \times 0.5$ mm^3 for the shoulder. The electric properties of the tissues in this model, which includes highly detailed sub models for eyes and ears, exhibit the same properties as the properties of tissues for SAR assessment, as published by the FCC. It represents another valuable tool in studying the effects of short-range EM radiation on wireless-device users.

See "A New High-Resolution Electromagnetic Human Head Model," *IEEE Antennas & Propagation Magazine*, Vol. 58, No. 5, Oct. 2016, p. 32.

SCAVENGING ENERGY from 800-MHz Wireless Sources

ENERGY IS A valuable resource that can be harvested from many different sources, including from wireless radio signals. Armed with an efficient rectenna, which is a combination of an antenna and a rectifying circuit, an electronic device can literally extract dc power from the air, so as to power an electronic device and/or recharge its batteries.

As part of the recent International Microwave Symposium (IMS) student design competition for wireless energy harvesting, students were invited to share their design efforts on developing rectennas for use at different wireless frequency bands. Valentina Palazzi of the University of Perrugia and Massimo Del Prete and Marco Fantuzzi of the University of Bologna, both in Italy, rose to the challenge. They developed a broadband rectenna with 25% bandwidth centered at 800 MHz (700 to 900 MHz).

The student engineers experimented with the mechanical configuration of the antenna design, choosing a planar antenna with a tapered slot for broad impedance bandwidth and low losses. With the aid of CST Studio Suite electromagnetic (EM) simulation software, the students were able to simulate and optimize the performance of the planar antenna design to achieve a fractional bandwidth of 22.3%.

The planar antenna, with dimensions of $130 \times 140 \times 0.254$ mm^3, provides maximum gain of 3.6 dBi across the operating bandwidth with input power levels of –10 to 0 dBm. Maximum efficiency is 65%. To complete the rectenna, a number of different commercial diodes were considered for the rectifier circuit design. Once diodes were selected, matching circuits were developed for an efficient connection to the antenna, and multiple measurements were made to confirm that prototype performance was fairly close to computer-simulated performance.

See "Scavenging for Energy," *IEEE Microwave Magazine*, Vol. 18, No. 1, Jan./Feb. 2017, p. 91.

HAND FLEX™ CABLES

Hand Flex Cables conform to any shape required.

from $9.75 ea. (qty.1-9) DC to 18 GHz

Get the performance of semi-rigid cable, and the versatility of a flexible assembly. Mini-Circuits Hand Flex cables offer the mechanical and electrical stability of semi-rigid cables, but they're easily shaped by hand to quickly form any configuration needed for your assembly, system, or test rack. Wherever they're used, the savings in time and materials really adds up!

Excellent return loss, low insertion loss, DC-18 GHz. Hand Flex cables deliver excellent return loss (33 dB typ. at 9 GHz for a 3-inch cable) and low insertion loss (0.2 dB typ. at 9 GHz for a 3-inch cable). Why waste time measuring and bending semi-rigid cables when you can easily install a Hand Flex interconnect?

Two popular diameters to fit your needs. Hand Flex cables are available in 0.086" and 0.141" diameters, with a tight turn radius of 6 or 8 mm, respectively. Choose from SMA, SMA Right-Angle, SMA Bulkhead, SMP Right-Angle Snap-On and N-Type connectors to support a wide variety of system configurations.

Standard lengths in stock, custom models available. Standard lengths from 3 to 50" are in stock for same-day shipping. You can even get a Designer's Kit, so you always have a few on hand. Custom lengths and right-angle models are also available by preorder. Check out our website for details, and simplify your high-frequency connections with Hand Flex! *RoHS compliant*

SMA SMA Right Angle SMA Bulkhead SMP Right Angle Snap-On N-Type N-Type Bulkhead

Mini-Circuits®

www.minicircuits.com P.O. Box 350166, Brooklyn, NY 11235-0003 (718) 934-4500 sales@minicircuits.com

Product Trends

PETRA HAMMES | Principal Characterization Engineer, Ampleon
STEVE LOYSEL | Principal RF Applications Engineer, Ampleon
MAREK SCHMIDT-SZALOWSKI | RF Modeling Engineer, Ampleon
NELSY MONSAURET | Modeling Engineer, Ampleon
JOS VAN DER ZANDEN | RF Engineer, Ampleon
www.ampleon.com

A Robust, Large-Signal Model for LDMOS RF Power Transistors

Accurate empirical LDMOS transistor models are critical to achieving first-pass design success.

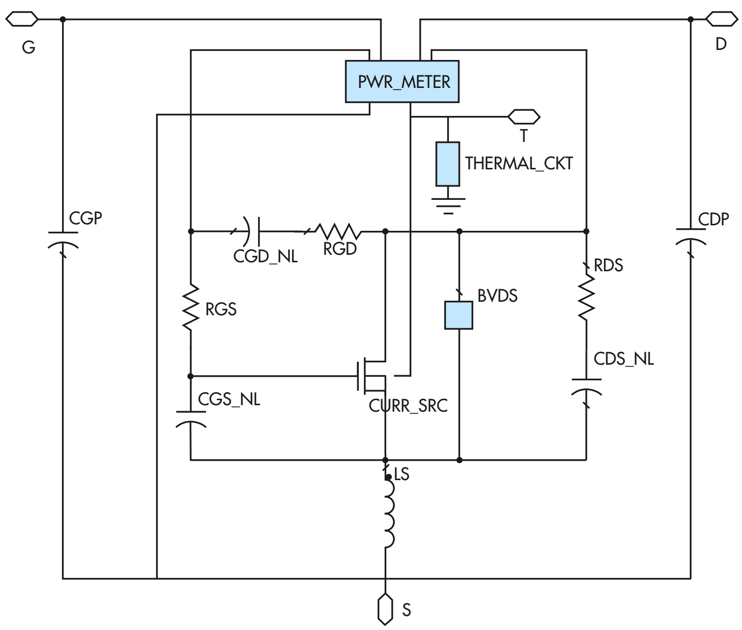

1. This is a top-level representation of the model, with gate, drain, and source terminals as well as the thermal node.

2. Shown below are pulsed and non-pulsed IV curves at room temperature.

WHEN MODELING TRANSISTOR behavior, models generally divide into three categories: physical, empirical, and behavioral. Each has its own advantages and disadvantages, making it more or less suitable for modeling different types of transistors for different applications.

The physical model is at one side of the spectrum. Although it is complex, it relates to the physics and layout of the device. Thus, the physical model generates physical insight and is inherently suitable for statistical analysis. At the other side of the spectrum is the behavioral model, a black box that is easily extracted and represents measured data (S-parameters or X-parameters).

A compromise in terms of functionality, ease of extraction, and robustness is offered by the empirical model. It is generally some form of compact model with physical components described by non-physical fitting functions. The suitability of this model to describe the performance in the region outside of where the model was extracted depends both on the extraction method and the formulas used in the model.

Ampleon (*www.ampleon.com*) has chosen to develop its own empirical models for the newest LDMOST tech-

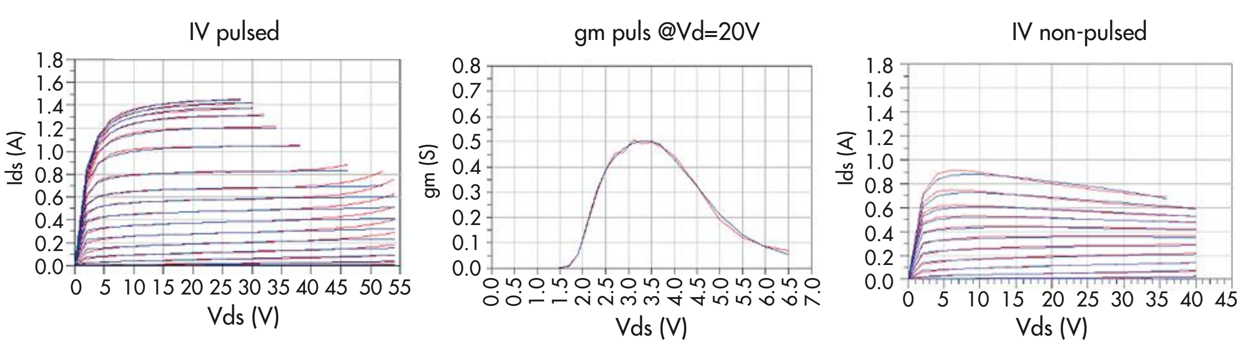

nologies. This development has been driven by the fast time-to-market needs of these models, which are intended to provide accurate simulation results for the targeted applications.

Ampleon LDMOST technology is primarily aimed at base-station applications. In the early days, LDMOST operated in Class AB in feed-forward systems. Today, two- or three-way Doherty amplifiers in combination with digital pre-distortion (DPD) systems are the norm for efficient base stations. To enable accurate modeling of the Doherty configuration, modeling the Class C behavior of the LDMOST is crucial. Therefore, a focus was placed on this aspect while extracting and generating the new model.

This article describes the extraction and performance of the core model. Three power amplifiers (PAs) in a Doherty configuration are then simulated. The results are shown to illustrate the model performance and usability of these models for a Doherty design.

EXTRACTION FLOW AND METHODOLOGY

The extraction flow is based on current-voltage (IV) curves over temperature, S-parameters, and large-signal RF performance in the region where the model should describe the transistor behavior accurately. The current source, extrinsic parasitics, and intrinsic parasitics are then extracted *(Fig. 1)*.

All measurements are performed on wafer. Thus, the de-embedding needed to obtain the response of the LDMOST by itself is minimized. Measuring an unpackaged transistor does limit the size of the LDMOST that can be measured. Ground-signal-ground RF probes, which are needed for accurate measurements, are limited in terms of current- and power-handling capability. Typical gate peripheries of around 6 mm have been used, keeping the number of fingers greater than two in order to avoid extraction of a model based on end-fingers only.

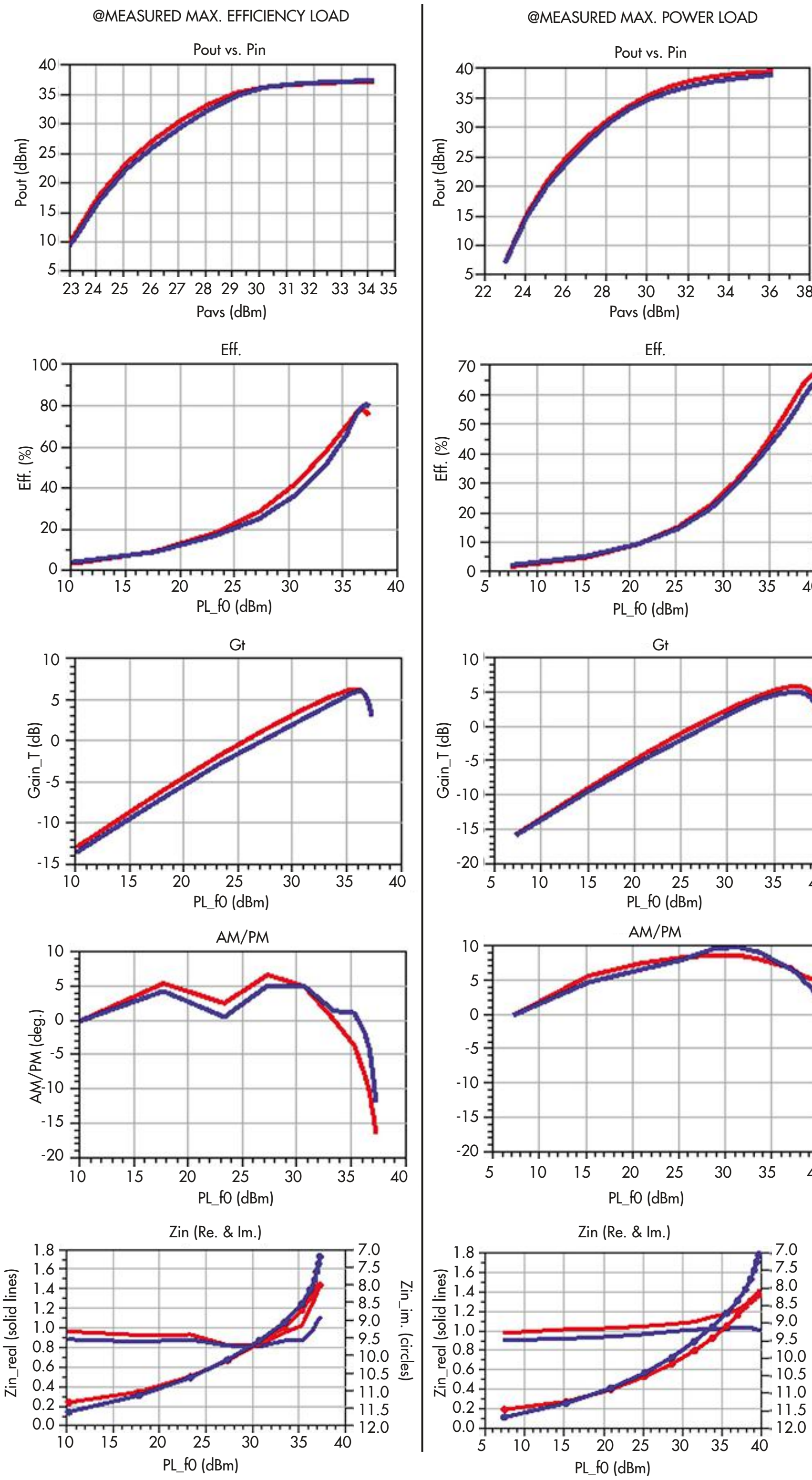

3. This image illustrates Class C pulsed RF performance at 2.5 GHz with maximum efficiency (left) and maximum power load states (right), with measured results in red and simulated results in blue.

from $139.95 (qty. 1-9)
Rugged connectorized package
0.75 x 0.74 x 0.46"

from $11.95 (qty. 20)
3x3 mm MMIC

0.5 to 8 GHz
LOW NOISE AMPLIFIERS
IN/OUT Termination Matched!

Low noise, high dynamic range, high output power, and flat gain from 0.5 to 8 GHz, all in a single amplifier! Mini-Circuits' popular ultra-wideband LNAs are now available in both a 3x3mm QFN for your PCB and a rugged connectorized package to facilitate your cable assemblies. Both models are matched over the 0.5 to 8 GHz range*, making them a snap to use for sensitive, high-dynamic-range receivers, instrumentation, defense systems, LTE, WiFi, S-Band and C-Band radar, SatCom and more! They're available off the shelf for a great value, so visit minicircuits.com and place your order today for delivery as soon as tomorrow!

FEATURES:
- *Low Noise Figure, 1.3 dB*
- *High Gain, 21 dB*
- *Excellent Gain Flatness, ±0.7 dB†*
- *High IP3, +35 dBm*
- *High POUT, +23.2 dBm*

*See datasheet for suggested application circuit for PMA3-83LN+
†Flatness specified over 0.5 to 7 GHz

Mini-Circuits®

www.minicircuits.com P.O. Box 350166, Brooklyn, NY 11235-0003 (718) 934-4500 sales@minicircuits.com

553 revOrig

During the model extraction, stringent specs are placed on IV performance, S-parameter accuracy at multiple bias points, and final RF performance accuracy with regard to gain, efficiency, and impedances. When these conditions are met, the model can be successfully used for monolithic microwave integrated-circuit (MMIC) design, as well as for discrete power Doherty designs.

In addition, designers and customers can request a special version of the model. With this version, the internal current source (the center of the model in Fig. 1) can be accessed to monitor the internal current and voltage waveforms.

DC VALIDATION

The formulas of the current source are fitted utilizing both non-pulsed and pulsed IV measurements over temperature. Measurements are performed using AMCAD Engineering's *(www.amcad-engineering)* PIV-240-10 pulsed IV solution. In addition, the thermal model, which describes the thermal behavior of the device, is extracted. A multi-section thermal circuit is implemented to capture the thermal time constants in the device.

For large RF power transistors in a package, the thermal behavior is largely dominated by the thermal characteristics of the die's surroundings. Therefore, the internal thermal circuit can be negated by an external thermal circuit.

The formulas in the current source of the model have been optimized in such a way as to accurately represent the currents in Ampleon's three latest 28-V LDMOST technologies, as well as in its 50-V LDMOST technology. *Figure 2* demonstrates the general fit of all IV curves after fitting the current source parameters.

Due to the non-physical nature of the model, a complete new extraction needs to be done for each new technology. There are no physical parameters in the model that can reflect the process change. However, as stated in the introduction, time-to-market of a model is quite fast for these models, since measurement and extraction of the model is much less complicated compared to physical model extraction.

S-PARAMETER VALIDATION

The wideband pulsed S-parameters are measured at several bias points covering the total IV plane. The PIV-240-10 is used in combination with an N5242 PNA-X network analyzer for these measurements.

The extrinsic and intrinsic parasitics are extracted and the voltage dependence on the intrinsic parasitics is determined. The modeled trends in the S-parameters over all bias points are verified. Special attention is paid to the Class C and AB bias points.

LOAD-PULL VALIDATION

Load-pull measurements are used to validate the compact transistor model with the proper load terminations for optimal RF performance. The impedances presented to the transistor are varied in such a way that the generated load plane includes the maximum efficiency and the maximum power load states. A comparison is made between measured and modeled RF performance. To obtain an overall good fit for both small- and large-signal performance of the model, the extrinsic and intrinsic parasitics are fine-tuned in an iterative optimization process.

Measurements are performed using Maury Microwave's *(www.maurymw.com)* MT2000 active load-pull system. In the system at Ampleon today, the fundamental- and second-harmonic source and load terminations can be controlled, while the third-harmonic terminations are only measured. To keep the accuracy of the measured environment, these measured fundamental-, second-, and third-harmonic terminations are presented to the model

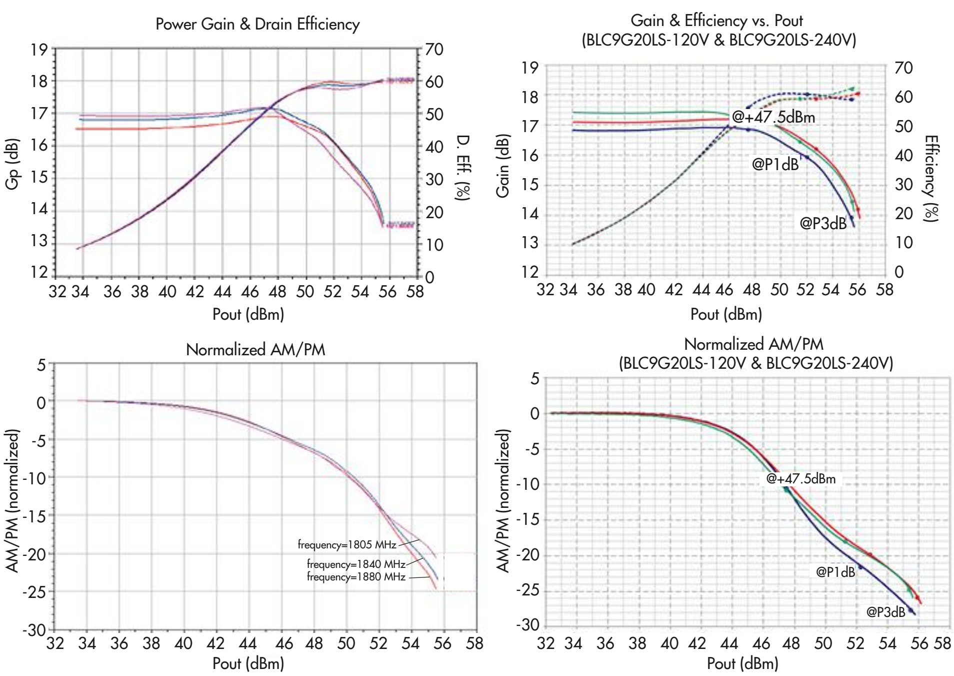

4. Shown is the RF performance of the 3-way Doherty amplifier from 1,805 to 1,880 MHz. Both simulated (left) and measured (right) transducer gain, efficiency, and AM/PM conversion are shown.

(Continued on page 40)

(Continued from page 36)

when comparing the measured and the modeled RF performance.

Special emphasis is placed on the actual frequency of operation of the transistor during extraction. However, a wider frequency range is also verified. Stringent specs are again placed on the RF performance of the model.

Performance is verified for Class AB bias (V_d = 28 V) and for Class C bias (V_g = 0.3 V, V_d = 28 V). Gain, efficiency, power, AM/PM, as well as input impedance are verified at the maximum efficiency and maximum power load states. *Fig. 3* illustrates the results for Class C operation. Furthermore, a tradeoff occurs between the simulated load-pull contours and the power efficiency.

The model performance is verified over a wider frequency range, demonstrating good behavior for both Class AB and Class C operation. Optimal load impedances are predicted by the model and the input impedance is modeled accurately. This very good prediction of the active device will allow designers to generate amplifier products—both discretes and MMICs—as described in the next sections.

3-WAY DISCRETE DOHERTY DESIGN MODELING

Combining the core model with bond-wire and package models enables the generation of accurate models of packaged power RF transistors. This led to the design of a 3-way Doherty.

The model of the BLC9G20LS-120V transistor assesses the feasibility of a 3-way Doherty with high performance in the frequency band from 1,805 to 1,880 MHz. Matching of the transistor is realized with ideal microstrip lines. Some realistic losses are added in order to characterize insertion losses on a standard printed-circuit board (PCB). The fast simulation time of this model made it possible to fine-tune the amplifier for maximum performance.

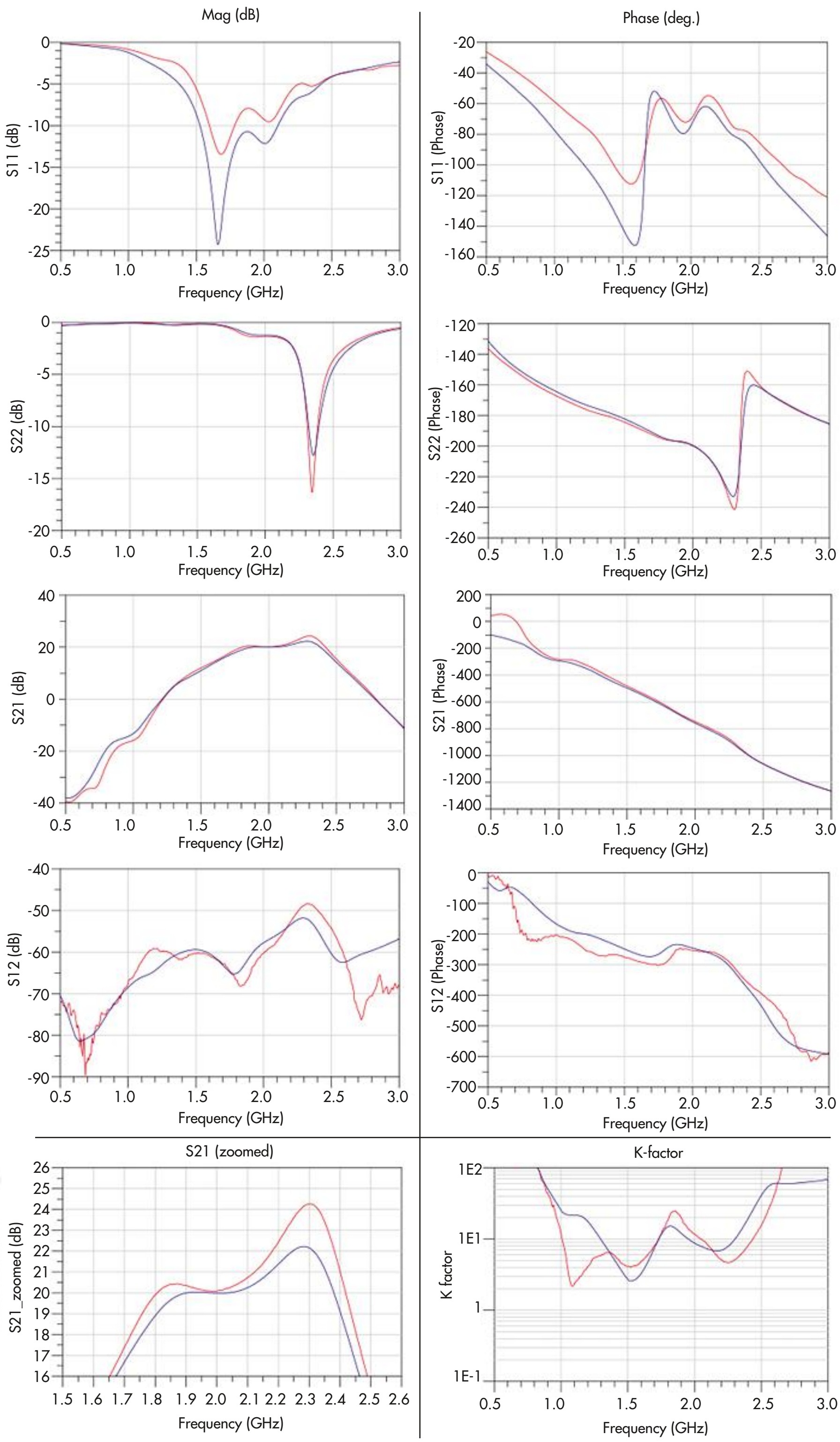

5. These plots depict the small-signal behavior over a broadband frequency range of an integrated Doherty MMIC at bias conditions of 28 V and 90 mA. Measured results are in red; simulated results are in blue.

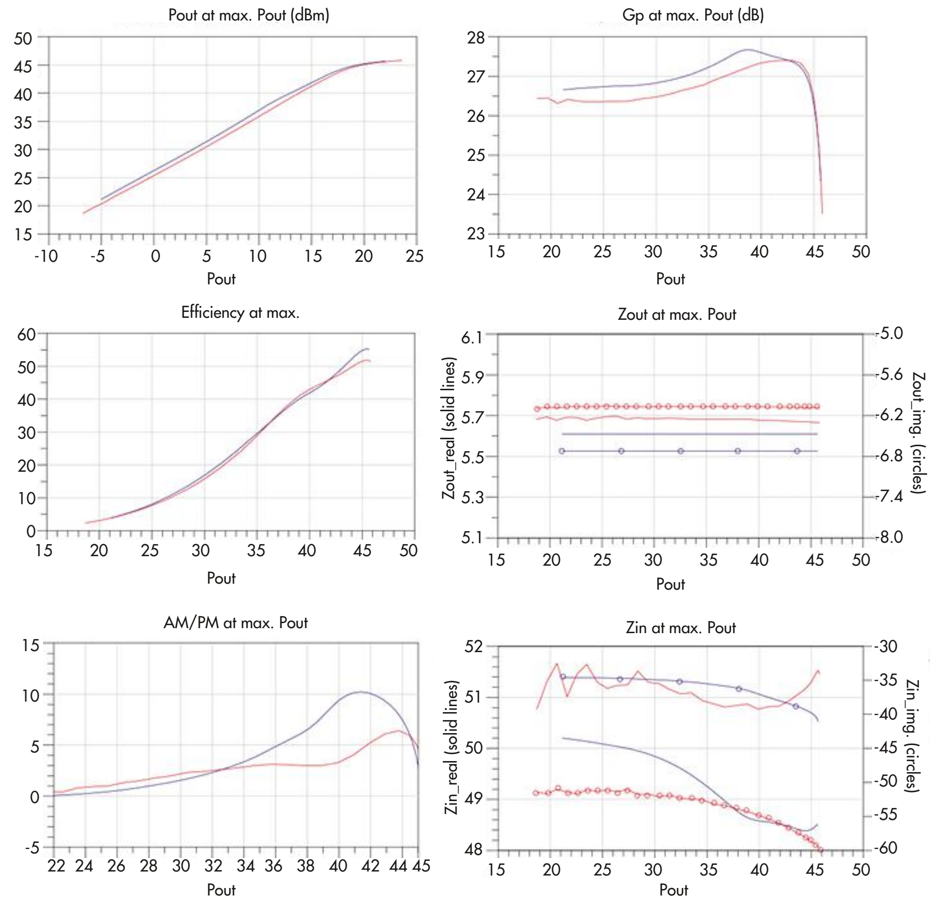

6. Shown is the RF performance at 2.14 GHz for the maximum power load impedance of an integrated Doherty MMIC at bias conditions of 28 V and 100 mA (carrier). Measured results are in red; simulated results are in blue.

The output combiner and input splitter are added to simulate the complete Doherty behavior. The peaking amplifiers are biased to attain the desired turn-on. The input phase is adjusted so that the three branches are able to power-combine in phase.

This Doherty architecture has been implemented in a real circuit with the BLC9G20LS-120V transistor used to create the main amplifier. Meanwhile, the BLC9G20LS-240PV transistor is used to create both peaking amplifiers in a push-pull package.

Figure 4 shows both simulated and measured gain, efficiency, and AM/PM. It can be seen that the behavior is very similar and the absolute values are also quite close. This validates that the device model is suitable to study a complex architecture like a 3-way Doherty.

2-GHZ INTEGRATED DOHERTY MMIC MODELING

In addition, using passive MMIC components that have been validated in a separate process allows designers to derive an integrated Doherty MMIC, such as the BLM8D1822S-50PBG, with a very good level of predictability. This capability is illustrated in *Figs. 5 and 6* for small- and large-signal operation, respectively.

A good match between modeled and measured data is observed for both ON and OFF states in small-signal operation, with special attention given to S_{22} and K-factor prediction. The same level of correlation is obtained in large-signal operation, taking into account parameters like gain, efficiency, output power, and AM/PM while also looking at input and output impedance prediction.

CONCLUSION

Compact transistor modeling is the most crucial step in a successful design flow. It can lead to first-pass design success and faster time-to-market when used in conjunction with circuit simulators. Ampleon's new empirical LDMOST model has proven to be very accurate. The IV behavior over temperature is characterized well, as are predictions for the S-parameters. While main emphasis is placed on the S-parameters at Class AB and C bias points, S-parameters are well characterized at different bias points, too.

Characterizing the load-pull behavior at RF frequencies is most important. The model is optimized for several frequency ranges of application, satisfying stringent specs with regard to gain, efficiency, power, and impedance levels. Other important qualities of the model are its ease of extraction and its robustness with the ADS and Microwave Office circuit simulators. The Ampleon model is therefore suitable for modeling high-power discrete designs, as well as medium-power MMIC designs. The model is especially well-suited for Doherty amplifiers because of its high level of Class C prediction.

As was shown, the AM/PM prediction of the model is quite accurate. The model also predicts distortion very well when excited by two tones. Investigations are still ongoing in this area. Harmonic load-pull accuracy is under examination as well.

Lastly, breakdown phenomena are currently only implemented very crudely into the model. This is another area to be investigated in the future. mw

JACK BROWNE | Technical Contributor

Basics of Modulation and Demodulation

Radio waves can carry audio, video, and digital information over great distances by using changes in a carrier wave's amplitude, frequency, or phase to represent the information being transmitted.

INFORMATION CAN BE sent from a transmitter to a receiver by means of modulation and demodulation, respectively, whether those signals are light waves moving through optical cables, radio waves through metallic cables, or radio waves propagating through the air. The electromagnetic (EM) waves that transport the information are referred to as carrier signals, while the information they carry may be in the form of audio, video, or data.

By changing the amplitude, frequency, or phase, or a combination of the three signal characteristics, information can be added as modulation to a signal. Due to the increased amount of information for transmission and reception, signal-modulation techniques have advanced in their capabilities to handle more data for a given amount of occupied bandwidth, although they have also grown more complex in the process.

Modulation of a radio wave can be performed by varying one or more of its signal components—amplitude, frequency, or phase—while keeping its other signal components constant. (Pulse modulation is yet another form of modulation, without a carrier, in which pulses with precisely known characteristics are transmitted and details can be learned about a target by receiving the reflected pulses from the target.)

AM & FM

The simplest form of carrier modulation, amplitude modulation (AM), has long been the basis for sending audio information to listeners with radios operating at carrier frequencies from about 535 to 1,605 kHz in the commercial broadcast band. AM is also used for maritime communications and navigation, as well as aircraft navigation, at carrier frequencies from 30 to 535 kHz.

In AM radio broadcasts, the amplitudes of the lower and upper sidebands of the center frequency of a broadcast channel are modulated with the audio content from a radio station, to be demodulated at the receiver of a listener. The lower and upper sidebands extend out from the carrier frequency, usually occupying a total bandwidth of about 25% around the carrier frequency. The audio content from a received AM radio wave can be recovered or demodulated by using a diode to rectify the signals and extract the audio content, or else via filtering to separate the high-frequency carrier signal from the audio content.

In frequency modulation (FM), the frequency of the carrier signal is varied as a function of the message or information. As with AM, audio content is the most commonly transmitted information using FM, such as in commercial FM broadcast radios operating on channels from 88 to 108 MHz. FM can be created by applying message signals directly to a voltage-controlled oscillator (VCO), so that the VCO's output will be a function of the input signal.

Phase-modulation and -demodulation techniques are more complex than modulation and demodulation based on amplitude and frequency. However, they provide the benefit of higher data rates for the amount of bandwidth consumed. Phase modulation is the basis for many digital modulation formats, in which a modulated signal is divided into in-phase (0 deg.) and quadrature (90 deg.) signal components. In contrast to sending video or audio information, digitized information can be easily transmitted by means of digital modulation formats since the modulated information need not be sent continuously in time, but rather can be sent in bursts or staggered with time and reconstructed at the receiver and demodulator.

KEYING IN ON DIGITAL MODULATION

Digital modulation relies on digital signal processing, such as digital-to-analog converters (DACs) at a receiver and analog-to-digital converters (ADCs) at a transmitter to transform analog information (e.g., audio or video) into a digital form that can then be represented by varying the characteristics of a carrier wave. The three fundamental types of digital modulation—amplitude-shift-keying (ASK), frequency-shift-keying (FSK), and phase-shift-keying (PSK) modulation—use changes in amplitude, frequency, and phase to represent digital bits "0" and "1."

In ASK, the signal amplitude is varied as a function of the information to be transmitted, and all other parameters of the signal remain constant. When sending digital information, one amplitude represents a 0 digital bit while a higher or lower amplitude represents the 1 bit. Waveforms with ASK have the rapidly changing amplitude levels representing a digital bit stream.

In FSK, two different frequencies are used to represent the digital 0 and 1 values. The shift in frequencies in FSK is implemented in different ways, notably in a noncoherent or coherent format. In noncoherent FSK, discontinuities exist between the frequencies that represent the digital bits. Termed "mark" and "space" frequencies, they are used as kinds of frequency gaps to separate the bit-representing frequencies. In coherent FSK, the changes in bit-representing frequencies are instantaneous, without phase discontinuities between the frequencies.

In PSK, the phase of the carrier is discretely changed to denote the different digital bits. The phase can be changed in relation to a reference phase, such as using 0 deg. for a 0 digital bit and 180 deg. to represent the digital 1 bit, or if a difference of 180 deg. is used to denote different digital bits, one of the bits may be represented by a relative phase of –90 deg. and the other by +90 deg. In such a simple, biphase modulation format, the two phase angles of the carrier represent two digital bits of information, so that the modulation rate is equal to the bit rate. But if a greater number of phase angles is used, the bit rate can be increased in parallel with an increasing number of phase angles.

In a quadrature phase-modulation format such as quadrature phase shift keying (QPSK), where four phase angles are used to represent the digital bits, two bits of digital information are able to be carried with each phase angle, so that the information can be represented as 00, 01, 10, and 11. Similarly, if eight phase angles are employed in the phase-modulation scheme, then three digital bits can be represented by each of eight possible phase angles. In turn, the bit rate will increase as the number of phase angles grows in the phase-modulation scheme.

As a result, many digital-modulation formats based on changes in phase attempt to represent the greatest number of digital bits possible by variations in phase, so as to support the highest bit rates possible. This performance parameter of a modulated waveform, spectral efficiency, refers to the number of bits that can be transmitted during a given period of time and for a given portion of bandwidth, usually measured as b/s/Hz.

ASK can be affected by nonlinearities in a system—for example, any form of nonlinear distortion like nonlinear amplification—so it is essential that components with extremely linear performance be used to preserve the amplitude characteristics of a transmitted and received signal.

FSK, on the other hand, requires high frequency stability in a system's signal sources, such as VCOs used for local oscillators (LOs) in receivers and transmitters. To maintain high frequency stability, oscillators in FSK systems are typically stabilized by means of phase-locked loops (PLLs) to synchronize the frequency and phase of the system's frequency sources to a common reference source. In addition, PSK depends on tight phase tolerances in a system, such as the lengths of transmission lines, whereby variations can mean increasing phase errors with increasing transmission frequencies. mw

EDITOR'S NOTE: This is part one of a two-part article on the basics of modulation and demodulation. The next installment will examine some of the more complex forms of digital modulation, and explain the use of the time domain and pulsed signals in systems employing pulse modulation (e.g., military radars and automotive collision-avoidance systems). Part 2 will also review the types of hardware needed for each type of modulation/demodulation format, and which modulator/demodulator performance parameters are most critical to achieving good communications-systems performance with high spectral efficiency.

MICHAEL DALTON | Product Marketing Manager, Analog Devices
www.analog.com

IoT Growth Banks on Reliable Communication

To meet the needs of the Industrial Internet of Things (IIoT), communication systems must demonstrate a high level of reliability while maintaining low costs.

ACCORDING TO TECHNOLOGY industry researcher Gartner, the number of "things" in the Internet of Things (IoT) increases by 5.5 million each day. By 2020, the total number is expected to reach 20.8 billion. Given such explosive growth, it's imperative to examine the internet that will connect and enable communication between all of these things. Creating reliable wireless connectivity among devices is proving to be one of the IoT's greatest challenges.

The reliability of a communications system can be defined by the performance of two critical components: a radio transceiver and a communications microcontroller. This article discusses how components and solutions are able to maximize system-level reliability, enabling high-impact applications that provide mission-critical quality and integrity of data and insights.

Smart factories have the potential to significantly enhance manufacturing across all industries.

WHAT'S GOOD NOW IS NOT GOOD ENOUGH

Existing wireless-connectivity technologies for consumer devices do not always satisfy the performance demands of industrial and healthcare systems. The different priorities in these systems—including safety, accuracy, and time-sensitivity—heighten the need for increased reliability. Cellular systems come close, but are often unsuitable in terms of battery, cost, and data-throughput requirements.

Extremely reliable systems exist today for niche industrial and military applications. However, these are designed with reliability being the top priority and cost appearing further down the list. With the Industrial Internet of Things (IIoT), the challenge becomes delivering the same high level of reliability at a much lower system cost.

Let's consider several scenarios in which wireless capability was added to enhance the effectiveness of a system and mission-critical reliability of connectivity:

Smart Factory: Production Process Control for Industry 4.0

Connected devices are attractive in the manufacturing arena due to the potential improvements in overall yield. To achieve this, it is often necessary to gain remote control of various devices in the production chain to implement adjustments. An example is a control valve for a boiler operating in a chemical production process. Immediate and autonomous control of this valve can make real-time adjustments based on feedback from other stages in the process, leading to more optimized overall efficiency.

Smart Healthcare: Vital Signs Monitoring

Hospitals and care centers are looking to wireless connectivity to monitor patient vital signs. Clunky wired solutions can be replaced with wireless sensor patches connected through a local gateway. Such systems enable more effective patient monitoring while reducing the burden on healthcare staff.

Smart City: Event Sensing for Emergency Response

With advanced image and acoustic sensing and processing methods, systems mounted in public spaces (for example, on lampposts) can detect events like vehicle accidents and criminal activity with a high degree of confidence. This information can be relayed via wireless communications to the appropriate agency or unit, along with the location information, thus quickening the emergency response.

Ultra Small 2x2mm

2W ATTENUATORS DC-20 GHz from $1.99 ea.(qty. 1000)

Save PC board space with our new tiny 2W fixed value absorptive attenuators, available in molded plastic or high-rel hermetic nitrogen-filled ceramic packages. They are perfect building blocks, reducing effects of mismatches, harmonics, and intermodulation, improving isolation, and meeting other circuit level requirements. These units will deliver the precise attenuation you need, and are stocked in 1-dB steps from 0 to 10 dB, and 12, 15, 20 and 30 dB.

The ceramic hermetic ***RCAT*** family is built to deliver reliable, repeatable performance from DC-20GHz under the harshest conditions. With prices starting at only $4.95 ea. (qty. 20), these units are qualified to meet MIL requirements including vibration, PIND, thermal shock, gross and fine leak and more, at up to 125°C!

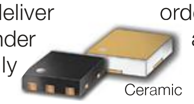

The molded plastic ***YAT*** family uses an industry proven, high thermal conductivity case and has excellent electrical performance over the frequency range of DC to 18 GHz, for prices starting at $2.99 ea. (qty. 20).

For more details, just go to minicircuits.com – place your order today, and you can have these products in your hands as soon as tomorrow!

RoHS compliant

FREE Simulation Models! Modelithics®

http://www.modelithics.com/mvp/Mini-Circuits/

Mini-Circuits®

www.minicircuits.com P.O. Box 350166, Brooklyn, NY 11235-0003 (718) 934-4500 sales@minicircuits.com

515 rev E

Wireless communication systems simplify the monitoring of patients in hospitals.

CHALLENGES IN BUILDING RELIABLE WIRELESS CONNECTIVITY IN COMPLEX ENVIRONMENTS

RF Obstacles Cause Missed Packets

Each of the examples mentioned above is subject to distinct environmental challenges that can negatively affect wireless communication. For example, the steel construction and thick walls of factories create large obstacles that may degrade the power of an RF signal to the point where it cannot be received by the target device. The sensitivity of the radio receiver used in the target device will determine the tolerance level of signal degradation. A change in sensitivity that is as low as 2 dB could be the difference between successful or unsuccessful reception of a signal. Communication-system designers must pay close attention to receiver sensitivity when selecting a radio.

Crowded Frequency Bands Cause Missed Packets

Connected devices will typically operate in the relevant industrial-scientific-medical (ISM) band for a given region. ISM bands are license-free and can be used for a wide range of applications that require wireless connectivity. The 2.4-GHz band is standardized globally and extensively used by Wi-Fi and Bluetooth devices. ISM spectrum is also available in sub-1-GHz bands—a common destination for IoT applications. The sub-1-GHz band is centered at 868 MHz in Europe and 915 MHz in the U.S.

A challenge arises when multiple devices located in close proximity share the same ISM band. Transmitting devices can interfere with nearby receiving devices, such as in public hospitals that have multiple machines within the same ISM band. A radio's ability to function properly in the presence of such interferers is measured by the blocking specification.

However, the challenge extends beyond devices operating within the ISM band. Without sufficient blocking capability, mobile phones or tablets operating nearby could cause a loss of communication in the system. In military and aerospace applications, very costly components are incorporated to mitigate the effect of interferers. Radios being used for mission-critical data, such as the applications mentioned, must achieve similar performance to military and aerospace without incurring the high cost of additional external components. Such radios will continue to receive messages with multiple interferers operating nearby.

Environmental Effects Degrade Performance

Radio transceivers are built on processes prone to performance variations that depend on their surrounding environment. Such variations include temperature changes, voltage-supply reductions as batteries discharge, and silicon manufacturing variations across devices. These real-life events can cause changes in the device's operating stability.

Let's look at an event-sensing emergency-response system operating on a street light. Cold winter temperatures could cause the output power of a device to vary or the receiver sensitivity to degrade, resulting in a loss of communication.

While less of a concern for a consumer device—which is rarely used in such extreme conditions—it would be unacceptable for an emergency-response system. At best, the cost is reputational damage to the end product, ending up in a service call to replace the faulty device. System designers must ensure that the components selected for the sensing and communication system are robust through the rigors of changing environmental conditions.

Corrupted Memory Can Lead to Unexpected Outcomes

Reliability is also a concern for the communications microcontroller. Although extremely reliable, both flash and nonvolatile memory can occasionally become corrupted. This

Smart cities can take advantage of wireless communications to respond to emergency situations.

may occur as a result of unintended effects caused by the operating environment, or intentionally through malicious hardware hacking.

Regardless of the mechanism, it is imperative that microcontrollers are equipped with the necessary integrity features to identify when a device has been corrupted. Once identified, the microcontroller can either correct the error or shut the device down, ensuring that the security of the wider system is not breached.

DESIGNING FOR RELIABILITY

Analog Devices' ADF7030-1 radio transceiver and ADuCM3029 Cortex-M3 microcontroller both help overcome the aforementioned challenges. They target performance levels and functionality features that lead to more robust communication links.

In many cases, the ADF7030-1 will be able to receive radio signals that are 3 dB lower than other similar radios. And with blocking numbers in excess of 100 dB, the ADF7030-1 can achieve a level of interference resilience comparable to military and aerospace equipment—without the need for additional costly external components. This ultimately lowers overall cost while ensuring communication is maintained in the noisiest RF environments.

Through generations of collaboration with leading industrial manufacturers, Analog Devices has developed methods for coping with real-life environmental effects on radio transceivers. As an example, the output power transmitted by a device using the ADF7030-1 varies by less than 0.2 dB over the full operating temperature range. Competing radios, on the other hand, often vary by up to 2 dB.

The ADuCM3029 is designed with flash and error-correction-code (ECC) parity checks to ensure errors caused by memory corruption are identified and corrected where possible. The microcontroller also comes with battery-monitoring capability in sleep mode. This ensures that unexpected drops in voltage are detected, and that the processor is in turn alerted to a possible malicious threat or power-supply malfunction. The end device then is able to take appropriate action, either by alerting an administrator or entering a safe mode, to make sure that the wider system is not compromised.

Technologies developed by Analog Devices inhabit every stage of the IoT signal chain, from sensing and measuring to interpreting and connecting the data. Certifying the quality and integrity of the information created through this chain is a core design principle, and a fundamental requirement to fulfill the true potential of the IoT.

DR. ALFRED GRAYZEL | Consultant, Planar Monolithic Industries Inc., 7311 Grove Rd., Ste. F, Frederick, MD 21704; (301) 662-5019
www.pmi-rf.com

Analyze RF JFETs for Large-Signal Behavior

A new field-effect-transistor architecture can be biased for improved efficiency and output power at RF and microwave frequencies.

Linear amplification is a requirement for processing many waveforms, although achieving high amplifier efficiency with linear performance might present a challenge. For example, terminating a JFET in an optimum resistance (R_{opt}) at one-half the maximum current, or $V_{dc}/(I_{max}/2)$, does not result in linear amplification with 50% efficiency.[1] For that reason, it is necessary to reconsider the way that FETs are analyzed. Linear models cannot be used—one must first solve the equations that describe a JFET's behavior to better understand and improve the performance.

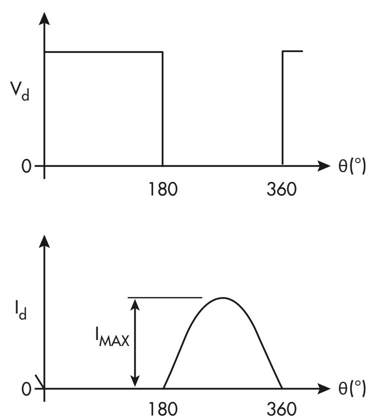

1. The plot shows a Class F drain-voltage and drain-current waveform.

In designing a linear, Class A amplifier, load-line analysis assumes that when the signal to a JFET's gate is sinusoidal, the drain current and voltage will also be sinusoidal in nature. As a result, that approach cannot be used for a FET amplifier. In a FET, when the drain voltage is greater than or equal to a saturated drain voltage (V_{dsat}), where V_{dsat} is the voltage at which pinchoff occurs, then the drain current of an n-type JFET can be found by Eq. 1:

$$I_{ds} = G_0(V_g - V_p - (2/3)(V_{bi} - V_p)\{1 - [(V_{bi} - V_g)/(V_{bi} - V_p)]^{3/2}\}) \quad (1)$$

where G_0 is the conductance of the FET channel when there is no depletion layer; V_g is the gate voltage; V_p is the pinchoff voltage; and V_{bi} is the "built-in" p-n junction potential.[2]

It can be seen from Eq. 1 that when V_g is a sinusoid, drain current I_{ds} contains harmonics; therefore, load-line analysis cannot be used. At saturation, I_{ds} is solely a function of the gate voltage. Equation 2 provides a good approximation for the drain current:

$$I_{ds} = I_{dss}(1 - V_g/V_p)^2 \quad (2)$$

where I_{dss} is the saturated drain current when the gate voltage is zero, $V_g = 0$.

When the gate voltage is set for a maximum value of zero and minimum value of V_p, the gate voltage can be found with Eq. 3:

$$V_g = (V_p/2)[1 - K\cos(\omega t)] \quad (3)$$

where K = 1. Substituting Eq. 3 into Eq. 2, with K = 1, yields Eq. 4:

$$I_{ds} = I_{dss}[3/8 + (1/2)\cos(\omega t) + (1/8)\cos(2\omega t)] \quad (4)$$

The dc power can be determined by Eq. 5:

$$P_0 = (3/8)I_{dss}V_0 \quad (5)$$

while the output power at the fundamental frequency (P_1) can be found using Eq. 6:

$$P_1 = I_1^2R_{opt}/2 = (I_{dss}/2)^2R_{opt}/2 = I_{dss}\,V_0/4 \quad (6)$$

where $R_{opt} = V_0/(I_{dss}/2)$ is the load resistance thought to be the optimum value[1] as determined by load-line analysis when setting the "knee voltage" equal to zero. Parameter I_1, which is the magnitude of the current at the fundamental frequency, is equal to $I_{dss}/2$ as indicated by Eq. 4. Equations 5 and 6 yield an efficiency of 66.7% when calculating P_1/P_0. The efficiency is greater than 50% due to the second-harmonic current consumption, thus decreasing the magnitude of the dc current. Since the amplifier has second-harmonic components of both current and voltage, it is not linear.

Current I_{ds} is a function of gate voltage V_g and not of the load impedance. If the load impedance presents a short-circuit condition at the second-harmonic frequency, only the fundamental frequency will appear at the output of the amplifier. In order for the drain voltage to always be greater than or equal to the saturated drain voltage V_{dsat}, the optimum load resistance R_L will be represented by Eq. 7:

$$R_L = 2(V_0 - |V_p|)/I_{dss} \quad (7)$$

The fundamental-frequency output power (P_1) is given by Eq. 8:

$$P_1 = I_1^2R_L/2 = I_{dss}(V_0 - |V_p|)/4 \quad (8)$$

and the efficiency by Eq. 9:

$$Eff = (2/3)(V_0 - |V_p|)/V_0 \quad (9)$$

Substituting Eq. 2 into Eq. 3, the output current at the fundamental frequency (I_1) is equal to $0.5(I_{dss})K\cos(\omega t)$. Thus, the output voltage (I_1R_L) and the input voltage at the fundamental frequency, given by Eq. 3, are linearly related, indicating that the amplifier is truly linear.

Large-signal nonlinear analysis based on device physics must be performed to arrive at the correct solution for a FET model. Unfortunately, many incorrect waveforms result from using linear models. The FET channel must be treated as a resistance that is a function of the gate voltage, and the drain voltage and current follow Ohm's Law, or $I(t) = V(t)/R(t)$. If at any time (t_0) the drain voltage is equal to zero, then the drain current must also be equal to zero at that time. Any set of waveforms in which drain current flows when the drain voltage is zero is not possible with a FET, including Class E and F waveforms *(Fig. 1)*.

THE "GRAYZEL JFET"

When the drain voltage of a JFET is exactly equal to V_{dsat}, the conditions are those of *Fig. 2a*,[2] where pinchoff occurs exactly at the drain of the transistor. If the drain voltage is increased by ΔV, the point at which pinchoff occurs moves toward the source a distance of ΔL *(Fig. 2b)*.

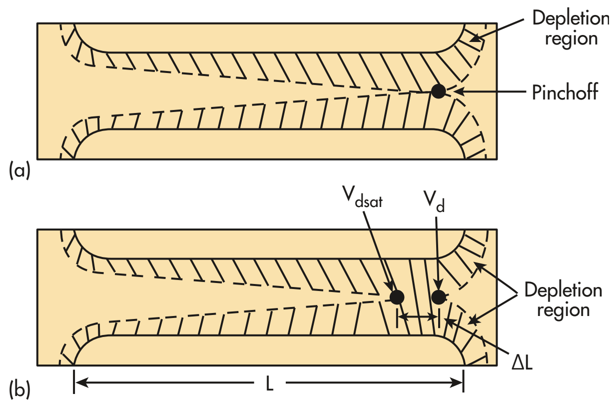

2. The diagrams depict a FET channel under different conditions: when the drain voltage equals the pinchoff voltage (a) and when the drain voltage exceeds the pinchoff voltage (b).

Over the length ΔL, at the drain, the voltage is completely depleted. Only minority carriers remain and the resistance is quite large. Voltage ΔV drops across this depleted region and, due to the high resistivity in the depleted region, ΔL is very small. For ΔL << L, which represents the usual case, the depletion from source to pinchoff point will be essentially identical in shape and have effectively the same resistance from the source to the point where pinchoff occurs.[2] There is hardly any change to drain current, which is equal to V_{dsat} divided by this resistance. This explains why the value of the drain current is nearly constant for drain voltages greater than V_{dsat}.

The instantaneous power P(t) dissipated in the depleted region is equal to $I_d(t)\Delta V(t)$. Integrating this product over a cycle setting of $\Delta V(t) = 0$ for $\Delta V(t) < 0$ yields the total dissipated power in the totally depleted region. In addition, ohmic losses develop in the portion of the channel that is not completely depleted.

Since voltage ΔV(t) drops across the depleted region ΔL, it does not contribute to the output power and simply degrades the efficiency. It is therefore clear that, for high efficiency, the depletion region must be minimized. Ideally, when converting dc power to RF power, the channel should have no depletion at all for one-half the cycle and should be completely cut off for the other one-half cycle. With the optimum load, this should yield the maximum dc-to-RF efficiency. To accomplish this, a new (patented) FET model is presented that will be referred to as the "Grayzel JFET."

Figure 3 shows a simplified schematic of a JFET with a drain voltage of 7 V dc. Along the channel, the potential has values of 0, 1, 2, 3, 4, 5, 6, and 7 V. The junction is progressively back-biased, causing greater depletion at the drain than at the source. *Figure 4* shows a simplified schematic diagram of the "Grayzel JFET." The P+ region is divided into N sections that are insulated from one another, forming N p-n junctions. (In Fig. 4, N is equal to 8 as an illustrative example.)

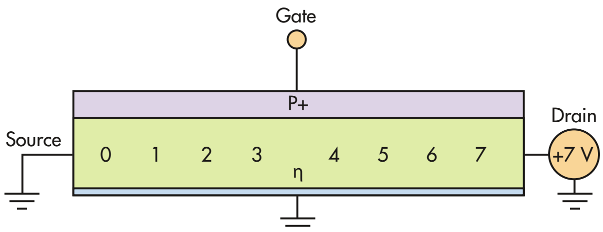

3. A voltage drop occurs down the FET channel for a drain voltage of +7 V dc.

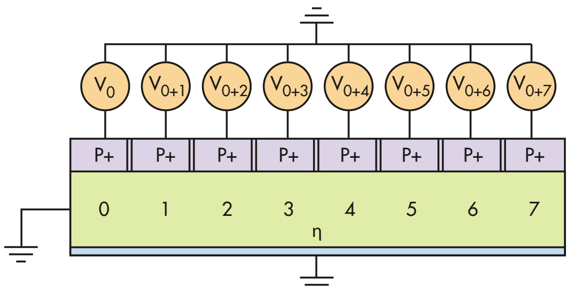

4. Each p-n junction in this Grayzel JFET model is reverse-biased at voltage V_0.

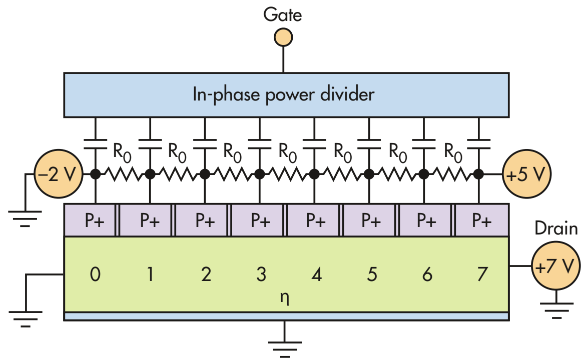

5. This diagram of a Grayzel JFET model shows each p-n junction biased at –2 V dc and with in-phase RF voltage provided by means of an in-phase power divider.

Each p-n junction is biased to ground separately as shown in Fig. 4—the first at V_0 and the eighth at $V_0 + 7$. With a drain voltage of 7 V, all of the p-n junctions will have the same dc voltage V_0 across their junctions and hence, to a good approximation, all of the junctions will act in unison.

Consider as an example of a Grayzel JFET a device where all p-n junctions are completely depleted when back-biased with a voltage of –4 V dc. The gate voltage is then equal to –4 V dc, and the drain current is approximately zero. A square wave varying from –2 to +2 V is applied to each of the p-n junctions through an eight-way, in-phase power divider *(Fig. 5)*. The p-n junctions are biased such that each p-n junction has a bias voltage of –2 V dc when the drain voltage is equal to 7 V dc. The channel will be without depletion for about one-half of the cycle and cutoff for approximately the other one-half. For very large N, the conductance of the channel approaches an ideal square wave varying between 0 and G_0, where G_0 is the value of the conductance of the channel when there is no depletion region.

This p-n biasing arrangement represents just one example, though. The p-n junctions can be biased individually, as shown in Fig. 4, or by other means. The act of dividing the gate into multiple sections is applicable to all types of FETs. *Fig. 6* shows an example of the Grayzel MOSFET with the gate divided into N sections, with N = 6.

SPECIAL CASE

One might also want to consider a special case for the Grayzel JFET: In this instance, odd-order harmonics are short-circuited and the even-order harmonics are open-circuited. In addition, for one-half of the cycle, the JFET is cut off; for the other half of the cycle, the depletion region in the channel is of minimal width. The conductance is thus a square wave varying between 0 and G_0, where G_0 is the conductance when the depletion region in the channel is of minimal width. If $\theta = 2\pi ft = \omega t$, where f represents the fundamental frequency of the square wave, the Fourier series of the square wave can be given by Eq. 10a:

$$G(t) = 0.5G_0 + g(t) \quad (10a)$$

where:

$$g(t) = (2G_0/\pi)(\cos\theta - \cos(3\theta)/3 + \cos(5\theta)/5 - \cos(7\theta)/7 + \ldots$$
$$= (2G_0/\pi)\Sigma^{\infty}_{k=1}(-1)^{k-1}\cos[(2k-1)\theta]/(2k-1) \qquad (10b)$$

The FET is terminated in an admittance $Y(\omega)$, which at the fundamental frequency has a value G_L. The value of $Y(\omega)$ is zero at the even harmonics and infinite at the odd harmonics of the fundamental frequency. The drain voltage, therefore, has only even harmonics and the drain current has only odd harmonics. The drain voltage, $V_d(t)$, is chosen to take the form of Eq. 11a:

$$V_d(t) = V_0 + v(t) \quad (11a)$$

where:

$$v(t) = V_1\cos(\theta) + \Sigma^{\infty}_{k=1}(V_{2k})\cos(2k\theta) \quad (11b)$$

This form was chosen for the following reason: According to Eq. 10, the value of the conductance of the channel is equal to G_0 when $-90° < \theta < +90°$ and the channel is cut off for the remainder of the cycle. As a result, current will only flow when $-90° < \theta < +90°$. Since the current is equal to $V_d(t)G(t)$, $V_d(t)$

Ultra-Wideband
MMIC SPLITTER|COMBINERS

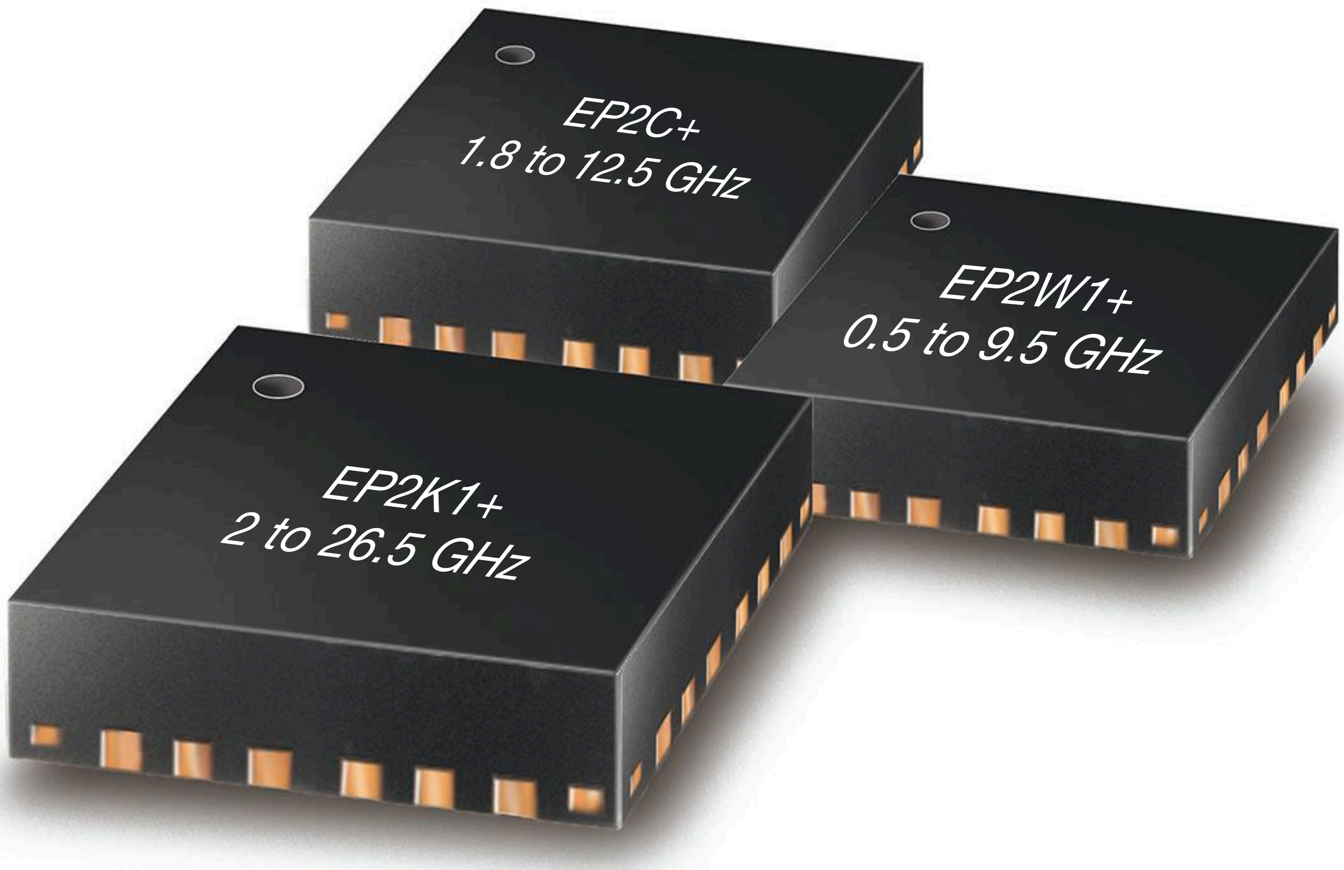

Single Unit Coverage as Wide as **2 to 26.5 GHz**

Models from $5.56 *ea. (qty.1000)*

THE WIDEST BANDWIDTH IN THE INDUSTRY IN A SINGLE MODEL!

Our new EP-series ultra-wideband MMIC splitter/combiners are perfect for wideband systems like defense, instrumentation, and all cellular bands through LTE and WiFi. These models deliver consistent performance across the whole range, so you can reduce component counts on your bill of materials by using one part instead of many! They utilize GaAs IPD technology to achieve industry-leading performance, high power handling capability and efficient heat dissipation in a tiny device size, giving you a new level of capability and the flexibility to use them almost anywhere on your PCB! They're available off the shelf, so place your order on minicircuits.com today, and have them in hand as soon as tomorrow!

- Series coverage from 0.5 to 26.5 GHz
- Power handling up to 2.5W
- Insertion loss, 1.1 dB typ.
- Isolation, 20 dB typ.
- Low phase and amplitude unbalance
- DC passing up to 1.2A

EP2K-Series, 4x4x1mm
EP2W-Series, 5x5x1mm

Mini-Circuits®

www.minicircuits.com P.O. Box 350166, Brooklyn, NY 11235-0003 (718) 934-4500 sales@minicircuits.com 549 Rev B

One might also want to consider a special case for the Grayzel JFET: In this instance, odd-order harmonics are short-circuited and the even-order harmonics are open-circuited.

will have its maximum value centered at $\theta = 0°$ and will thus be equal to the sum of cosines.

The bias voltage V_0 in Eq. 11a is the same for all of the p-n junctions, with the Grayzel JFET progressive-biased as described earlier. There will, however, be a variation of the depletion region along the channel because of v(t) in Eq. 11a. This variation will be small, and is therefore neglected in this analysis.

The amplifier shown in *Fig. 7a*, where the FET is a Grayzel JFET, will be analyzed with the aid of the circuit in *Fig. 7b*. Voltage v(t), given by Eq. 11a, appears across the RF choke in series with the dc battery, across the load G_L in series with blocking capacitor C, and across the nonlinear susceptance G(t) given by Eq. 10a. The choke, which is in series with the dc battery, has voltage v(t) across it, but negligible RF current flowing through it. Drain current $I_d(t) = I_0 + i(t)$ is equal to the product $G(t)[V_d(t)]$. Current i(t) flows in a loop through the termination $Y(\omega)$ *(Fig. 7)*. In turn, dc voltage V_0 is dropped across the blocking capacitor C.

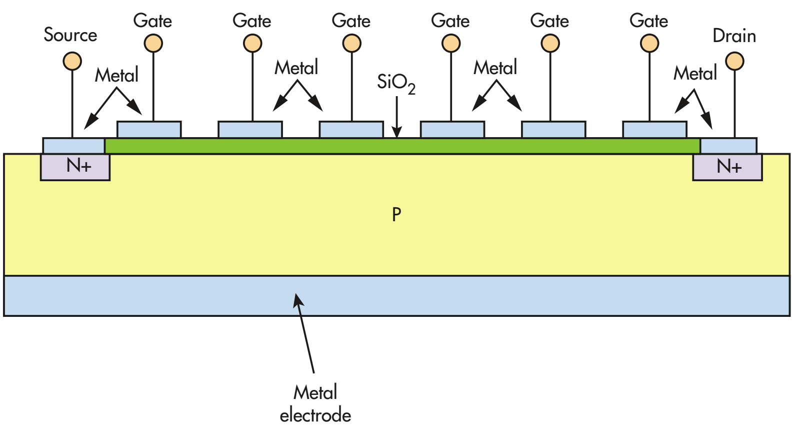

6. This is an example of the thinking behind a Grayzel MOSFET, with the gate divided into sections (six in this case).

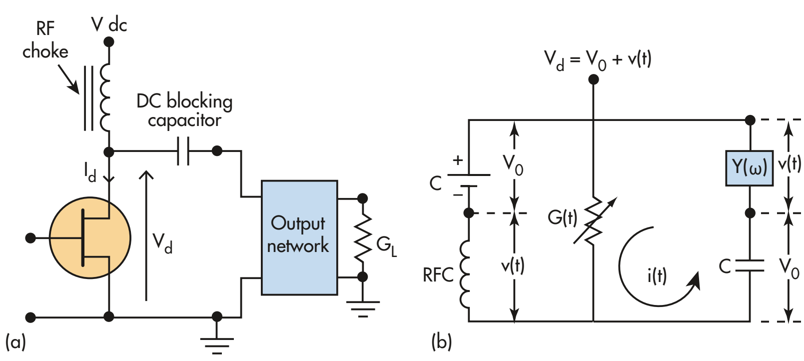

7. These schematic diagrams show a conventional JFET amplifier (a) and the equivalent circuit for a JFET amplifier based on the Grayzel nonlinear JFET model (b).

The drain current is given by Eq. 12a:

$$I_d(t) = [V_0 + v(t)][0.5G_0 + g(t)]$$

$$= 0.5V_0(G_0) + V_0[g(t)] + 0.5G_0[v(t)] + v(t)g(t)$$

$$= 0.5V_0(G_0) + v(t)g(t)$$

$$+ V_0[(2G_0/\pi)(\cos\theta - \cos(3\theta)/3 + \cos(5\theta)/5 - \cos(7\theta)/7 + \ldots)$$

$$+ 0.5G_0(V_0)(V_1\cos\theta + V_2\cos(2\theta) + V_4\cos(4\theta) + V_6\cos(6\theta) + \ldots] \quad (12a)$$

where:

$$v(t)g(t) = (V_1\cos\theta)(2G_0/\pi)(\cos\theta - \cos(3\theta)/3 + \cos(5\theta)/5 - \cos(7\theta)/7 + \ldots)$$

$$+ (V_2\cos 2\theta)(2G_0/\pi)(\cos\theta - \cos(3\theta)/3 + \cos(5\theta)/5 - \cos(7\theta)/7 + \ldots)$$

$$+ (V_4\cos 4\theta)(2G_0/\pi)(\cos\theta - \cos(3\theta)/3 + \cos(5\theta)/5 - \cos(7\theta)/7 + \ldots)$$

$$+ (V_6\cos 6\theta)(2G_0/\pi)(\cos\theta - \cos(3\theta)/3 + \cos(5\theta)/5 - \cos(7\theta)/7 + \ldots \quad (12b)$$

The drain current can therefore be written as the sum of the dc term, the odd harmonics, and the even harmonics:

$$I_d(t) = I_0 + \Sigma^{\infty}_{k=1}(I_{2k-1})\cos(2k-1)\theta + \Sigma^{\infty}_{k=1}(I_{2k})\cos(2k)\theta \quad (13)$$

Using the identity $\cos(x)\cos(y) = 0.5[\cos(x + y) + \cos(x - y)]$, the even harmonics can be found from Eq. 12 by means of Eq. 14:

(Continued on page 84)

MOUQUN DONG | RF Applications Engineer, California Eastern Laboratories Inc.
4590 Patrick Henry Dr., Santa Clara, CA 95054; (408) 919-2500; www.cel.com

Analyze Transient Delays in GaAs MMIC Switches

The fast speeds of GaAs MMIC switches can be hindered by step voltage functions employed for bias sequencing of power amplifiers.

High-frequency GaAs switches are widely used to route signals through RF/microwave circuits and systems. GaAs monolithic-microwave-integrated-circuit (MMIC) switches are the most common type of microwave switch used for communications applications, and they can provide typically fast switching speeds.

However, under certain conditions, longer-than-expected settling times (longer than indicated by the product datasheet) can occur, which can severely degrade system-level performance—especially for packet-based communication systems. These delays, which are relatively unknown to RF/microwave designers, result from a transient effect in GaAs MMIC switches. Fortunately, solutions are not difficult to achieve, once the problem has been properly identified. This holds especially true for systems involving multiple dc and RF/microwave signal sources.

GaAs MMIC switches rely on field-effect transistors (FETs) for their functionality. A FET has three terminals: gate, drain, and source. The main current path or channel is between drain and source, while the gate operates as a control terminal. In a GaAs FET amplifier, input signals are applied to the gate while the output is available at the drain, with the source typically connected to ground.

But in a switch, a FET behaves like a voltage-controlled resistor, with drain and source as conducting terminals and the gate as control. The two conducting terminals are essentially symmetric with respect to the gate, so the distinction between source and drain is not overly important in a GaAs FET switch. The gate controls the two logic levels or switch states of the resistor device: "on" when resistance is low and "off" when resistance is high.

Figure 1 shows a simple circuit, comprised of two FETs, for realizing a switching function. Some low-cost RF/microwave switches are constructed with this simple configuration,

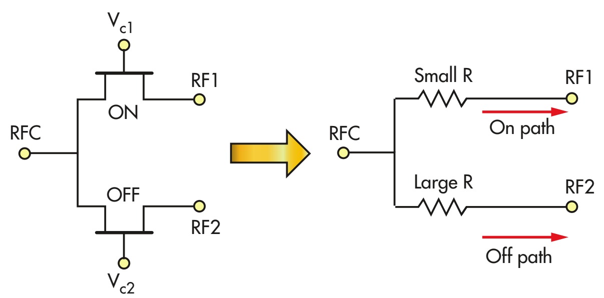

1. The two FETs are combined to form a switch circuit, with its equivalent circuit also shown.

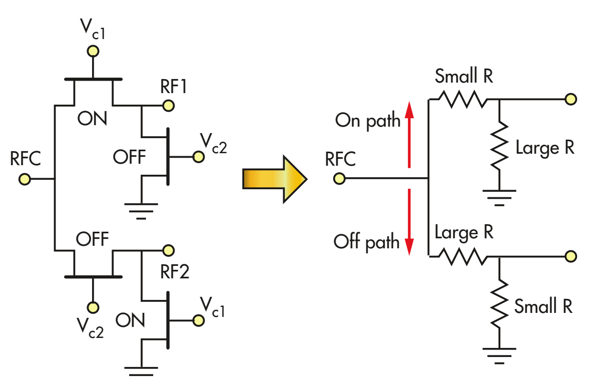

2. A switch circuit can be formed of series and shunt FETs, with its equivalent circuit also shown.

although a series FET in its off state does not yield very high switch isolation. Isolation can be increased by adding a shunt FET in its on state *(Fig. 2)*.

Adding a small shunt resistance to the large series resistance *(Fig. 2, again)* can further increase the signal attenuation of the off signal path, increasing isolation. For the on signal path, the shunt FET is set to its off state, corresponding to a configuration with a small series resistance and a large shunt resistance. The large shunt resistance has negligible effect on the on-path insertion loss.

GaAs MMIC switches have evolved with time. Pseudomorphic high-electron-mobility-transistor (pHEMT) active devices and other technology now offer improved performance compared to earlier GaAs FETs. These devices operate in depletion mode, where a negative gate voltage with respect to drain source is required to turn off the channel or, in terms of switching functionality, a negative voltage is required to turn transistors to their off states.

Figure 3 plots a typical transistor drain-source current, I_{ds}, versus gate-source voltage, V_{gs}, with V_{th} representing the threshold voltage above which the transistor becomes a conductor. For switch applications, the on state is achieved by biasing V_{gs} slightly positive, while the off state is achieved by setting V_{gs} below V_{th}. Detailed analyses of transistors operating in switch applications are available in the literature.[1,2]

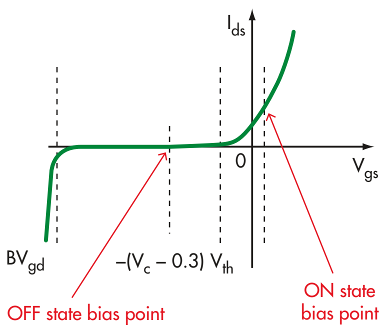

3. These are the I_{ds}-V_{gs} curves of a GaAs FET used in MMIC switches. The bias points for ON and OFF states are indicated. The threshold voltage, V_{th}, and breakdown voltage, BV_{gd}, are also shown.

Figure 4 shows how dc bias is established for the on and off transistor states in a GaAs MMIC switch consisting of series and shunt FETs. The gate resistors R_{gs1}, R_{gs2}, R_{gp1}, and R_{gp2} are mainly for isolation of RF paths from the dc supply, and they normally have a value of about 10 kΩ. The source capacitors in the shunt FETs (Q_{p1} and Q_{p2}) are used for blocking dc to ground and providing an RF short.

These capacitors require only moderate values to achieve a low impedance to ground at higher frequencies. This is due to the fact that the equivalent impedance of the series transistors in their off state is usually high enough for good low-frequency isolation. The behavior of the dc currents from the gate to the drain and source of a pHEMT can be modeled as a diode with the gate serving as an anode.

When the diode is forward-biased (the gate voltage is positive with respect to the drain/source), the channel is conductive and the transistor is in its on state. If the diode is reverse-biased (below the threshold voltage), the channel is open and the transistor is in its off state. Since the circuit is symmetric with respect to control logic levels V_{c1} and V_{c2}, only one logic configuration need be considered, where V_{c1} equals the high (H) state and V_{c2} represents the low (L) or grounded state.

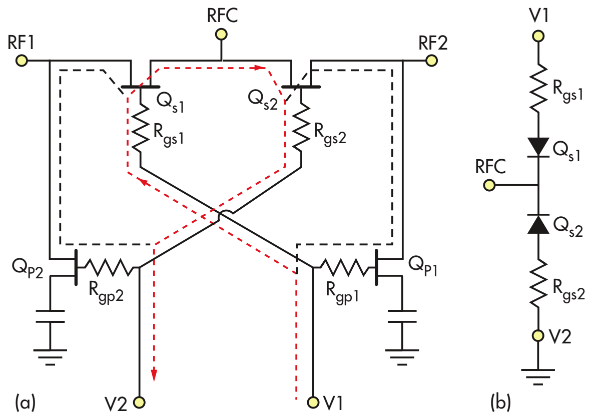

4. The block diagram (a) shows an SPDT GaAs MMIC switch with shunt FETs, with current paths for logic high and low levels at V_{c1} = H and V_{c2} = L; and (b) the dc equivalent circuit for the current path.

Figure 4a displays the dc current distribution and flow for the assumed logic configuration. The gates for transistors Q_{s1} and Q_{p1} are forward-biased, while the gates for Q_{s2} and Q_{p2} are reverse-biased, corresponding to a switch configuration of on for the RFC-to-RF1 path and off for the RFC-to-RF2 path. There are three main current paths from pin V_{c1} (logic high) to pin V_{c2} (logic low). Although a full circuit analysis is possible, only one path ($V_{c1} \rightarrow Q_{s1} \rightarrow Q_{s2} \rightarrow V_{c2}$; the red dashed line) will be considered at this time.

Figure 4b shows the dc equivalent circuit for this current path, where the transistors have been replaced by two diodes that are forward- and reverse-biased, respectively. This simplified equivalent circuit is for dc bias consideration only; the equivalent capacitances between the drain/source and gate, which in fact are partially short at RF frequencies, are not included. One of the RF ports, RFC, is between the two diodes. The dc voltage at the RFC port is lower than logic high V_{c1}, roughly by the amount of a forward voltage drop for the diode (which is typically about 0.3 V for the FETs used in MMIC switches).

A similar analysis will show that the dc voltages at RF ports RF1 and RF2 are essentially the same as that at the RFC port. For the other switch logic configuration, where V_{c1} is low and V_{c2} is high, the voltages at all RF ports are effectively unchanged. For a steady-state condition, the dc voltages at the RF ports are about 0.3 V less than the logic high level, regardless of the logic configuration.

For a FET switch to function properly, each FET must be biased according to design specifications, and any external dc voltage present or resistive load on the internal dc bias current paths will impact the bias conditions for a FET switch's active devices. For this reason, a dc blocking capacitor must be used at all RF ports to isolate the internal dc bias circuitry from external circuitry surrounding the switch.

The choice of dc blocking capacitor is usually based on the switch manufacturer's recommendations. But when the settling time for a FET switch's dc bias is much longer than the switching speed specified in the switch's datasheet, the choice of dc blocking capacitor should be reconsidered. A long settling time for the dc bias condition can also result in long delays for the RF output power of the switch to reach a steady-state condition, a problem for many modern communication systems.

Figure 5 shows a case where an RF switch can have a potentially long settling time at its output port. It is an antenna diversity application where the output port of a power amplifier (PA) is connected to a single-pole, double-throw (SPDT) switch. The switch's two output ports are connected to two antennas. The PA is powered by an external supply, V_{PA}, at the RF output pin through an inductor choke. This is a standard bias scheme for RF transistors and is also widely used for various RF PA ICs. In this case, a dc voltage is present on the RF signal line.

Normally, dc blocking capacitor C_{blk} should be sufficient to protect the switch's bias circuitry from interference caused by the PA's supply voltage. However, for improved efficiency, the PA's power supply is often programmed to turn on before the start of an RF transmission and turned off at the end of the transmission. The PA's turn-on process will cause a sudden change in voltage on the switch side of the blocking capacitor, with charge movement inside the switch to and from the V_{c1} and V_{c2} pins.

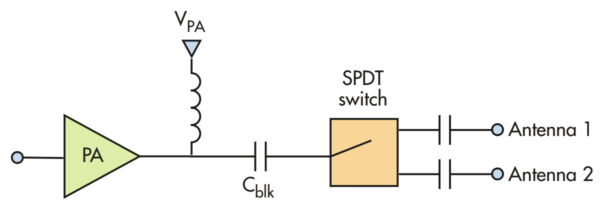

5. These PA bias and switch circuits serve an antenna diversity application.

If the switch control logic is set before V_{PA} starts, the bias condition of the switch will be disturbed by the onset of V_{PA}, which may affect the switch's performance in terms of settling time. If the switch has not settled before the arrival of an RF signal, system performance will be degraded. The actual settling time will be determined by the time for charge buildup on C_{blk} according to a new steady-state voltage across the capacitor. Although this transient phenomenon is strongly correlated to the switch's characteristics, several other factors will affect the settling time, which therefore cannot be fully characterized by switch specification.

Figure 6 shows a measurement setup for analyzing these transient effects on GaAs FET switch settling time. Although the induced transient voltage on the RF ports is expected to be the root cause of the unsettling condition of the switch's RF performance, it is difficult to directly probe the voltage on the RF ports without introducing loading effects for both the dc voltage and RF signals. From an application perspective, the most relevant concern in this case is RF performance—notably insertion loss—and it is insertion loss, rather than dc voltage, that is monitored with this test setup. A 2.4-GHz signal is applied to the switch's RFC port with supply voltage to the switch port held steady at $V_c = 3$ V dc. A power detector monitors RF power at RF1, while RF2 is terminated with a 50-Ω load.

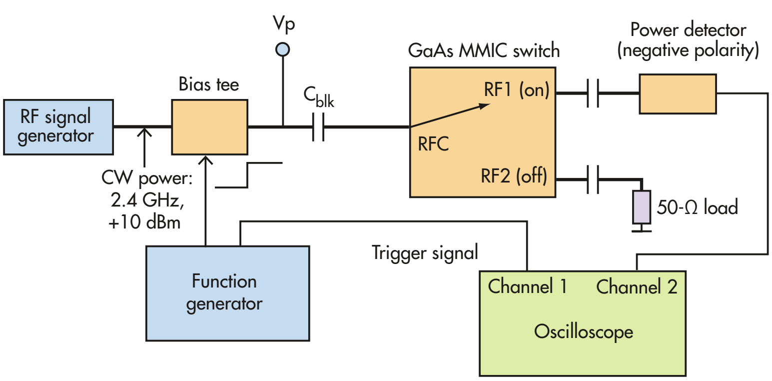

6. This measurement setup was used for analyzing settling times in GaAs MMIC switches.

To simulate the PA supply, a step function from the function generator is injected at the outside of the dc blocking capacitor (V_p in Fig. 6). A bias-T isolates the RF path from the function generator. The choke inductor of the bias-T slightly slows the rise time of the step function to about 1 μs, which is still insignificant compared with the settling times observed in the experiments.

Referring to Fig. 4, the RFC port is essentially connected to RF1 port through Q_{s1} which is in the ON state (RF2 is isolated from RFC because Q_{s2} is in the OFF state). Therefore, in principle, the capacitance values of C_{blk} on both RFC and RF1 ports will affect the transient characteristics of the switch in this specific logic configuration. For simplicity, the same capacitance value is used for all dc blocking capacitors in the experiments.

The charging/discharging process in this case is similar to the transient behavior of a resistive-


HIGH DYNAMIC RANGE
MMIC AMPLIFIERS
PGA-SERIES
5 to 6000 MHz

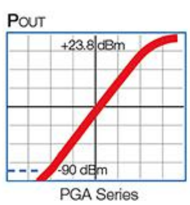
POUT
+23.8 dBm
-90 dBm
PGA Series

capacitive (RC) circuit with a step-function stimulus. But unlike an RC circuit, the dc bias circuit of a switch is nonlinear. In addition, the step response being considered here is the RF power or insertion loss at the switch output, rather than voltage. While the insertion loss is strongly affected by the switch dc bias condition, the quantitative relationship between the two parameters is not obvious.

As a result, the settling time cannot be easily calculated using an RC time constant. Nevertheless, it is expected that the resultant settling time of the RF output power is strongly influenced by the C_{blk} value and the equivalent impedance (the ratio of voltage to current) of the transistor bias circuit.

For these experiments, an SPDT GaAs MMIC switch was used, specified to 3 GHz with relatively low output power at 0.1-dB compression rating of $P_{0.1dB}$ = +23 dBm. The device has low supply current of about 5 nA. Such a switch is suitable for battery-powered, short-range wireless applications.

Figure 7 shows the responses of output RF power to a step function for three different C_{blk} values. The power detector has negative polarity, so any drop shown on the oscilloscope corresponds to an increase in RF power. The amplitude of the step function, V_{step}, was chosen to be the same as the switch supply voltage of 3 V.

In response to the step function, the RF power initially drops about 10 dB, indicating a severe disturbance in the dc bias condition inside the switch due to the step function at the RFC port. After this initial drop, the RF power gradually recovers to a steady-state level. The time intervals between the onset of the step function and the point when RF power is fully recovered are utilized as the time constant in this measurement. They are 1.5, 3.5, and 9 ms for C_{blk}= 8, 22, and 56 pF, respectively.

The order of magnitude of the measured time constants is in reasonable agreement, with a calculation using RC as time constant if R is taken as the equivalent impedance for a steady-state condition. The measured results confirm that the time constant is roughly proportional to C_{blk}, at least in the range of capacitance values studied in the experiments.

The impact of the amplitude of the step function, V_{step}, was also examined with a series of measurements using additional values of V_{step}=1.4, 2, and 4 V for C_{blk}=22 pF. As expected, the magnitude of the initial drop in RF power is strongly affected by V_{step}, but the transient time constant remains essentially the same *(Fig. 8)*.

For a true RC circuit, the step responses at the rising and falling edges are expected to be symmetric with respect to the steady-state value, but this is not the case here. The rising edge of the step function causes a considerable drop in RF power at the switch output *(Fig. 7a)*, while the falling edge of the step function has no discernible effect. This asymmetry can

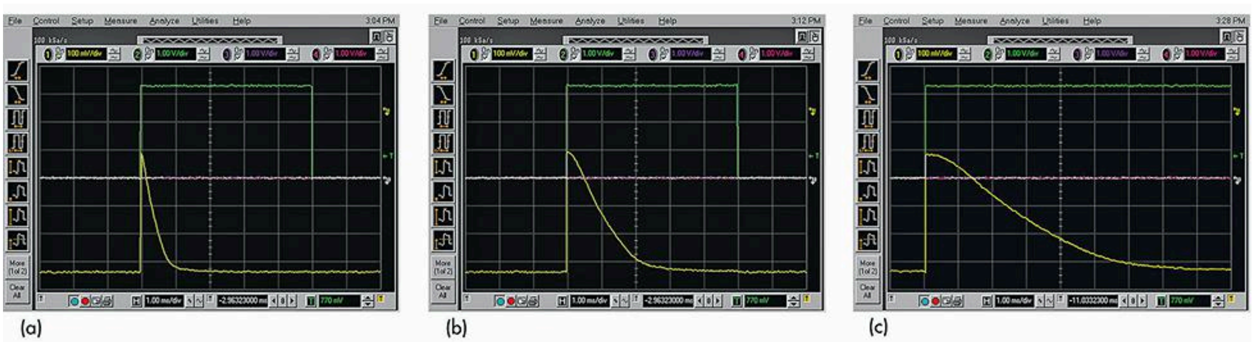

7. The effects of step functions on RF switch output power are shown for three different blocking capacitors, C_{blk} : (a) 8 pF, (b) 22 pF, and (c) 56 pF. The amplitude of the step function, V_{step}, is 3 V and the initial power drop, ΔP, is 10 dB.

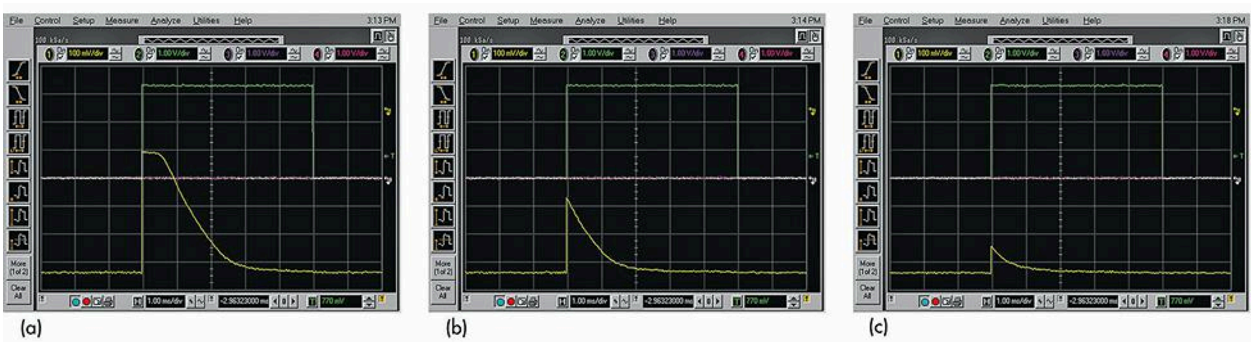

8. These are the responses in RF output power for three additional step-function amplitudes: (a) V_{step} = 4 V and ΔP=10 dB, (b) V_{step} = 2 V and ΔP=5 dB, and (c) V_{step} = 1.4 V and ΔP=1.2 dB, with a blocking capacitor, C_{blk}, of 22 pF.

be attributed to the characteristics of diodes in the equivalent circuit *(Fig. 4b)*. At the rise of the step function, the increasing voltage on C_{blk} pushes electrical charges (positive) away from C_{blk} and into the switch.

The discharge paths are through transistors Q_{s1} and Q_{s2}; both are in reverse-biased condition with RFC as the reference point. The equivalent impedance in this direction is very high, resulting in a long settling time. On the other hand, at the falling edge of the step function, charge flows in the opposite direction through a forward-biased diode. The equivalent impedance is much less in this direction, and the corresponding transient process is negligible. In this direction, the time constant essentially equals the switching speed quoted in the datasheet for a GaAs MMIC switch.

To analyze the effects of equivalent impedance on an RC circuit, a different switch was used in the experiments—one with higher supply current and much lower equivalent impedance, a model CG2185X2 SPDT switch from CEL. It is a medium-power GaAs MMIC switch suitable for wireless applications to 6 GHz. The supply current used in experiments with this device was 1.9 µA, or about 400 times larger than the supply current used previously.

Figure 9 shows the step response for this device using the same conditions for the higher-impedance device in Fig. 7.

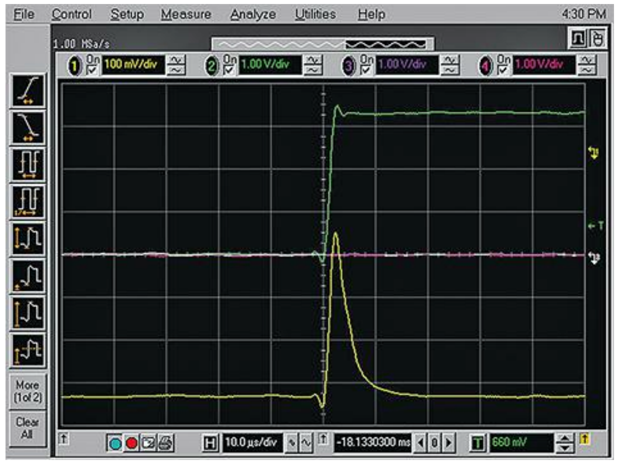

9. This is the step response in RF output power for a model CG2185X2 SPDT switch, with C_{blk} =22 pF and V_{step} =3 V.

The initial power drop is similar to the earlier device, but the settling time is much shorter, at about 10 µs.

This confirms that the equivalent impedance indeed affects the transient behavior in a similar manner as resistance in an RC circuit. It also explains why problems with longer settling times are more prominent with low-power switches with lower supply currents (i.e., higher equivalent impedances). Of course, the low-current requirements of such switches makes them well-suited for low-power wireless systems, where long battery life is important. RF designers concerned with long switch settling times in a system should pay attention to the design of power-sequencing functions in that system.

Power sequencing of RF components such as PAs can also be a concern for the reliability of GaAs MMIC switches. A low-power GaAs MMIC switch may be rated for maximum control voltage of around 6 V and run at actual control voltages as high as 5 V. Since the voltage on the switch's RF ports is typically below the control voltage by about 0.3 V, the dc voltage on the RF ports can be close to a switch's maximum rating, especially if a relatively high control voltage is used.

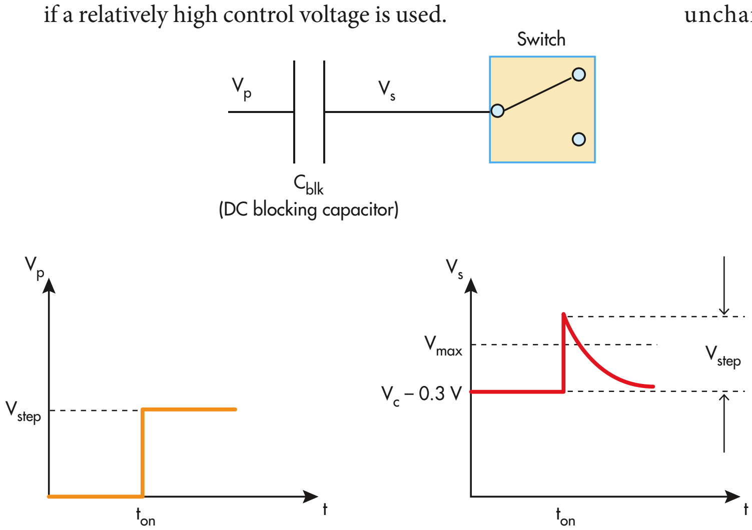

10. This is the step response of the voltage on the switch side of a dc blocking capacitor, where V_{c1} – 0.3 V is the steady-state voltage on the RF ports and V_{max} is the maximum rating of the supply voltage for a given switch model.

Power sequencing of RF components such as PAs can also be a concern for the reliability of GaAs MMIC switches.

Figure 10 shows a case where the transient voltage on an RF port of a switch, V_s, induced by a voltage step function, V_p, can momentarily exceed the maximum rating of the switch supply voltage. The step response of V_s can be analyzed by realizing that at the onset of the step function, t_{on}, the voltage across the dc blocking capacitor remains unchanged, and subsequent charging/discharging of the capacitor brings the voltage back to the steady-state level.

With t_{on}, the voltage V_s, in response to the step function V_p, jumps by the same amount as V_{step} and then returns to its steady-state level through an RC-like discharge process on C_{blk} *(Fig. 10)*. Even though the voltages on the RF ports are only briefly beyond the maximum rating, the condition can cause long-term performance degradation—if not immediate damage—to the switch. The situation can be avoided by delaying switch biasing until after the step function (such as PA power sequencing). mw

REFERENCES
1. Inder Bahl, *Control Components Using Si, GaAs, and GaN Technologies*, Artech House, Norwood, MA, 2014.
2. N. Jain and R. Gutmann, "Modeling and Design of GaAs MESFET Control Devices for Broadband Applications," *IEEE Transactions on Microwave Theory & Techniques*, Vol. 38, No. 2, February 1990, pp. 109-117.

JOE MADDEN | Principle Analyst, Mobile Experts
www.mobile-experts.net

Reversing 25 Years of ANTENNA DEGRADATION

As mobile communication ramps up in complexity, smarter antenna tuning could prove to be a game-changer in meeting demands.

Does anyone remember pulling out the antenna on your first mobile phone to make a call? Over the past 25 years, antenna design has changed radically for cell phones. While transitioning from 2G to 3G to LTE, we have incrementally and gradually sacrificed as much as 10 dB of link budget in some cases. It's shocking but true: The network has improved dramatically, so we've been able to compromise performance in the handset antenna without much backlash from consumers *(Fig. 1)*.

Multiple factors come into play here:

- The elimination of the extended antenna
- Metal-backed phone cases
- Multi-band antenna requirements, with carrier aggregation, Licensed Authorized Access (LAA), and multiple input, multiple output (MIMO)
- Smaller antenna form factors
- Time-to-market pressure that leaves little time for optimization

Most people didn't notice the reduction of antenna performance, because government agencies require conducted testing (with a connector at the antenna port), and carriers generally perform testing in a "free space" chamber environment. CTIA certification requires free-space testing, but only under fairly optimal conditions.

Dynamic performance testing with realistic hand-grip fixtures is rarely required by anyone. In fact, testing is often done with hand-grip fixtures using a foam spacer to avoid simulating the poor performance with a true hand. The industry is hiding from the truth: We have been throwing away performance by ignoring real-world conditions.

However, the 25-year trend of throwing away antenna performance is starting to turn in the other direction. We're starting to see handset OEMs investing in new technology that specifically targets improvements in total radiated power (TRP) and total isotropic sensitivity (TIS). The benefits can be huge.

1. Antenna efficiency is lost in the transition from external to internal antennas.

DIVERSITY

In addition to tuning the main antenna, adding diversity antennas to the terminal can make a big difference. Most smartphones now include 2×2 MIMO for LTE, which prompted adding a second antenna to their designs for LTE frequency bands. According to LTE standards, the second antenna can be used for receiver diversity or for MIMO, depending on which mode is more advantageous with prevailing channel conditions.

Taking this concept one step further, a few handsets (e.g., the Google Pixel and the Galaxy S7) now use four antennas in key LTE bands to support choices like 4-way receiver diversity and 4×4 MIMO. The gain in throughput is not obvious in a free-space test. However, in the real world, with hands gripping metal-backed phones, the impact of additional antenna options can be significant. Some vendor testing has revealed more than a 60% increase in throughput.

Mobile operators are starting to invest in 4×4 MIMO for some base stations, but it's clear that this capability will not be implemented everywhere. Therefore, we expect the architecture of the smartphone to include diversity switches that allow for either 4×4-MIMO operation or 4-way receiver diversity, enabling the best possible performance in all situations.

TUNING

Aperture tuning was introduced 10 years ago and has become a standard part of any smartphone that includes multiple bands between 700 and 960 MHz. In most smartphones today, it is implemented as a simple switch that changes the electrical length of the antenna, thus changing its resonant frequency from one band to another. Some handsets use MEMS devices for this purpose.

In addition to frequency tuning, more than 100 smartphone models now include impedance-match tuning, which adapts for the impact of a hand on the phone *(Fig. 2)*. Closed-loop impedance-match tuning can recover more than 4 dB of lost performance in radiated power, which translates directly into user benefits such as:

- **Longer battery life:** As much as an hour per day longer for typical users.
- **More stable data sessions:** TDD links tend to be dropped due to uplink limitations. A 4-dB improvement in TRP greatly improves the stability of the LTE link.
- **Higher data throughput:** Both uplink and downlink benefit from higher signal quality.

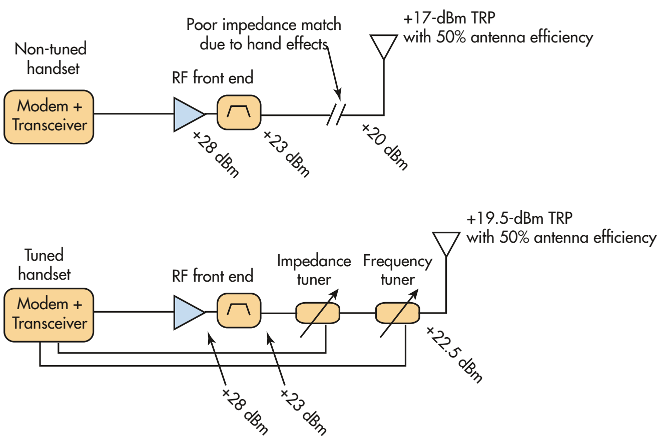

2. Mismatch loss due to hand effects can be eliminated with closed-loop tuning.

CARRIER AGGREGATION

Many people believe that antenna tuning is incompatible with carrier aggregation (CA), especially where CA is implemented for low-low band combinations or high-high band combinations. However, the closed-loop tuning used today can be adapted for different scenarios. Mobile Experts forecasts adoption of impedance-match tuning and possibly aperture tuning, even in the low-low CA case. The modem will need to make some new decisions about what tuning settings are required for a wideband match versus a narrowband match. This is the next natural step in evolution.

Notably, CA can include multiple licensed bands, but also incorporate LAA, 3.5-GHz Citizens Broadband Radio Service (CBRS), and other bands. The algorithm can get pretty complex when combinations of licensed and unlicensed bands are constantly changing.

WHAT'S COMING NEXT

The industry pattern has started to change. Ten years ago, handset OEMs recognized the inferior performance of some antenna choices they were making, but they were not willing to spend another two dollars per handset to fix the problems. Today, handset OEMs are voluntarily choosing to use tuning solutions. These solutions have been simplified and "systemized" so that the cost is much lower than before. New handsets employ a combination of diversity and tuning to improve everyday performance by 4 dB—and up to 10 dB for some cases.

If the 600-MHz auction results in new spectrum for mobile handsets, we expect all of the problems with antenna performance to get even worse. Lower operating frequencies translate into electrically short antennas—the antenna dimensions are smaller than a wavelength.

Being electrically short causes poor efficiency in general for the antenna, forcing system engineers to rely on a more resonant antenna with more narrowband performance to reduce electrical losses. As the 600-MHz band comes onto the market and CA is required with 700- or 850-MHz bands, we can expect much more sophisticated use of "systemized" tuners that can optimize for multiple bands in a dynamic environment *(Fig. 3)*.

The key lies in considering the antenna as a system, not a component. Handset OEMs are dealing with dozens of bands, and their products are intended to work in countless frequency combinations. The solution to the complexity is smarter antenna tuning.

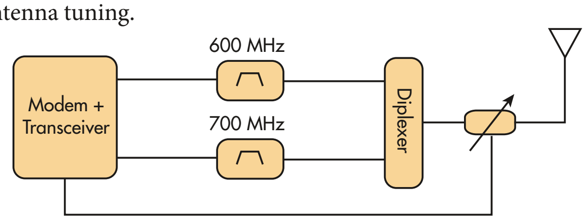

3. System-level closed-loop design can adapt for broadband performance.

Modem suppliers that implement advanced closed-loop antenna algorithms will be able to squeeze much more performance out of the handset. This is not a small technical detail, but a major impact—closed-loop tuning can effectively double the handset's true power. The result will be longer battery life and higher data speed for anybody who holds a phone in their hand. Yes, that means you. mw

GaN ENTERS 5G TERRITORY

FIFTH-GENERATION (5G) networks promise to offer significantly better performance than today's wireless networks. Specifically, these performance improvements include faster data rates, greater area traffic capacity, and lower latency. Greater network efficiency is another advantage expected with 5G. In the white paper, "Gallium Nitride—A Critical Technology for 5G," Qorvo discusses the role that gallium-nitride (GaN) technology is likely to play in future 5G networks.

According to the white paper, 5G promises to deliver latency below 1 ms, 20-Gb/s peak data rates, and area traffic capacity of 10 Mb/s/m^2. In addition, 5G is expected to offer improved efficiency, allowing for a more "green" communications network. Furthermore, objectives of 5G include delivering increased power levels and utilizing frequencies as high as 100 GHz.

To meet green network goals, 5G networks are likely to utilize GaN technology. GaN possesses a number of characteristics that allow for an improved overall efficiency in the RF chain. Its entrance into the base-transceiver-station (BTS) market space is detailed, as GaN technology has yielded greater efficiency in this arena. Moreover, the white paper notes that manufacturers must offer several GaN variations that span a wide array of frequencies and power levels to meet a diverse range of 5G requirements.

**Qorvo Inc.,
7628 Thorndike Rd.,
Greensboro, NC 27409;
(336) 664-1233;
www.qorvo.com**

In addition, according to the paper, GaN will overtake traditional semiconductor technologies in applications like higher-frequency, size-constrained small cells. Another prediction is that low-voltage GaN will ultimately find its way into mobile handsets. GaN can also operate in high-temperature environments, making it well-suited for passively cooled, all-outdoor base-station electronics, as well as automobile applications.

Lastly, millimeter-wave frequencies are discussed, as they are heavily tied to 5G. The white paper explains that GaN is an excellent fit for higher-frequency, wide-bandwidth applications. And with millimeter-wave applications utilizing beamforming technology, RF subsystems will therefore require a large number of active elements driving a relatively compact aperture. GaN technology is primed for such applications, as it can satisfy performance and small package-size requirements.

UNDERSTAND IEEE 802.11AX PA TEST REQUIREMENTS

THE UPCOMING IEEE 802.11ax standard is intended to enhance wireless connectivity, offering more consistent and reliable high-throughput Wi-Fi in crowded user environments. Such environments include places like busy airports and stadiums. The power amplifier (PA) is a critical component in a Wi-Fi transmitter, because its performance affects wireless coverage area, data-rate capacity, and battery life. Achieving the desired PA performance becomes even more challenging in IEEE 802.11ax applications for a number of reasons—all of which are discussed in LitePoint's application note, "Testing Power Amplifiers for 802.11ax."

**LitePoint,
965 West Maude Ave.,
Sunnyvale, CA 94085;
(866) 363-1911;
www.litepoint.com**

IEEE 802.11ax is expected to improve spectral efficiency in real-world environments, leveraging a number of technologies from cellular 4G LTE. Unlike the IEEE 802.11ac standard, which only operates in the 5-GHz frequency band, IEEE 802.11ax is intended to operate in both 2.4- and 5-GHz bands. IEEE 802.11ax also utilizes orthogonal-frequency-division multiple-access (OFDMA) technology. Another key aspect is the utilization of 1024-quadrature amplitude modulation (1024-QAM).

Some of the challenges associated with IEEE 802.11ax PAs surround error-vector-magnitude (EVM) requirements, which will be more stringent than those put forth by IEEE 802.11ac. The aforementioned OFDMA technology also impacts PA transmit performance and PA test requirements. Yet another challenge surrounding IEEE 802.11ax PA testing concerns dc voltage supply errors.

Digital pre-distortion (DPD) is an important feature likely to be deployed with next-generation IEEE 802.11ax chipsets. PA performance must therefore be validated when DPD is implemented. As a result, the PA linearization achievable with DPD is able to be quantified. Furthermore, OFDMA technology adds other variables that must be considered.

The application note concludes with a description of an IEEE 802.11ax test setup, explaining that all test system errors must be minimized. In essence, the entire integrated test system must be optimized to imitate real-world operating conditions. The test setup includes a number of LitePoint's instruments, including the z8653 vector signal analyzer (VSA), the z8751 vector signal generator (VSG), and the z5211 arbitrary waveform generator (AWG).

JACK BROWNE | Technical Contributor

POCKET-SIZED ANALYZERS Scan Millimeter-Wave Frequencies

Barely larger than many smartphones, this line of ultraportable spectrum analyzers doesn't skimp on performance, with models available for measurements to 110 GHz.

1. The Spectrum Master MS2760A family of portable spectrum analyzers are pocket-sized USB-powered instruments available in models operating to 110 GHz.

MILLIMETER-WAVE FREQUENCIES OFFER untapped bandwidth for many different applications, for those able to deliver practical wireless solutions in frequency bands such as 60 and 77 GHz. A major part of achieving those solutions includes the capability to test performance levels at such high frequencies, both for a device under test (DUT) and its operating environment. Fortunately, making measurements at millimeter-wave frequencies just became much easier with the introduction of the Spectrum Master MS2760A family of portable spectrum analyzers *(Fig. 1)* from Anritsu Co. *(www.anritsu.us.com)*.

Performance is impressive, with fast sweep speeds (11 s to sweep across a 110-GHz frequency range), wide dynamic ranges (100 dB to 110 GHz), and broad frequency ranges. Six different models cover ranges of 9 kHz to 32 GHz through 9 kHz to 110 GHz. What might be even more astounding is the size of these "ultraportable" instruments—these spectrum analyzers are no larger than a cell phone. They make use of a USB connection to a PC, laptop, or tablet, and its display screen to show measured results.

The millimeter-wave spectrum analyzers can be brought to a DUT, rather than the other way around *(Fig. 2)*. USB-powered MS2760A spectrum analyzers are almost like having a test laboratory in a pocket, and they represent the types of measurement tools that will help deliver millimeter-wave wireless technology to the masses.

As mentioned, six available Spectrum Master MS2760A models offer frequency coverage starting at 9 kHz for each and topping out at 32, 44, 50, 70, 90, and 110 GHz (with the 90-GHz version offered for locations where export licenses are required for frequencies above 90 GHz). Size is not the only "small" thing about these instruments—their cost allows multiple instruments to be purchased for the price of a single, larger benchtop instrument.

While millimeter-wave wireless applications are not about to become commodity items overnight, the millimeter-wave spectrum is gradually becoming more crowded. These frequencies have been in use in military applications, and for some time commercially in automotive electronic safety systems—notably at 77 GHz in collision-avoidance radar systems. The coming application of millimeter-wave bands for Fifth-Generation (5G) cellular wireless communications systems is expected to truly unleash the use of available wide bandwidths in support of the many communications and entertainment functions to be offered by service providers.

Testing these higher-frequency millimeter-wave-frequency systems will require suitable test equipment, including spectrum analyzers with not only sufficient frequency range, but also acquisition bandwidth. In addition, other performance parameters will come into play, such as frequency sweep speeds, when large segments of bandwidth must be scanned for potential operating environment issues (e.g., interference and coexistence with other high-frequency signal sources and their harmonic signals).

The Spectrum Master MS2760A ultraportable spectrum analyzers incorporate a number of patented technologies to squeeze the measurement capabilities of a full-sized, benchtop spectrum analyzer into those palm-sized packages, including

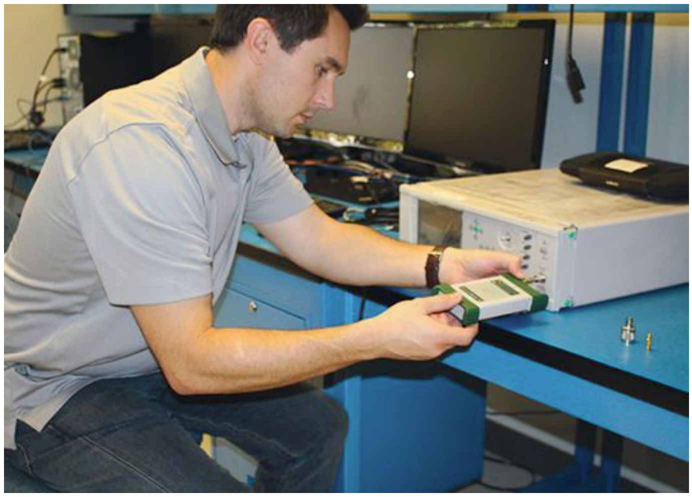

2. The Spectrum Master spectrum analyzers are small enough to connect directly to a DUT to eliminate the need for lossy, expensive interconnecting cables at millimeter-wave frequencies.

shockline nonlinear transmission line (NLTL) technology. This enables the construction of receiver circuitry covering frequencies from audio through millimeter waves with excellent amplitude accuracy and with amplitude flatness that remains typically within ±1 dB, even for a near-110-GHz frequency range.

Signal power tends to decrease with increasing frequency, with conventional mixer-based technologies exhibiting losses that increase with rising frequencies. The nonlinear characteristics of the NLTL circuits enables them to achieve flat amplitude response over such wide frequency spans.

The consistent frequency response and wide dynamic range of each Spectrum Master's internal receiver circuit boards and its transmission lines are preserved in the coaxial realm by means of a wideband planar-to-coaxial transition, terminating in different test port connectors depending on the frequency range of the particular Spectrum Master model.

For operation to 70 GHz, for example, 1.85-mm V-connectors (named for their V-band frequency range) are used. In regards to the highest-frequency model, 1-mm coaxial connectors enable connections to DUTs, antennas, and other measurement accessories operating at frequencies to 110 GHz. Models operating to 32 and 44 GHz use 2.92-mm K connectors.

Depending on the choice of frequency range, these pocket-sized spectrum analyzers are ready for high-frequency measurements in commercial, industrial, and military markets, including for automotive safety systems, military electronic-warfare (EW) systems, microwave radios, and satellite-communications (satcom) systems. The small size and versatility of the analyzers encourages production and even research environments to operate with multiple test stations.

In research, this equates to a more thorough investigation of a new design or technology. In production, it translates to more products that are ready to ship. And at millimeter-wave frequencies, the number of products expected to ship is projected to eclipse all that has come before at frequencies above 30 GHz.

In addition to the large number of production-line measurements needed to supply the hardware requirements of growing millimeter-wave applications, on-site testing *(Fig. 2, again)* will be essentially for qualification and maintenance of 5G wireless communications networks employing millimeter-wave frequencies. Due to the short-range propagation of millimeter-wave signals and their attenuation by buildings and other obstacles (even by people), wireless-communications coverage with millimeter-wave frequencies will require large numbers of antennas and antenna arrays and possibly multiple-input, multiple-output (MIMO) techniques for the best use of maintaining signal coverage with multiple antennas.

Having pocket-sized, battery-powered analyzers capable of characterizing such high-frequency networks and their antennas will allow 5G network technicians to bring the testbench with them. In fact, with the small size of the Spectrum Master millimeter-wave spectrum analyzers, the test instruments can be connected directly to a DUT, such as an antenna, for simplified testing. In this way, the loss (and the cost) of interconnecting millimeter-wave coaxial cables can be eliminated from the measurement setup.

The six millimeter-wave Spectrum Master portable spectrum analyzers operate with some form of controller, such as a tablet or laptop running Windows 7, 8.1, or 10. They are controlled remotely by small computer peripheral interface (SCPI) via a USB connection. The spectrum analyzers provide a number of "smart" measurements, including channel power, adjacent channel power, and occupied bandwidth.

Up to six measurement traces with individually selected detectors can be shown on the controller's screen at once, and as many as 12 total markers positioned on the traces to display the fine details of a measurement. Various limit-line functions can be set for frequency and amplitude for upper and lower limits *(Figs. 3 and 4)*. Sweep functions include single and continuous sweeps. In terms of amplitude, signal traces are able to be displayed in ranges of 1 to 15 dB/division, in 1-dB steps, with 10 divisions shown on the display screen.

CHECKING THE SPECS

The novelty of squeezing the essential elements of a spectrum analyzer into a package measuring just 6.1 × 3.3 × 1.1 in. (155 × 84 × 27 mm) and weighing just 9 oz. (255 g) doesn't obscure the fact that these high-performance measurement instruments are reaching frequencies not commonly displayed. The Spectrum Master millimeter-wave spectrum analyzers provide the sensitivity, dynamic range, and sweep speeds to identify interference when it becomes a problem and to keep track of signals in frequency bands of interest, no matter how high.

They also feature the measurement capabilities and bandwidths to screen for harmonic signals from lower-frequency signals, since otherwise harmless microwave signals can produce second- and third-harmonic signal components that become problems when they fall within a target millimeter-wave frequency band.

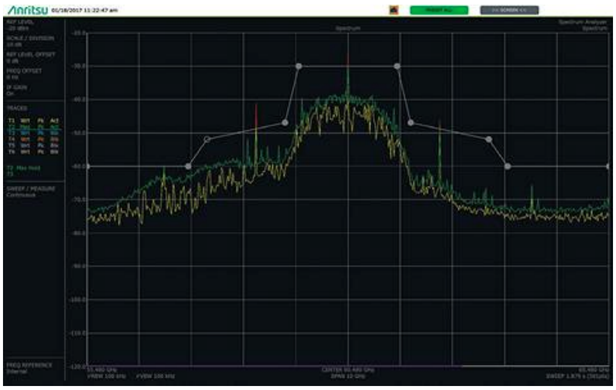

3. Limit lines can be set to make measurements per required wireless standards, such these screen traces with a spectral mask created for IEEE 802.11ad.

4. Markers can be placed where needed on signal traces to indicate measured values, with or without a trace marker shown on the screen to easily identify the markers.

The Spectrum Master ultraportable spectrum analyzers tune frequency with resolution of 1 kHz across their different frequency ranges. Measurements can be made with resolution bandwidths (RBWs) and video bandwidths (VBWs) from 10 Hz to 3 MHz and with sweep speeds approaching 7 s for a near-70-GHz span. Reference levels can be set from −120 to +30 dBm, with maximum safe input power as high as +20 dBm. The displayed average noise level (DANL) is typically −132 dBm from 40 to 70 GHz and −134 dBm or better for most of the frequency range below that. The DANL is typically better than −127 dBm through 110 GHz.

The analyzers operate with very good spectral purity, with typical spurious levels of −95 dBc and worse-case spurious levels of −85 dBc. Second-harmonic performance measured for a 1-GHz input signal at 0 dBm is typically −60 dBc, with maximum second-harmonic level of −60 dBc for a 1-GHz input signal at an input level of −20 dBm. The coaxial input is well matched to 50 Ω, with a typical VSWR of 1.29:1 to 12.4 GHz (18-dB return loss), 1.43:1 to 26.5 GHz (15-dB return loss), 1.58:1 to 40 GHz (13-dB return loss), and 2.10:1 to 70 GHz (9-dB return loss).

The millimeter-wave spectrum analyzers are equipped with a USB 3.0 Type-C connector from which they are completely powered by the host controller. The analyzers feature an internal frequency reference with ±1-ppm/year aging rate and ±0.2-ppm frequency accuracy, as well as input/output connections for an external 10-MHz reference source. For in-field measurements, the performance levels of the spectrum analyzers apply to temperatures from −10 to +50°C. A 12-month calibration cycle is recommended for the analyzers; they ship with a three-year warranty. mw

ANRITSU CO., 1155 East Collins Blvd., Ste. 100, Richardson, TX 75081; (800) 267-4878, (972) 644-1777, www.anritsu.com

JACK BROWNE | Technical Contributor

RF ICs Aim for Higher Functional Densities

Whether for analog, digital, power, or a combination of functions, IC designs are targeting increased functionality in smaller footprints.

MODERN ELECTRONIC PRODUCTS, such as cellular telephones and computers, continue to deliver increased functionality in smaller packages. Higher-density integrated circuits (ICs) are enabling this trend, while being designed for lower power consumption and increased efficiency. Advances in semiconductor processing, semiconductor materials, and device packaging all contribute to the "densification" of all IC types, which makes it possible to design and develop smaller circuits and smaller electronic products.

High-frequency ICs for RF and microwave applications are fabricated on a number of different substrate materials, including silicon wafers and III-V group compound semiconductor materials such as gallium arsenide (GaAs) and gallium nitride (GaN). GaAs has the high electron mobility to support high-frequency circuits well into the millimeter-wave frequency range (30 to 300 GHz), while GaN is a wide-bandgap material with high breakdown voltage and excellent high-power capabilities.

As with GaAs, GaN devices were initially developed for military/aerospace applications, such as solid-state radars and portable radio transmitters. But GaN-based ICs are becoming widespread for commercial applications, such as monolithic microwave integrated-circuit (MMIC) power amplifiers for wireless cellular base stations, and even at millimeter-wave frequencies as high as 77 GHz, in automotive collision-avoidance radar systems.

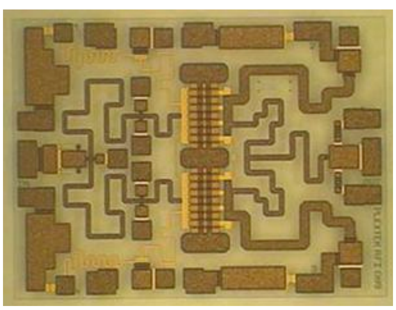

1. An example of high power from a small IC size, this GaN MMIC amplifier provides 25 W output power from 10 to 12 GHz. *(Courtesy of Plextek RFI)*

GOING WITH GaN

The spread of GaN semiconductor technology in both discrete-device and IC forms has been rapid during the past few years, with semiconductor foundries worldwide exploring the material's capabilities for high output power at high frequencies. Single-function MMICs such as power amplifiers and switches are available from a large number of suppliers, with some beginning to offer ICs that feature a combination of functions—e.g., switches and multistage amplifiers—on the same chip.

Silicon has been a semiconductor material of choice for many years, since it is a readily available material and inexpensive. As ICs moved higher in frequencies during the 1970s, however, the frequency limitations of devices fabricated on silicon substrates became apparent. Early U.S. Department of Defense (DoD) funding accelerated the development of GaAs substrate material for higher-frequency discrete devices and ICs. Along the way, additional compound semiconductor substrate materials, including indium phosphide (InP) or silicon germanium (SiGe) for high frequencies and silicon carbide (SiC) for high power, have been developed in different semiconductor foundries. That being said, GaN has become the current "material of interest" for a wide range of applications.

Although ICs can be fabricated on pure GaN wafers, more often than not, the GaN layers are formed on a backing layer (such as GaN-on-Si or GaN-on-SiC) to leverage some benefit from the second material—e.g., the low cost of silicon. Thermal management is a key concern when striving for higher levels of integration with GaN-based semiconductors. The high power density of GaN discrete devices and ICs results in large temperature rises in small areas.

Applications that require high power levels even in peak form, such as pulsed phased-array radars with multiple amplifiers, are being made more compact, although the heat generated by the active GaN devices must be effectively managed. Even the most efficient GaN amplifiers will generate heat that must be effectively dissipated.

Developers working with GaN-on-Si and GaN-on-SiC processes are exploring the thermal issues, especially for semiconductor processes capable of minute device features. Semiconductor foundries often offer fabrication services for multiple

substrate materials like GaAs and GaN, although the GaN process will be either on Si or SiC. Many commercial foundries focus on GaN-on-SiC fabrication services due to the excellent thermal properties of the SiC substrate material. These include Wolfspeed/Cree *(www.wolfspeed.com)*, HRL Laboratories *(www.hrl.com)*, United Monolithic Semiconductors (UMS; *www.ums-gaas.com*), Qorvo (*www.qorvo.com*), and WIN Semiconductors (*www.winfoundry.com*). Some foundries offering GaN IC fabrication services may not be as well known, such as defense contractors BAE Systems *(see p. 75)* and Northrop Grumman (*www.northropgrumman.com*).

One attractive feature of GaN-on-Si semiconductor processes has been their low cost and the opportunities to apply the benefits of GaN outside of RF/microwave designs. GaN transistors are noted for their low on-state resistance and low parasitic capacitance, characteristics that enable fast switching speeds when used in power supplies.

Navitas Semiconductor (*www.navitas.com*), for example, has focused on energy applications for GaN and developing GaN ICs for power control and supplies. GaN Systems *(www.gansystems.com)* has applied HEMTs fabricated with GaN-on-Si technology to power electronics, such as dc-dc converters with fast switching speeds. Infineon Technologies *(www.infineon.com)* has explored a variety of applications for GaN ICs, from audio amplifiers to microwave switching. Efficient Power Conversion (*www.epc.co.com*) also uses GaN devices for audio amplifiers.

GaN-based ICs are growing smaller over time, even as suppliers learn to handle thermal issues while cutting product costs. Though GaN MMIC amplifiers, for example, are still available from many suppliers in ceramic packages with excellent thermal conductivity to effectively dissipate heat from the GaN ICs, a growing number of GaN MMIC amplifiers are now available in lower-cost plastic packages. Nevertheless, users are advised to ensure that adequate heat-sinking is provided around the device at the circuit level.

Smaller die sizes promote more compact circuit designs and the opportunity to supply the ICs in smaller packages. The smaller die sizes also bring economic benefits for semiconductor suppliers. As researchers at Plextek RFI *(www.plextekRFI.com)* discovered when developing a GaN MMIC power amplifier for X-band radar applications *(Fig. 1)*, high power was possible even in extremely small die size.

The GaN HEMT amplifier MMIC was fabricated at WIN Semiconductors using a 0.25-μm gate-length process, resulting in a GaN MMIC amplifier die measuring 1.5 × 2.5 mm. In addition to meeting a customer's need for high output power of 25 W from 10 to 12 GHz in a small size for phased-array radars needing multiple channels of amplification, many amplifiers were produced per wafer. For the 4-in. GaN-on-SiC wafers used at the time of the work, about 2,300 amplifiers were fabricated per wafer.

Of course, GaN MMICs have some ways to go to match the levels of integration available in high-frequency silicon CMOS ICs, or even GaAs MMICs for that matter. But growing demands for wireless communications services and equipment with higher data rates, and the loads that are expected to be placed on wireless networks by new applications, is driving chip designers to find ways to pack more functionality into less space.

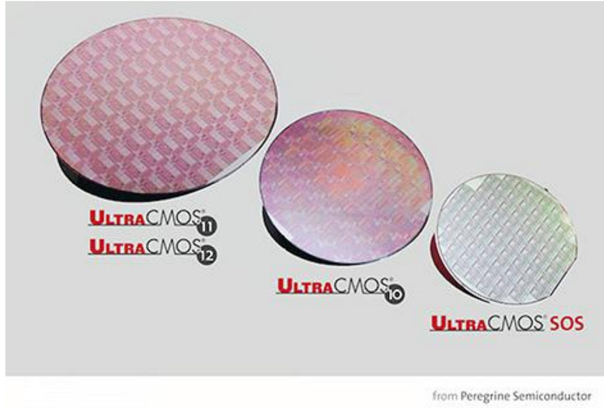

2. Silicon RF/microwave semiconductor technology continues to advance, as demonstrated by the latest generation of a high-speed silicon-on-insulator (SOI) process technology. *(Courtesy of Peregrine Semiconductor)*

While digital IC designers have almost routinely achieved high circuit densities in their ICs, the design constraints of RF/microwave ICs often throw roadblocks in the way of RF chip designers who are seeking to shrink the size of their ICs. These challenges include the importance of impedance matching as well as providing sufficient isolation between multiple on-chip signal sources.

Nonetheless, the design team for the ADR6612 and ADR6614 ICs from Analog Devices *(www.analog.com)* deserve much credit for their accomplishments of fabricating complete radio receivers and transmitters with multiple LOs for frequencies from 0.7 to 3.0 GHz on one chip.

Although the transceivers are not sold in die (chip) form, they are small enough to fit within 48-lead LFCSP housings that measure just 7 × 7 mm. The implications of this level of integration are significant, especially for systems that must provide functionality while remaining physically "unnoticeable."

Silicon RF/microwave ICs will not be quickly forgotten. As Peregrine Semiconductor *(www.psemi.com)* recently demonstrated, silicon CMOS technology is not close to reaching its top frequency. The firm recently announced the latest generation of its silicon-on-insulator (SOI) technology with low on-resistance and off-capacitance for a transition time of 80 fs.

The UltraCMOS 12 process *(Fig. 2)*, developed in conjunction with foundry Global Foundries *(www.globalfoundries.com)*, fabricates devices on 300-mm-diameter SOI wafers for relatively high yields. The process is able to fabricate ICs that can reach well into the upper reaches of the millimeter-wave frequency range. mw

JACK BROWNE | Technical Contributor

Facility Fabricates GaAs and GaN Devices

This well-equipped facility contains the equipment—and the people with the know-how—needed to create and manufacture GaAs and GaN semiconductors.

The BAE Microelectronics Center (MEC) and its foundry houses people and equipment needed for the research and production of high-performance microwave, millimeter-wave, and even optical semiconductor devices, circuits, and modules.

NOT EVERY DEFENSE/AEROSPACE electronics systems supplier can point to a full-fledged semiconductor foundry in its midst. But the Microelectronics Center (MEC) at BAE Systems *(www.baesystems.com)* is a full-featured, full-service compound-semiconductor foundry that can meet the company's most challenging needs for high-performance, high-frequency semiconductors. The MEC can transform software design files into wafers full of high-performance, RF/microwave discrete and integrated-circuit (IC) semiconductors based on compound semiconductor materials such as gallium arsenide (GaAs) and gallium nitride (GaN).

The BAE MEC *(see photo)* encompasses a total area of 70,000 ft.^{2}, including 12,000 ft.^{2} of Class 100 IC fabrication clean-room space, as well as Class 10,000 and 100,000 clean rooms for the qualification of advanced high-frequency semiconductor devices and the assembly/test of higher-level MMIC-based assemblies. The facility features extensive environmental control equipment to ensure the highest levels of cleanliness.

Also supporting the facility are automated-test-equipment (ATE) systems that include vector network analyzers (VNAs) with frequency extension well into the millimeter-wave ranges. The MEC is accredited as a Category 1A Trusted Supplier by the U.S. Department of Defense (DoD).

The facility relies on in-house molecular-beam-epitaxial (MBE) reactors to grow pseudomorphic high-electron-mobility-transistor (PHEMT) and metamorphic HEMT (MHEMT) active device layers on GaAs semiconductor wafers. GaN starting wafers, sourced from carefully qualified suppliers, are grown on thermally conductive silicon-carbide (SiC) substrates by means of metal-organic chemical vapor deposition (MOCVD). The MEC can form device features as fine as 20 nm via electron-beam lithography; the facility has already developed and produced millimeter-wave semiconductors operating as high as 200 GHz.

In addition to RF/microwave/millimeter-wave devices based on GaAs, indium phosphide (InP), and GaN, the MEC has also performed R&D for production of photonic and integrated optoelectronic devices and circuits, including optoelectronic ICs (OEICs) and focal plane arrays.

The facility added high-volume GaN module production capabilities in 2015, renovating the facility the following year for efficient co-location of staff working on R&D and production. This included those involved with material growth and wafer processing, as well as with device and module design, test, and manufacturing. Economies of scale in working with larger wafers began back in 2004 with 6-in.-diameter GaAs wafers for the production of GaAs pHEMTs and MESFETs. Through the use of automated wafer-handling systems, defects can be minimized and the benefits of high yields from these large wafers can be realized.

Customers are the beneficiaries of such high-volume semiconductor production, with cost reductions typically a function of increased yields. For mature semiconductor processes like GaAs, large volumes of devices are needed for both commercial and defense systems. The BAE MEC has shown its capabilities to meet high-volume military requirements for GaAs devices, with nearly 1 million GaAs MMIC devices delivered for F-22 production applications. The facility expects to be able to handle similar requirements for GaN devices. mw

BAE SYSTEMS, 95 Canal St., Nashua, NH 03064; (603) 885-4321, www.baesystems.com

IEEE

MTT-S®

WAMICON

IEEE Wireless and Microwave Technology Conference

WAMICON 2017

Hilton Cocoa Beach Oceanfront

Cocoa Beach, Florida

April 24-25, 2017

JOIN US

The 18th annual IEEE Wireless and Microwave Technology Conference (WAMICON 2017) will be held in Cocoa Beach, Florida on April 24-25, 2017. The conference will address up-to-date multidisciplinary research needs and interdisciplinary aspects of wireless and RF technology. The program includes both oral and poster presentations as well as tutorials and special sessions. The conference also features an active vendor exhibition area and an array of networking opportunities.

Conference Highlights

- **Keynote Speaker:**

Paul Colestock, Founder and Head of the Exploratory Design Group
Global Foundries
"The impact of Silicon as an emerging technology for 5G Circuits and System Solutions"

Registration includes:

- Access to all technical sessions and keynotes
- Breakfast and lunch both days. Morning and afternoon beverage/snack breaks
- Monday evening awards banquet

Visit ***www.wamicon.org*** for complete details.

Exhibit & Sponsorship Opportunities Available!
Email: jassurian@reactel.com • dzavac@tte.com

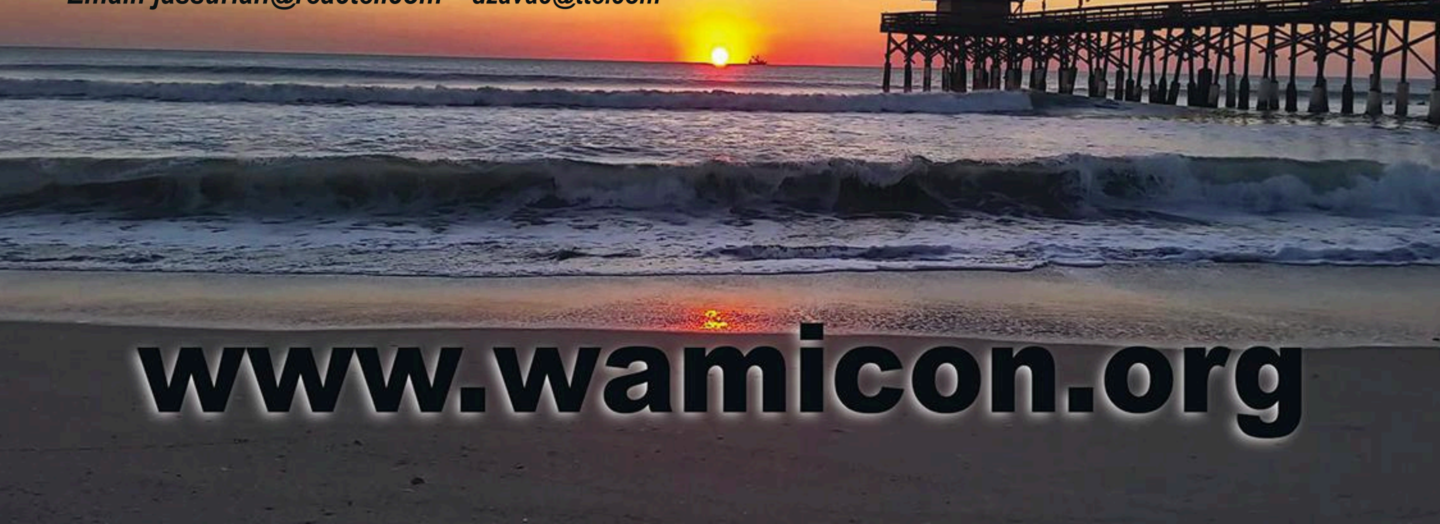

JACK BROWNE | Technical Contributor

FREQUENCY SYNTHESIZERS Rack Up Performance to 20 GHz

Leveraging a combination of standard and customized integrated circuits, these frequency synthesizers deliver high levels of performance.

ONE OF THE RF/microwave industry's leading suppliers of integrated circuits (ICs) is also a major consumer of them—specifically, as part of higher-level electronic designs. Well known for its data converters and receiver/transmitter ICs, Analog Devices *(www.analog.com)* is also adept at finding spots for many of its own ICs in block diagrams representing modules and even rack-mount systems for commercial, test, military, and even space applications.

As an example, the HMC-T2220 synthesized signal generator is a legacy product from the acquisition of Hittite Microwave Company a decade earlier that has been enhanced and upgraded to meet the needs of both avionics and automatic-test-equipment (ATE) applications. It is broadband, low in noise, and fast in switching speed, and manufactured alongside many of those smaller ICs that are more familiar to many high-frequency systems designers.

The HMC-T2220 synthesized signal generator *(see figure)* has the broad frequency range—10 MHz to 20 GHz—that makes it a candidate both for automated testing and adaptation to electronic-warfare (EW) systems. It is assembled with standard phase-locked-loop (PLL) frequency-synthesizer ICs as well as custom ICs developed specifically for this design, including tunable filters, a triplexer, eight-way multiplexer, a voltage-controlled oscillator (VCO), and a combination fractional-divider/phase-detector PLL with improved spurious performance.

These customized devices push forward superior performance while reducing size, weight, power, and cost. Several mechanical configurations have been developed, including a robust, 19-in.-wide rack-mountable unit for harsh environments. Although perhaps not well known, Analog Devices has the capability to quickly turn a set of function and performance requirements into a customized design and follow-up production.

This full-featured frequency synthesizer operates from 10 MHz to 20 GHz and is based on standard and custom analog and digital ICs that might be more familiar to many specifiers.

Having many of the necessary ICs close at hand *(see sidebar)* helps shorten lead times. With respect to designs featuring a heavy blend of analog and digital engineering, possessing the in-house expertise to combine RF, analog, and digital technologies at the device, circuit, and system levels offers major advantages toward achieving high circuit densities (small size)—with minimal power consumption and the highest reliability for critical applications.

Returning to the example of the HMC-T2220 synthesized signal generator, it was originally developed as a miniature test signal generator with high performance that could be easily moved around a research or manufacturing facility. It has been transformed into different versions, all with excellent broadband performance, but differing in digital functionality and control.

In general, the signal generator can tune quickly, with typical frequency switching speed of 300 μs and frequency-tuning resolution of 1 Hz. It provides generous output power, with +24 dBm at 10 MHz, +26 dBm at 1 GHz, +25 dBm to 10 GHz, +24 dBm to 15 GHz, and +20 dBm to 20 GHz. Output power can be adjusted with 0.1-dB resolution. With the RF power switched off, the power at the RF output port measures −80 dBm. Output power accuracy is typically better than ±2 dB below 50 MHz and better than ±1 dB above 500 MHz.

The single-sideband (SSB) phase noise is typically −113 dBc/Hz offset 1 kHz from a 1-GHz carrier and −135 dBc/Hz offset 1 MHz from the same carrier, and typically −86 dBc/Hz offset 1 kHz from a 20-GHz carrier and −112 dBc/Hz offset 1 MHz from the same carrier. Spurious rejection is −57 dBc or better for all frequencies 10 GHz or greater and −65 dBc or better for all frequencies less than 10 GHz. Second harmonics are −31 dBc or better below 10 GHz and −55 dBc at 20 GHz. Third-harmonic levels are −44 dBc at 10 MHz, −52 dBc at 1 GHz, and −58 dBc at 10 GHz.

The frequency synthesizer can be operated manually or under computer control, via USB, GPIB, and Ethernet ports and a computer running drivers supplied with the synthesizer. The drivers and graphical user interface (GUI) software that accompanies them are compatible with Windows XP, Vista, and 7. It is one example of the system-level design capabilities that work with many of the company's own ICs as building blocks. On a smaller scale, those design capabilities can also yield many other functions within a system block diagram, including power amplification *(see sidebar)*. mw

ANALOG DEVICES INC., One Technology Way, P.O. Box 9106, Norwood, MA 02062-9106; (781) 329-4700, www.analog.com

GaN IS JUST THE START

TO MEET AMPLIFICATION demands in high-frequency systems, Analog Devices has invested in GaN as the semiconductor material of choice for high-power RF/microwave amplification. On a smaller scale than the frequency synthesizer, the company assembles hermetic high-power-amplifier (HPA) modules based on GaN monolithic microwave integrated circuits (MMICs), with all necessary power sequencing and biasing connections made to the die within the module packaging. The modules are manufactured and fully tested within the confines of Analog Devices and are conservatively rated to meet their stated performance levels over wide environmental operating conditions.

One example of the in-house-manufactured GaN HPAs is model HMC8113, which operates from 2 to 6 GHz with more than 500 W typical saturated output power. It is supplied in a rugged, rack-mount housing *(Fig. 1)* with self-contained power supply, along with bias sequencing and bias protection to prevent damage. The large enclosure includes sufficient heat sinking in order to provide suitable thermal management for the range of GaN semiconductors.

For broadband applications requiring a somewhat smaller enclosure, another example is model HMC8114 *(Fig. 2)*, an HPA module with 90 W typical saturated output power from 6 to 18 GHz. The HMC8113 and HMC8114 are both ideal for EW applications. These and other GaN HPAs are designed with advanced thermal-management techniques and thermal modeling to minimize performance degradation due to self-heating effects. They incorporate numerous innovative design strategies, such as power-combining techniques developed to trim losses due to discontinuities and transmission-line mismatches. Many of the lessons learned in developing high-performance RF ICs are demonstrated in these higher-level modules and system-level assemblies. ■

1. The HMC8113 is a GaN power amplifier capable of more than 500 W saturated output power from 2 to 6 GHz. It comes in a rugged rack-mounted housing.

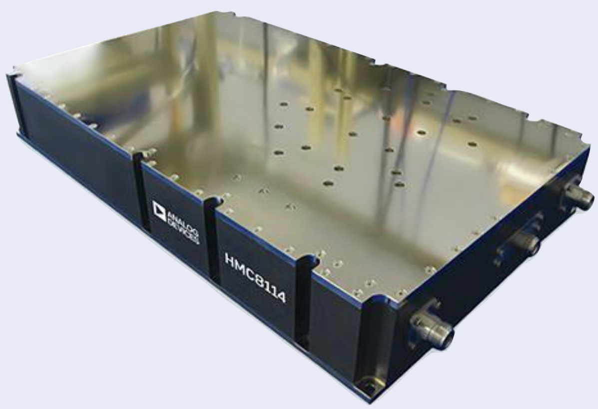

2. The HMC8114, a GaN power-amplifier module, offers more than 90 W saturated output power from 6 to 18 GHz. It is housed in a compact package with coaxial connectors.

(Continued from page 27)

In terms of spectrum sharing, what challenges do you think will arise due to the IoT and the potentially massive number of wireless devices?

The IoT has been rightly touted as the next revolution in the mobile ecosystem, although it presents many challenges. As vendors demand lower-priced IoT components, the IoT will be populated by a huge number of low-cost, thin-margin, spectrum-using devices manufactured by vendors new to the wireless space. Many offerings will be anomalous, non-compliant devices that use out-of-spec frequencies, bandwidths, and power levels.

Various well-known protocols have been developed over the years to support IoT, but none of them have gained mass-market penetration. One limiting factor to their adoption has been a lack of ubiquitous coverage. Cellular networks provide adequate coverage, but the deployed protocols have proven to be inefficient for many IoT uses. As a result, power-consumption expenses are too high for many lower-power devices.

In recent years, 3rd Generation Partnership Project (3GPP) standards such as LTE-M (LTE modified for IoT) and Narrowband-IoT (NB-IoT) have been modified to support IoT devices more efficiently. Nationwide IoT networks utilizing LTE-M are just starting to be deployed, and will support a variety of services including utility meters, vending machines, etc. This will result in a massive number of devices sending small bursts of traffic, which will increase the overall utilization of the spectrum.

While these new cellular standards and technologies will expand the number of IoT devices, they won't be the only protocols in use. Existing protocols will continue to be used where ubiquitous coverage is not needed, leveraging unlicensed spectrum in many cases. Regardless of the protocol, efficient spectrum sharing will keep being challenged by increased utilization of the spectrum, the distributive nature of the IoT devices, and more short bursts of traffic, which will make it harder to sense and predict the spectrum utilization. Advanced machine-learning algorithms will be required to detect the patterns in traffic and appropriately determine opportunities to share the spectrum.

What spectrum-management challenges do you expect to see as a result of 5G?

The introduction of 5G has the potential to revolutionize a number of industries by providing ultra-reliable, high-throughput, low-latency communication links. This will support applications ranging from autonomous vehicles to IoT network traffic.

To meet this vision, the network will have to be very dynamic. Multiple deployment paradigms will be supported, including licensed spectrum, shared spectrum, and unlicensed spectrum. Sharing and aggregation will be done both within the same band, as well as between bands having very different propagation characteristics, like sub-6-GHz and millimeter-wave.

The concepts pioneered in LTE, such as heterogeneous networks and inter-cell interference coordination, and the anticipated sharing between access and backhaul, will allow LTE deployment to reach full potential. Taken together, these 4G features will create new and unique spectrum-management challenges.

During 5G network operation, not only will RF carriers be set up and torn down quickly, but the transmission formats used on those carriers will change rapidly in order to optimize waveforms to meet the application's needs. This will require adaptive algorithms that can sense the spectrum and share it appropriately. To boost network capacity, 5G will also have to make extensive use of MIMO techniques to simultaneously send and receive multiple data signals over the same channel. This will make sensing the network's spectrum use more challenging, due to the high directivity of MIMO signals. Sensing the network in one location may not reveal potential interference in another location.

5G will also support very short (<1 ms) transmission intervals and fast switching between uplink and downlink transmissions, which will create greater challenges in sensing the network. Traditional survey methods will be insufficient with 5G. Instead, a network of sensors will have to be utilized that continuously monitors the network to fully understand spectrum usage.

Lastly, what is your vision of the RF spectrum and spectrum sharing in the future?

Spectrum is a finite natural resource. Advanced wireless signal-processing and optimized dynamic-allocation techniques will continue to enable increasingly efficient use of this resource. However, vastly scaled user demand for both military and commercial applications such as IoT, machine-to-machine (M2M) communications, and advanced multimedia data services will outstrip the gains made by improved spectral efficiency alone.

To address the growing need and financial opportunities posed by these applications, spectrum substrata must be allocated more narrowly and maximized through spatial system-level techniques such as very small, extremely high-density cells.

To support 5G protocols, highly adaptive heterogeneous wireless networks and standards will be needed to achieve optimal spectrum utilization throughout the network.

Beyond these breakthroughs in making effective use of bandwidth, our ability to dynamically sense the wireless-network environment and adapt to it will be paramount. This cognitive-sensing component will be critical to the design of end-user devices and to the evolution of the wireless infrastructure itself. Only through cognitive sensing will we be able to monitor and enforce spectrum-usage rules, maintain our awareness of network anomalies and spectrum interference, enable spectrum sharing, and deploy the wireless data analytics needed to simultaneously serve many mission needs. mw

PRIOR TO LGS Innovations, Kevin Kelly held senior positions within General Dynamics Advanced Information Systems and Lockheed Martin. He has served in board/advisory positions with the Innovative Technologies Council of INSA, AFCEA, IEEE, the National Advisory Council for GWU SEAS, and others.

JACK BROWNE | Technical Contributor

SPECTRUM ANALYZER Fits in Your Palm

This portable 8-GHz spectrum analyzer teams with a PC and online software applications, providing both on-location spectrum monitoring and EMI/EMC testing.

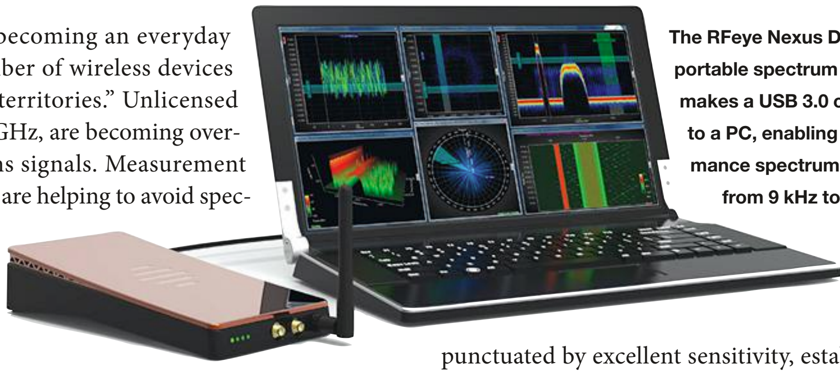

The RFeye Nexus Desktop DR-8 portable spectrum analyzer makes a USB 3.0 connection to a PC, enabling high-performance spectrum monitoring from 9 kHz to 8 GHz.

SPECTRUM MONITORING IS becoming an everyday event, given the growing number of wireless devices vying for their own "spectral territories." Unlicensed frequency bands, such as 2.45 GHz, are becoming overcrowded with communications signals. Measurement tools (e.g., spectrum analyzers) are helping to avoid spectral clutter and interference, achieving coexistence among these many wireless signals.

And fortunately, spectrum analyzers like the RFeye Nexus Desktop DR-8 from CRFS *(www.crfs.com)* are evolving to meet the measurement needs of this ever-changing wireless environment, packing sensitive and accurate measurement capabilities from 9 kHz to 8 GHz into a package that can truly fit into the palm of your hand.

The RFeye Desktop spectrum analyzer *(see photo)* works with a laptop or other PC to make simple spectral measurements in the field. The analyzer is supported with different online measurement applications that allow such functions as signal monitoring, interference hunting, and even testing for electromagnetic interference (EMI) and electromagnetic compatibility (EMC).

The pocket-sized instrument's looks are deceiving: It appears nothing like the traditional portable spectrum analyzer with large screen and handle. Weighing less than 1 kg and relying on the computer's microprocessor for programming and the computer's display screen for information readouts, this analyzer looks more like the commercial wireless communications devices it is measuring. Yet, the compact package houses a highly sensitive, wide-dynamic-range radio receiver with the low phase noise needed to detect and correctly identify different signals across its frequency span.

In addition to its wide frequency bandwidth, the spectrum analyzer has the measurement agility to spot frequency-hopping signals. It provides instantaneous measurement bandwidths as wide as 100 MHz that can be swept across its total frequency range at speeds to 400 GHz/s. The analyzer features frequency-tuning resolution of 1 Hz for studying the finest details of a captured signal. Its wide dynamic range is punctuated by excellent sensitivity, established by excellent phase-noise performance and low noise figures.

For example, the single-sideband (SSB) phase noise is less than −125 dBc/Hz offset 20 kHz from carriers below 0.5 GHz and less than −115 dBc/Hz offset 20 kHz from carriers greater than 1 GHz. The typical noise figures are 12 dB from 9 kHz to 100 MHz, 7 dB from 100 MHz to 2.4 GHz, and 8 dB from 2.4 to 8.0 GHz.

The RFeye Nexus Desktop DR-8 portable spectrum analyzer is supported by a company with a strong background in measuring spectral activity and with a number of effective software tools for use with its different hardware instruments. RFeye Monitor software, for example, is networked software that monitors and collects spectrum data through 6 GHz from numerous networked RFeye Nodes. It can be programmed with frequency masks and alarms, as well as used to check spectrum activity and occupancy per licenses and regulations.

The RFeye Desktop Nexus DR-8 is equipped with a USB 3.0 port, along with three female SMA connectors for RF/microwave signal interconnections (e.g., to antennas for remote spectrum monitoring). The spectrum analyzer can be run through a browser on any Windows- or Linux-compatible PC. The firm expects that RFeye Desktop users will take advantage of its online software measurement tools, but will also contribute some of their own measurement software applications as they learn more about the capabilities of this palm-sized RF/microwave spectrum analyzer. mw

CRFS INC., 4230-D Lafayette Center Dr., Chantilly, VA 20151; (571) 321-5470; www.crfs.com

CHRIS DeMARTINO | Technical Editor

Create Accurate EM ANTENNA MODELS

This software tool can produce electromagnetic (EM) models of antennas for use in higher-level simulations.

RF/MICROWAVE ENGINEERS ARE well-acquainted with "black box" models that characterize components in terms of S-parameters. These models, when incorporated into design software tools, enable engineers to conduct higher-level simulations. However, creating similar models of antennas has proven to be a more difficult task.

One company, the Microwave Vision Group (MVG), is focused on providing accurate electromagnetic (EM) models of measured antennas. These models can then be exported to various computational-electromagnetic (CEM) software tools, allowing for simulations of complex environments. Because such antenna models can be used to represent a measured source in numerical simulations of complex scenarios, they essentially link numerical simulations and antenna measurements. As a result, it becomes possible to analyze deployed antenna performance in complex scenarios.

The INSIGHT software developed by MVG can be used to create EM models based on an antenna's measured radiation pattern. By post-processing the measured data, the software can generate an Equivalent Current (EQC) model. This model, which is in the form of a black box, is based on Huygens' formulation. The equivalent antenna model can then be exported to a number of CEM tools from vendors such as Altair *(www.altair.com)*, ANSYS *(www.ansys.com)*, Computer Simulation Technology (CST; *www.cst.com*), and others *(see figure)*.

Specifically, the measured radiation pattern, which can be near-field and/or far-field data, is subsequently loaded into INSIGHT. After loading of the measurements, the next step involves configuring the measurement data and the geometry. INSIGHT can then perform measurement post-processing, providing users with 3D visualization and current animations. The measured field and the fields reconstructed from equivalent currents are visualized.

One example of this scenario is a reflector system fed by a dual-ridge horn. The system consists of the horn, which is the source antenna, and the reflector. Once the radiation pattern of the horn itself is initially measured, the measured data can be post-processed to obtain an equivalent black box model. This model then is able to be exported to a CEM tool to simulate the entire reflector system.

VALIDATING THE TECHNIQUE

MVG's white paper, "Finding the Missing Link: Bringing Together Numerical Simulation and Antenna Measurement to Understand Deployed Antenna Performance," discusses the case of a flush-mounted monocone antenna on a flat structure. This analysis is presented to validate the link between antenna measurements and CEM simulations.

The validation structure consists of MVG's SMC2200 monocone antenna mounted on a flat structure. Measurements were performed with the StarLab measurement system. The measured data is then post-processed by INSIGHT to create a 3D EM model of the monocone antenna. Next, the model is exported to six different CEM simulators to simulate the plate with the monocone antenna. Simulations are performed at 5.28 GHz.

The results of each simulation are compared with a reference measurement. If the peak directivities of all simulations are close to the measured value, it demonstrates a successful validation. Directivity radiation patterns at 5.28 GHz are also presented, illustrating agreement between measured and simulated results. mw

THE MICROWAVE VISION GROUP; www.mvg-world.com

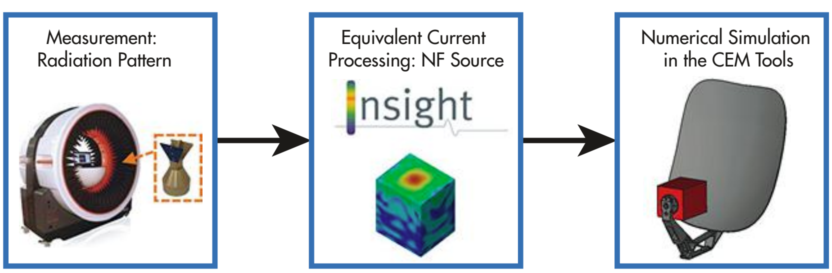

This figure illustrates the steps needed to incorporate an EM antenna model into a numerical simulation.

Product SPOTLIGHT

The latest product information presented by
Mini-Circuits®
www.minicircuits.com

Low-Noise Amp Has High IP3 from 0.5 to 15 GHz

Mini-Circuits' PMA2-153LN+ is GaAs MMIC amplifier with low noise figure, high gain, and high output third-order intercept (IP3) from 0.5 to 15.0 GHz. Based on E-PHEMT technology, the low-noise amplifier (LNA) features noise figure of 2.3 dB at 0.5 GHz, 2.8 dB at 10.0 GHz, and 3.8 dB at 15.0 GHz. The gain is typically 19.0 dB at 0.5 GHz, 16.0 dB at 10.0 GHz, and 12.5 dB at 15.0 GHz. The output power at 1-dB compression is typically +15.3 dBm at 0.5 GHz, +14.8 dBm at 10.0 GHz, and +11.2 dBm at 15.0 GHz. The IP3 performance is typically +27.3 dBm at 0.5 GHz, +26.7 dBm at 10.0 GHz, and +24.0 dBm at 15.0 GHz. The surface-mount amplifier is supplied in a 2 × 2 mm surface-mount MCLP housing. It is a good match for radar and wireless communications receivers and operates over temperatures from -40 to +85°C. It typically draws 66 mA from a +6 V dc supply.

Plug-In 75-Ω Diplexer Covers DC to 1220 MHz

Mini-Circuits' DPLC-8510A0+ is a 75-Ω plug-in diplexer with wide total frequency range of DC to 1220 MHz. It provides a lowpass frequency range of DC to 85 MHz with typical insertion loss of 1.1 dB and highpass range of 102 to 1220 MHz with typical insertion loss of only 1.4 dB. The passband return loss for both bands is typically 24 dB. The stopband rejection is typically 42 dB from 102 to 1220 MHz for the lowpass port and typically 42 dB from DC to 85 MHz for the highpass port. The plug-in diplexer exhibits low group-delay variations and is an excellent choice for DOCSIS® 3.1 data-over-cable systems as well as for multiband radio systems. It has an operating temperature range of -40 to +85°C.

Bidirectional SMT Coupler Handles High Power to 512 MHz

Mini-Circuits' SYDC-10-52VHP+ is a rugged surface-mount bidirectional coupler with 10-dB coupling, ±0.4 dB coupling flatness, and low loss from 30 to 512 MHz. It handles as much as 35 W power with load VSWRs as high as 2.0:1 and as much as 10 W power with output open- or short-circuit conditions. The mainline insertion loss is only 0.5 dB across the frequency range. Input and output return loss is typically better than 20 dB across the full frequency range. The bidirectional coupler, with as much as 22-dB directivity, measures 0.75 x 0.52 x 0.43 in. and has an operating temperature range of -40 to +65°C.

Power Splitter/Combiner Channels 5 to 1300 MHz

Mini-Circuits' SXPS-4-13-75+ is a four-way, 75-Ω 0° surface-mount power splitter/combiner with wide frequency range of 5 to 1300 MHz. It is suitable for many broadband applications, including in DOCSIS® systems. The typical insertion loss is 1.5 dB across the full frequency range, with better than 22 dB typical fullband isolation between ports. The high-performance splitter/combiner features amplitude unbalance controlled to within 0.25 dB and phase unbalance of typically 1° across the full frequency range. The sum port VSWR is typically 1.15:1 while the VSWR at the other four ports is typically 1.50:1 or less. The miniature divider/combiner measures just 0.44 x 0.74 x 0.19 in. and is supplied in a shielded package with wraparound terminations to simplify soldering.

MMIC Mixer Die Converts Frequencies from 5.0 to 21.5 GHz

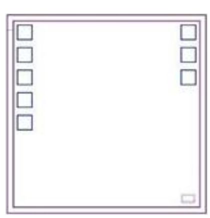

Mini-Circuits' MDB-24H-D+ is a MMIC frequency mixer die that can be used for upconversion and downconversion of signals from 5.0 to 21.5 GHz. Based on InGaP HBT semiconductor technology, the unpackaged die integrates baluns and local oscillator (LO) in a footprint of only 1278 × 1278 ×100 μm. The mixer has an RF/LO frequency range of 5.0 to 21.5 GHz and intermediate-frequency (IF) range of DC to 5 GHz. Typical conversion loss is 6.9 dB at 5.0 GHz, 9.0 dB at 10 GHz, and 10.3 dB at 21.5 GHz for an IF of 30 MHz. The RoHS-compliant double-balance mixer exhibits 44-dB typical LO-to-IF isolation. It is ideal for integration in hybrid circuits for commercial and military communications and radar systems.

Coaxial Slope Equalizer Runs 1300 to 2900 MHz

Mini-Circuits' ZEQ-5-292-S+ is a slope equalizer with wide frequency range of 1300 to 2900 MHz and steady drop in attenuation, from a minimum of 4.8 dB at 1300 MHz to a minimum of 0.2 dB at 2900 MHz. In fact, the minimum deviation in the attenuation slope with frequency is ±0.4 dB. The component features well-matched VSWR of typically 1.10:1 across the full frequency range. Well suited for L- and S-band satellite communications applications, the RoHS-compliant slope equalizer is supplied with SMA male input connector and SMA female output connector. It is designed for operating temperatures from -40 to +85°C.

(Continued from page 54)

$I_{2k} = G_0\{0.5V_{2k} - (2V_1/\pi)(-1)^k/[(2k-1)(2k+1)]\}$ (14)

Since the currents at the even harmonics are zero, it is possible to solve for voltage V_{2k} by setting current I_{2k} equal to zero in Eq. 14, thus yielding Eq. 15:

$V_{2k} = (4/\pi)(V_1)(-1)^k/[(2k-1)(2k+1)]$ (15)

Collecting the terms in cosθ in Eq. 12, the value of the current at the fundamental frequency I_1 can be found by Eq. 16:

$I_1 = (G_0)\{2(V_0)/\pi + 0.5(V_1) - (2/\pi)\ \Sigma^{\infty}_{k=1}(-1)^k V_{2k}/[(2k-1)(2k+1)]\}$ (16)

Substituting Eq. 15 into Eq. 16 yields Eq. 17a:

$I_1 = (G_0)(2(V_0)/\pi + V_1\ (0.5 - (8/\pi^2)\Sigma^{\infty}_{k=1}\{1/[(2k-1)(2k+1)]\}^2)$ (17a)

The term $(0.5 - (8/\pi^2)\ \Sigma^{\infty}_{k=1}\{1/[(2k-1)(2k+1)]\}^2)$ was found to converge in the limit to $(\pi/2)^2$ as k approaches infinity. (This limit was first estimated and then verified by computer program.) Substituting for $(0.5 - (8/\pi^2)\Sigma^{\infty}_{k=1}\{1/[(2k-1)(2k+1)]\}^2)$, the limit $(\pi/2)^2$ in Eq. 17a yields Eq. 17b:

$I_1 = G_0[2(V_0)/\pi + (2/\pi)^2 V_1]$ (17b)

At the fundamental frequency $Y(\omega) = G_L$, and as can be seen from Fig. 7, $I_1 = -(G_L)(V_1)$.

By equating I_1 as given by Eq. 17b to $-(G_L)(V_1)$:

$2(G_0)(V_0)/\pi + (G_0)(V_1)(2/\pi)^2 = -(G_L)(V_1) = -(X)(G_0)(V_1)$ (18)

where $X = G_L/G_0$. Solving Eq. 18 yields Eq. 19:

$V_1 = -(2/\pi)(V_0)/[X + (2/\pi)^2]$ (19)

The dc current I_0 is found from Eq. 12 to have two terms. The first term is $0.5(G_0)(V_0)$. The second dc term results from the product $[(2G_0/\pi)\cos\theta](V_1\cos\theta)$ and is equal to $(G_0)(V_1)/\pi$. Thus,

$I_0 = 0.5(G_0)(V_0) + (G_0)(V_1)/\pi = 0.5(G_0)(V_0)(1 + (2/\pi)/V_1/V_0)$ (20a)

Substituting Eq. 19 into Eq. 20a yields:

$I_0 = 0.5(G_0)(V_0)(X)/[X+(2/\pi)^2]$ (20b)

The efficiency of the Grayzel FET model for this special case can be found in the following way. The dc power is equal to $(I_0)(V_0)$. Multiplying Eq. 20b by voltage V_0 yields Eq. 21:

$P_0 = (I_0)(V_0) = 0.5(G_0)(V_0)^2(X)/[X+(2/\pi)^2]$ (21)

The output power at the fundamental frequency P_1 is found by Eq. 22:

$P_1 = 0.5(G_L)(V_1)^2 = [2(V_0)^2(G_L)/\pi^2]/[X+(2/\pi)^2]^2$ (22)

The efficiency (Eff) is then:

$Eff = P_1/P_0 = (2/\pi)^2/[X+(2/\pi)^2]$ (23a)

and the efficiency (to three-places accuracy) is:

$Eff = P_1/P_0 = 0.405/(X + 0.405)$ (23b)

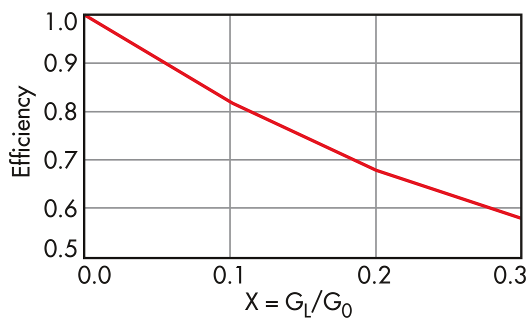

8. Efficiency is plotted as a function of parameter X for the Grayzel FET model, with even harmonics open-circuited and odd harmonics short-circuited.

Figure 8 shows a plot of efficiency as a function of X as given by Eq. 23. This special case where the amplifier is terminated in an open circuit for even harmonics and a short circuit for odd harmonics gives good results. However, it isn't necessarily an optimum termination. An analysis similar to what was performed here, but where the amplifier is terminated in an open circuit for odd harmonics and a short circuit for even harmonics, gave a poorer result. Optimization is required to determine an optimum termination. mw

ACKNOWLEDGMENTS

The author wishes to acknowledge the support given by Dr. Ashok Gorwara, CEO of Planar Monolithics Industries Inc. (PMI), and support provided by the staff of PMI.

REFERENCES

1. Steven C. Cripps, *RF Power Amplifiers For Wireless Communications*, 2nd ed., Artech House, Norwood, MA, 2006, pp. 22-24.

2. R.F. Pierret, *Field Effect Devices. Modular Series on Solid State Devices*, Addison-Wesley Publishing Company, Boston, MA, 1983, pp. 5-15.

Splitter-Combiner Goes Four Ways to 18 GHz

MODEL ZN4PD1-183W+ is a four-way, 0-deg. power splitter/combiner that is suitable for a wide range of signal-processing applications from 4 to 18 GHz. Capable of passing as much as 4 A current from the sum port to the other four ports (100 mA at each port), the 50-Ω splitter/combiner can handle as much as 30 W RF input power as a splitter. The insertion loss (above the theoretical 6-dB splitting loss) is typically 0.7 dB across the full frequency range. Minimum isolation between ports is 18 dB and typically 22 dB across the full frequency range. The VSWR at all ports is typically 1.40:1 or better. The phase unbalance is typically ±3 deg. across the full frequency range while amplitude unbalance is typically ±0.25 dB. The rugged four-way power splitter/combiner is supplied in an aluminum-alloy housing with SMA female connectors at all ports. It is designed for operating temperatures from –55 to +85°C.

MINI-CIRCUITS, P.O. Box 350166, Brooklyn, NY 11235-003; (718) 934-4500; *www.minicircuits.com*

Rad-Hard MOSFET Ready for Space

THE IRHNJ9A7130 radiation-hardened power MOSFET has been developed for space applications. It is based on 100-V, N-channel R9 semiconductor technology and supplied in a hermetic, surface-mount-device (SMD) package. It is suitable for high-speed switching applications in data converters and motor controllers and features an ESD rating of Class 2 per MIL-STD-750, Method 1020. It is rated for maximum continuous drain current of 35 A at +12 V dc gate-source voltage and 140 A current under pulsed conditions. Maximum power dissipation is 75 W. The peak diode recovery response is 13 V/ns. The transistor is designed to handle operating temperatures from –55 to +150°C.

IR HIREL, AN INFINEON TECHNOLOGIES CO., 101 North Sepulveda Blvd., El Segundo, CA 90245; (310) 252-7105; *www.infineon.com*

Smart Synth Tunes 240 to 760 MHz

MODEL FSW2476-50 is an intelligent interactive synthesizer (I2S) with an on-board microcontroller to simplify communications and programming. The low-noise signal source tunes from 240 to 760 MHz in 500-kHz steps with at least 0-dBm signal output power. It is designed for use with an external 10-MHz reference source, although the reference frequency is programmable. The synthesizer maintains excellent spectral purity for operating temperatures from –40 to +85°C, with typical phase noise of –95 dBc/Hz offset 1 kHz from the carrier, –98 dBc/Hz offset 10 kHz from the carrier, and –118 dBc/Hz offset 100 kHz from the carrier. Harmonics are typically –12 dBc, while typical spurious suppression is –85 dBc. The synthesizer operates with +5 and +25 V dc bias and has typical settling time of 3 ms. It is supplied in a RoHS-compliant, surface-mount package measuring 0.94 × 0.94 × 0.23 in.

SYNERGY MICROWAVE CORP., 201 McLean Blvd., Paterson, NJ 07504; (973) 881-8800; *www.synergymwave.com*

Divider Shares Signals Among Six Antennas

THE 151-215-006 resistive six-way power divider is designed for sharing signals among as many as six 50-Ω antennas operating from dc to 6 GHz. The nominal insertion loss above the customary division loss is –1 dB from dc to 5 GHz and –1.6 dB from 5 to 6 GHz, with worst-case amplitude tracking of ±0.5 dB. The VSWR is 1.50:1. The divider, which is supplied with SMA female coaxial connectors, has an operating temperature range of –20 to +100°C.

BROADWAVE TECHNOLOGIES INC., 170 Airport Pkwy., Ste. A, Greenwood, IN 46143; (317) 888-8316; *www.broadwavetech.com*

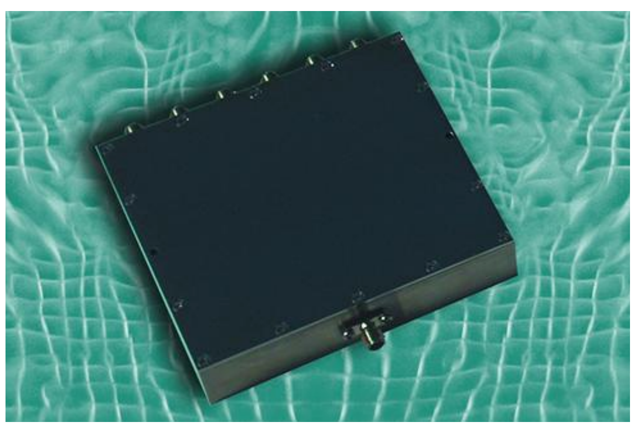

Spiral Inductors Span 1.5 to 300 nH

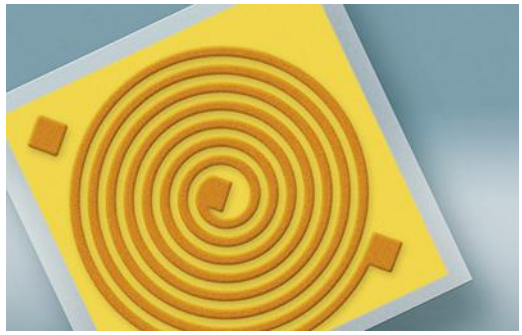

SPIRAL INDUCTOR coils are now available with inductance values from 1.5 to 300.0 nH, featuring 1.5 to 18.5 turns. The spiral inductor coils are produced in seven different square dimensions, all 0.12 in. thick: 0.030 × 0.030 in.; 0.040 × 0.040 in.; 0.045 × 0.045 in.; 0.055 × 0.055 in.; 0.065 × 0.065 in.; 0.075 × 0.075 in.; and 0.085 × 0.085 in. The spiral inductor coils, which are suitable for assembling microwave circuits and power supplies, are manufactured without chemical etching, using a thin-film process on quartz substrates with precision photolithography for excellent repeatability and consistency. A polyimide coating is applied on the quartz substrate to eliminate the need for conformal coating. The inductors can be attached by means of nonconductive epoxy and electrically connected via wirebonds.

SEMIGEN, 920 Candia Rd., Manchester, NH 03109; (603) 624-8311; *www.semigen.net*

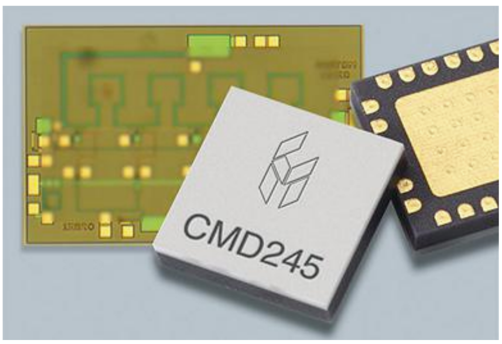

GaAs MMIC Amplifiers Promise Low Phase Noise

A LINE of broadband GaAs MMIC amplifiers has been developed for applications sensitive to the effects of phase noise. These five amplifiers, which are available in die and 4- × 4-mm QFN packages, achieve phase noise as low as –165 dBc/Hz offset 10 kHz from the carrier. Model CMD245 is a chip amplifier with 18-dB gain and 3-dB noise figure from 6 to 18 GHz; model CMD245C4 is the packaged version, with 4.5-dB noise figure. Model CMD246 is a chip amplifier with 17-dB gain and 3.5-dB noise figure from 8 to 22 GHz; model CMD246C4 is the packaged version, with 5-dB noise figure. Model CMD247 is a die amplifier with 13-dB gain and 5-dB noise figure from 30 to 40 GHz. All are self-biased with a single supply from +3 to +5 V dc.

CUSTOM MMIC, 300 Apollo Dr., Chelmsford, MA 01824; (978) 467-4290; *www.custommmic.com*

Multichannel LXI Digitizers Aid Low-Frequency Testing

A LINE of low-frequency digitizers includes units with as many as 24 synchronized input channels (with SMA connectors) for testing with 16-b resolution at sample rates to 250 Msamples/s or 14-b resolution at sample rates to 500 Msamples/s. The DN6.44x digitizers are ideal for testing arrays of antennas and sensors at analog bandwidths to 250 MHz. Switchable input impedances (50 Ω and 1 MΩ) and switchable input amplifiers provide six input ranges from ±200 mV to ±10 V. The digitizers are provided with operating software that controls the instrument from a host computer.

SPECTRUM SYSTEMENTWICKLUNG MICROELECTRONIC GmbH, Ahrensfelder Weg 13-17, 22927 Grosshansdorf, Germany; +49 (0) 4102-6956-0; *www.spectrum-instrumentation.com*

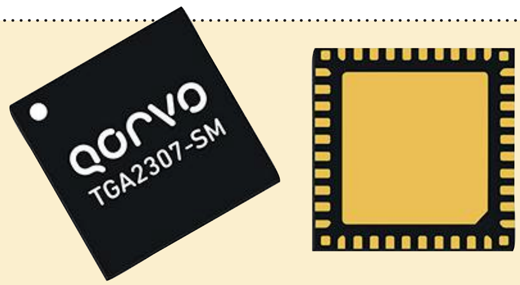

C-Band GaN Amplifier Boosts Satcom Signals

MODEL TGA2307-SM is a high-power GaN amplifier designed for satellite communications (satcom) or radar applications in the 5- to 6-GHz band. It provides 50 W saturated output power with pulsed signals with better than 28-dB small-signal gain. The amplifier features power-added efficiency (PAE) of better than 44% with large-signal gain of 20 dB. Supplied in a 6- × 6-mm QFN plastic package, the amplifier draws 500 mA current from a +28-V dc supply.

RFMW LTD., STOCKING DISTRIBUTOR FOR QORVO, 188 Martinvale Ln., San Jose, CA 95119; (408) 414-1450; e-mail: info@rfmw.com; *www.rfmw.com*

ADVERTISER	PAGE
A	
ANRITSU CORPORATION	C2, 40a-b
www.anritsu.com/test-measurement	
ARRA INC.	C3
www.arra.com	
AVTECH	6
www.avtechpulse.com	
B	
BOONTON	C4
www.boonton.com	
C	
CALIFORNIA EASTERN LAB	11
www.cel.com/switches	
CIAO WIRELESS INC	17
www.ciaowireless.com	
COILCRAFT	2
www.coilcraft.com	
COMMUNICATION CONCEPTS INC	70
www.communication-concepts.com	
D	
DBM CORP	43
www.dbmcorp.com	
F	
FAIRVIEW	24,25
www.fairviewmicrowave.com	
H	
HEROTEK INC	13
www.herotek.com	
K	
KOAXIS INC	44
www.koaxis.com	
L	
L-3 NARDA-MITEQ	3
www.nardamiteq.com	
LINEAR TECHNOLOGY CORPORATION	19
www.linear.com/product/LTC5549	
M	
M/A COM TECHNOLOGY SOLUTIONS, INC	8-9
www.macom.com/mmics	
MECA ELECTRONICS INC	7
www.e-MECA.com	
MICRO CIRCUIT LABORATORIES	49
www.microcircuitlabs.com	
MINI-CIRCUITS/SCI COMPONENTS	12, 14-15, 23, 29, 30-31, 35, 45, 47, 53, 59, 65, 67, 71, 73, 79, 83, 87
www.minicircuits.com	
N	
NEXYN CORPORATION	16
www.nexyn.com	
NI AWR	4
www.ni.com/awr	
NI MICROWAVE COMPONENTS	22
www.ni-microwavecomponents.com/quicksyn	
P	
PASTERNACK ENTERPRISES	32
www.pasternack.com	
PLANAR MONOLITHICS INDUSTRIES	1
www.pmi-rf.com	
POLYFET	61
www.polyfet.com	
PULSAR MICROWAVE CORP	18
www.pulsarmicrowave.com	
S	
SAGE MILLIMETER INC	38-39
www.sagemillimeter.com	
SR TECHNOLGIES	61
www.srtechnology.com	
SYNERGY MICROWAVE	37, 55
www.synergymwave.com	
W	
WAMICON	76
www.wamicon.org	
WAVELINE INC	62
www.wavelineinc.com	

This index is provided as an additional service by the publisher, who assumes no responsibility for errors or omissions.

Subscription Assistance and Information:
(ISSN 0745-2993)
Microwaves & RF is published monthly. Microwaves & RF is sent free to individuals actively engaged in high-frequency electronics engineering. In addition, paid subscriptions are available. Subscription rates for U.S. are $95 for 1 year ($120 in Canada, $150 for International). Published by Penton Media, Inc., 9800 Metcalf Ave., Overland Park, KS 66212-2216. Periodicals Postage Paid at Kansas City, MO and additional mailing offices. POSTMASTER: Send change of address to Microwaves & RF PO Box 2100, Skokie, IL 60076-7800. For paid subscription information, please contact Microwaves & RF at PO Box 2100, Skokie IL 60076-7800. Canada Post Publications Mail agreement No. 40612608. Canada return address: IMEX Global Solutions PO Box 25542, London ON N6C 6B2.

Get a piece of the ARRA pie...

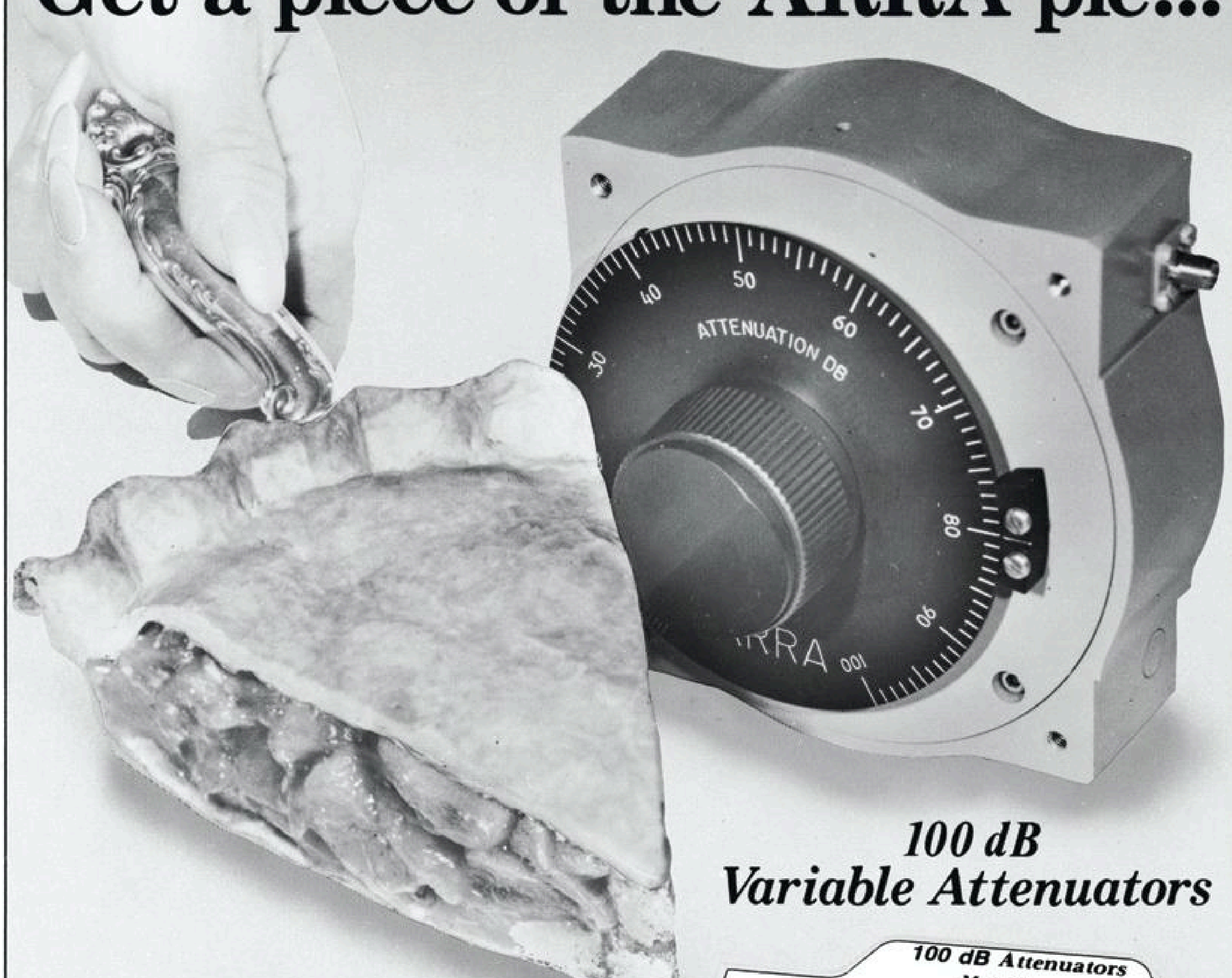

100 dB Variable Attenuators

100 dB Attenuators
Mmmm....

Freq Range	Atten vs Freq ·dB	Model #
500 - 1000 MHz	1.5	2952 - 100
900 - 1300 MHz	0.75	2-3952 - 100
1000 - 2000 MHz	1.5	3952 - 100X
2000 - 4000 MHz	1.5	4952 - 100 X
4000 - 8000 MHz	1.5	5952 - 100X

Insertion loss - 6 dB
VSWR - 1.5
Power - 15 cw
Temperature -30 to +120 C

Now, you can have your pie and eat it too! Only from ARRA! Four models that cover the 500 to 8000 MHz frequency range! Available in lower attenuation ranges. ***Customerized to your requirements with little or no additonal charge.*** Top performance. Super dial accuracy.

- Direct reading dial
- Extremely high reliability
- Non-contacting movable parts (our special recipe)
- High power version available (up to 200 W)
- Usage will not change calibration
- Attenuation will not vary with temperature
- Excellent phase characteristics
- Type N standard SMA connectors available

Applications include:
•TACAN •DME/IFF •Lab standards •Altimeter
Or any other requirements needing high attenuation and accurate dial reading.

Visit our website at www.arra.com
E-Mail: sales@arra.com

Some of the best attenuator recipes you can find are cooking at ARRA right now! Send for your copy today and get a piece of the ARRA pie.

. . . the last word in variable attenuators

ARRA INC.
15 Harold Court • Bay Shore NY 11706-2296

Tel 631-231-8400 Fax 631-434-1116

Don't Settle for Average.

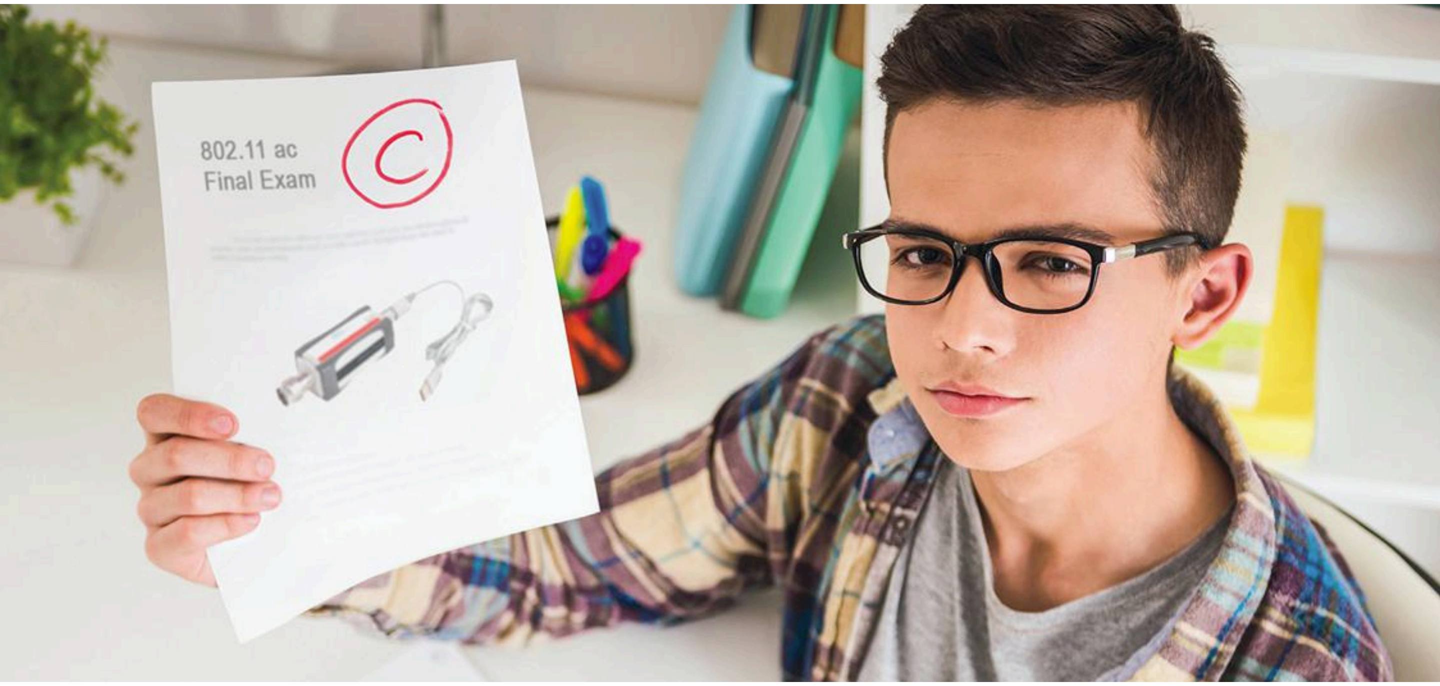

Demand Peak Performance.

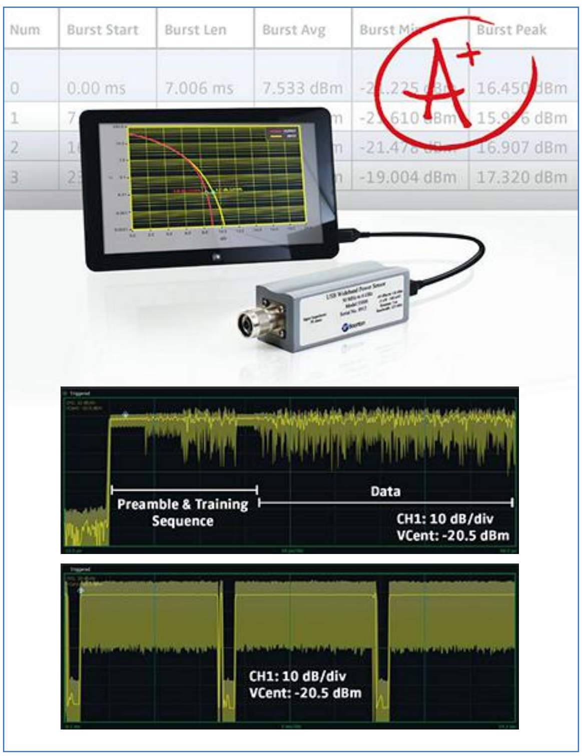

The 55 Series USB Peak Power Sensor

Real-Time Power Measurements for Complex Communications Signals

Others claim to have fast average measurements, but only the 55 Series measures continuous and burst average power faster than anyone in the industry. It adds wide-band peak and crest factor measurements, allowing you to see all aspects of your device's performance. This USB Sensor delivers results 100 times faster than conventional meters and with its *Real-Time Power Processing*™ technology captures all glitches with 100ps resolution.

- 195 MHz Video Bandwidth
- 3 ns risetime
- 100,000 measurements/sec
- 100 MHz Sample Rate
- Multi-channel synchronized measurements

For more information visit us at **www.boonton.com**
or call +1 973-386-9696.

Wireless Telecom Group
Boonton Microlab Noisecom

Boonton

Wireless Standards 2017

CELLULAR COMMUNICATION

LTE

FDD

Band	Uplink (MHz)	Downlink (MHz)	Bandwidth UL/DL (MHz)	Duplex Spacing (MHz)
1	1920 - 1980	2110 - 2170	60	190
2	1850 - 1910	1930 - 1990	60	80
3	1710 - 1785	1805 - 1880	75	95
4	1710 - 1755	2110 - 2155	45	400
5	824 - 849	869 - 894	25	45
6	830 - 840	875 - 885	10	45
7	2500 - 2570	2620 - 2690	70	120
8	880 - 915	925 - 960	35	45
9	1749.9 - 1784.9	1844.9 - 1879.9	35	95
10	1710 - 1770	2110 - 2170	60	400
11	1427.9 - 1447.9	1475.9 - 1495.9	20	48
12	699 - 716	729 - 746	17	30
13	777 - 787	746 - 756	10	-31
14	788 - 798	758 - 768	10	-30
17	704 - 716	734 - 746	12	30
18	815 - 830	860 - 875	15	45
19	830 - 845	875 - 890	15	45
20	832 - 862	791 - 821	30	-41
21	1447.9 - 1462.9	1495.9 - 1510.9	15	48
22	3410 - 3490	3510 - 3590	80	100
23	2000 - 2020	2180 - 2200	20	180
24	1626.5 - 1660.5	1525 - 1559	34	-101.5
25	1850 - 1915	1930 - 1995	65	80
26	814 - 849	859 - 894	35	45
27	807 - 824	852 - 869	17	45
28	703 - 748	758 - 803	45	55
29	N/A	717 - 728	11	N/A
30	2305 - 2315	2350 - 2360	10	45
31	452.5 - 457.5	462.5 - 467.5	5	10
32	N/A	1452 - 1496	44	N/A
65	1920 - 2010	2110 - 2200	90	190
66	1710 - 1780	2110 - 2200	70/90	400
67	N/A	738 - 758	20	N/A
68	698 - 728	753 - 783	30	55
252	N/A	5150 - 5250	100	N/A
255	N/A	5725 - 5850	125	N/A

TDD

Band	Uplink and Downlink (MHz)	Bandwidth (MHz)
33	1900 - 1920	20
34	2010 - 2025	15
35	1850 - 1910	60
36	1930 - 1990	60
37	1910 - 1930	20
38	2570 -2620	50
39	1880 - 1920	40
40	2300 - 2400	100
41	2496 - 2690	194
42	3400 - 3600	200
43	3600 - 3800	200
44	703 - 803	100
45	1447 - 1467	20
46	5150 - 5925	775

CDMA2000 1x/1xEV-DO

Band	Uplink (MHz)	Downlink (MHz)
Band Class 0	815 - 849	860 - 894
Band Class 1	1850 - 1910	1930 - 1990
Band Class 2	872 - 915	917 - 960
Band Class 3	887 - 925	832 - 870
Band Class 4	1750 - 1780	1840 - 1870
Band Class 5	410 - 483	420 - 493
Band Class 6	1920 - 1980	2110 - 2170
Band Class 7	776 - 788	746 - 758
Band Class 8	1710 - 1785	1805 - 1880
Band Class 9	880 - 915	925 - 960
Band Class 10	806 - 901	851 - 940
Band Class 11	410 - 483	420 - 493
Band Class 12	870 - 876	915 - 921
Band Class 13	2500 - 2570	2620 - 2690
Band Class 14	1850 - 1915	1930 - 1995
Band Class 15	1710 - 1755	2110 - 2155
Band Class 16	2502 - 2568	2624 - 2690
Band Class 18	787 - 799	757 - 769
Band Class 19	698 - 716	728 - 746
Band Class 20	1626.5 - 1660.5	1525 - 1559
Band Class 21	2000 - 2020	2180 - 2200

W-CDMA/HSPA/HSPA+

Band	Uplink (MHz)	Downlink (MHz)	Bandwidth (MHz)	Duplex Spacing (MHz)
1	1920 - 1980	2110 - 2170	60	190
2	1850 - 1910	1930 - 1990	60	80
3	1710 - 1785	1805 - 1880	75	95
4	1710 - 1755	2110 - 2155	45	400
5	824 - 849	869 - 894	25	45
6	830 - 840	875 - 885	10	45
7	2500 - 2570	2620 - 2690	70	120
8	880 - 915	925 - 960	35	45
9	1749.9 - 1784.9	1844.9 - 1879.9	35	95
10	1710 - 1770	2110 - 2170	60	400
11	1427.9 - 1447.9	1475.9 - 1495.9	20	48
12	699 - 716	729 - 746	17	30
13	777 - 787	746 - 756	10	-31
14	788 - 798	758 - 768	10	-30
19	830 - 845	875 - 890	15	45
20	832 - 862	791 - 821	30	-41
21	1447.9 - 1462.9	1495.9 - 1510.9	15	48
22	3410 - 3490	3510 - 3590	80	100
25	1850 - 1915	1930 - 1995	65	80
26	814 - 849	859 - 894	35	45

GSM/GPRS/EDGE/EDGE EVOLUTION

Band	Uplink (MHz)	Downlink (MHz)	Duplex Spacing (MHz)
T-GSM-380	380.2 - 389.8	390.2 - 399.8	10
T-GSM-410	410.2 - 419.8	420.2 - 429.8	10
GSM-450	450.4 - 457.6	460.4 - 467.6	10
GSM-480	478.8 - 486	488.8 - 496	10
GSM-710	698.0 - 716.0	728.0 - 746.0	30
GSM-750	777.0 - 792.0	747.0 - 762.0	-30
T-GSM-810	806.0 - 821.0	851.0 - 866.0	45
GSM-850	824.0 - 849.0	869.0 - 894.0	45
P-GSM-900	890.0 - 915.0	935.0 - 960.0	45
E-GSM-900	880.0 - 915.0	925.0 - 960.0	45
R-GSM-900	876.0 - 915.0	921.0 - 960.0	45
T-GSM-900	870.4 - 876.0	915.4 - 921.0	45
DCS-1800	1710.0 - 1785.0	1805.0 - 1880.0	95
PCS-1900	1850.0 - 1910.0	1930.0 - 1990.0	80

TD-SCDMA/TD-HSPA/TD-HSPA+

Band	Uplink and Downlink (MHz)	Bandwidth (MHz)
33	1900 - 1920	20
34	2010 - 2025	15
35	1850 - 1910	60
36	1930 - 1990	60
37	1910 - 1930	20
38	2570 -2620	50
39	1880 - 1920	40
40	2300 - 2400	100

GNSS (GLOBAL NAVIGATION SATELLITE SYSTEM)

GPS	
L1	1575.42 MHz
L2	1227.60 MHz
L3	1381.05 MHz
L4	1379.913 MHz
L5	1176.45 MHz
GLONASS	
L1	1602.0 MHz
L2	1246.0 MHz
L3	1202.25 MHz
Galileo	
E1	1575.42 MHz
E5	1191.795 MHz
E5a	1176.45 MHz
E5b	1207.14 MHz
E6	1278.75 MHz
BeiDou	
B1	1561.098 MHz
B1-2	1589.742 MHz
B2	1207.14 MHz
B3	1268.52 MHz

WIRELESS CONNECTIVITY

Name	IEEE Standard	Frequency Band	Data Rate
WLAN	IEEE 802.11a	5 GHz	54 Mbps
	IEEE 802.11b	2.4 GHz	11 Mbps
	IEEE 802.11g	2.4 GHz	54 Mbps
	IEEE 802.11n	2.4 GHz, 5 GHz	600 Mbps
	IEEE 802.11ac	5 GHz	6.93 Gbps
	IEEE 802.11af	54 - 790 MHz	26.7 Mbps for 6/7-MHz channels 35.6 Mbps for 8-MHz channels
	IEEE 802.11ah	< 1 GHz	Up to 40 Mbps
	IEEE 802.11ad	60 GHz	7 Gbps
Bluetooth		2.4 GHz	1 to 3 Mbps
ZigBee		2.4 GHz (worldwide) 915 MHz (U.S.) 868 MHz (Europe)	20 to 250 kbps
LoRaWAN		915 MHz (U.S.) 868 MHz (Europe)	0.3 to 50 kbps
Z-Wave		908.42 MHz (U.S.) 868.42 MHz (Europe)	Up to 100 kbps
THREAD		2.4 GHz	250 kbps
SIGFOX		915 MHz	Very Low
NFC		13.56 MHz	424 kbps
WirelessHART		2.4 GHz	250 kbps
Weightless		< 1 GHz	Up to 10 Mbps
LTE Cat-1		Cellular bands	Up to 10 Mbps
LTE Cat-0/LTE-M		Cellular bands	Up to 1 Mbps
Narrowband IoT (NB-IoT)		Cellular bands	Tens of kbps

microwaves&rf
TRUSTED ENGINEERING RESOURCE FOR OVER 50 YEARS